Solar-Terrestrial Centre of Excellence

Annual Report 2013

Belgian Science Policy Office
belspo

Royal Observatory of Belgium

RMI

BIRA-IASB

.be

STCE

Solar-**T**errestrial **C**entre of **E**xcellence

http://stce.be/

Ringlaan 3

B-1180 Brussels

Tel.: +32 2 373 0211

Fax: + 32 2 374 9822

Front-page: *The pieces of the puzzle on Sun and Space Weather were fit together during many gatherings, such as during seminars in the meeting rooms of the RMI, BISA and ROB, in the packed conference rooms of the Coronal Loops workshop and the 10th European Space Weather Week, and during the Open Door. In the background an SDO/AIA image from early December 2013, when the solar cycle was going through a new period of enhanced solar activity.*

Table of Contents

Preface

Dear reader,

Over the past few years, the Solar-Terrestrial Centre of Excellence has grown into a European and worldwide reference in the various sub-disciplines of solar-terrestrial physics. The expertise of the 3 participating institutes, combined into one multidisciplinary research frame, has indeed brought us enough critical mass to ignite a chain reaction towards ever deepening excellence.

In your hands, you hold the STCE Annual Report 2013. Successful research is often the result of sustained effort during many years. As in previous years, we have therefore chosen not to provide you an encyclopedic overview of all ongoing STCE activities, but instead only highlight what was particularly remarkable at the STCE in 2013. As you will see, even this selection of top stories fills an entire booklet. We hope you enjoy this year's selection while other ongoing activities are carefully bred for publication in coming issues.

As you will see, "communication" in all its facets (explicit in the first few chapters or implicit everywhere else) is considered crucial at the STCE, and also this report is part of that effort. The best communication is however a two-way process: if you would like to get more information about any of the particular topics or about any of the STCE activities, please do not hesitate to contact us.

Do challenge us with your questions, innovative ideas or proposals for collaboration!

Kind regards
Ronald Van der Linden
General Coordinator of the Solar-Terrestrial Centre of Excellence
Director General of the Royal Observatory of Belgium

Structure of the STCE

The Solar-Terrestrial Centre of Excellence is a project of scientific collaboration that focuses on the Sun, through interplanetary space, up to the Earth and its atmosphere.

The solid base of the STCE is the expertise that exists in the 3 Federal Scientific Institutes of the Brussels Space Pole: the Royal Observatory of Belgium, the Royal Meteorological Institute and the Belgian Institute for Space Aeronomy. The STCE supports fundamental solar, terrestrial and atmospheric physics research, is involved in earth-based observations and space missions, offers a broad variety of services (mainly linked to space weather and space climate) and operates a fully established space weather application centre. The scientists act at different levels within the frame of local, national and international collaborations of scientific and industrial partners.

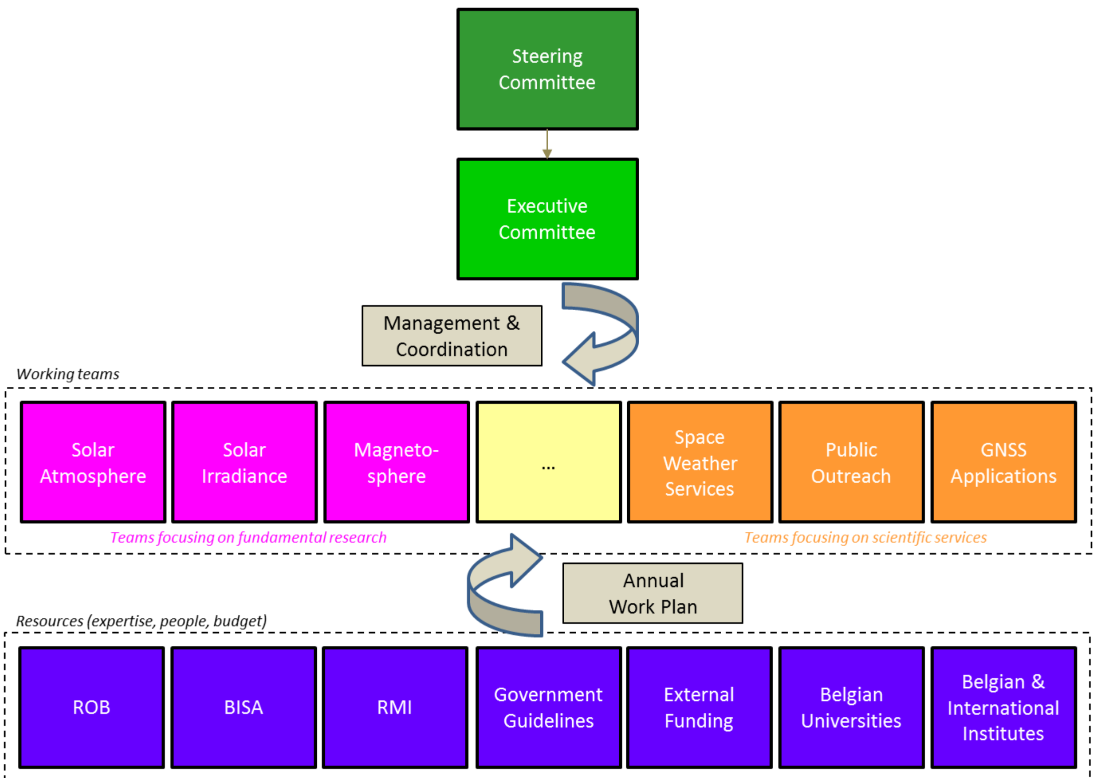

Figure 1: The STCE management structure

The STCE's strengths are based on sharing know-how, manpower, and infrastructure.

In order to optimize the coordination between the various working groups and institutions, as well as the available resources such as ICT, personnel and budget, a management structure for the STCE was put into place, consisting of a steering committee and an executive committee.

The ***steering committee*** takes all the final decisions on critical matters with regard to the STCE. It assures the integration of the STCE into the 3 institutions and the execution of the strategic plans. It is composed of:

- BELSPO Director General "Research Programs and Applications"

  Dr. Frank Monteny (BELSPO)

- Director General of each of the 3 institutions at the Space Pole

  Dr. Ronald Van der Linden (ROB)
  Dr. Daniel Gellens (RMI)
  Dr. Martine De Mazière (BISA)

The ***executive committee*** assures the global coordination between the working groups and the correct use of the budgetary means for the various projects. It also identifies new opportunities and is the advisory body to the Steering Committee. It is composed of:

- STCE Coordinator

  Dr. Ronald Van der Linden

- Representatives of the research teams in the 3 institutes

  Dr. David Berghmans (ROB)
  Dr. Carine Bruyninx (ROB)
  Dr. Johan De Keyser (BISA)
  Dr. Michel Kruglanski (BISA)
  Dr. Stanimir Stankov (RMI)
  Dr. Steven Dewitte (RMI)
  Dr. Hugo De Backer (RMI)

A promotional movie giving a flavor of the STCE's tasks, interactions and various research programs can be found via the STCE website (in English, and subtitled in French and Dutch).

Figure 2: An international team of researchers and ICT specialists getting ready for a seminar on the operation of the radio antenna in Humain.

Monitoring Space Weather: Solar-Terrestrial Highlights in 2013

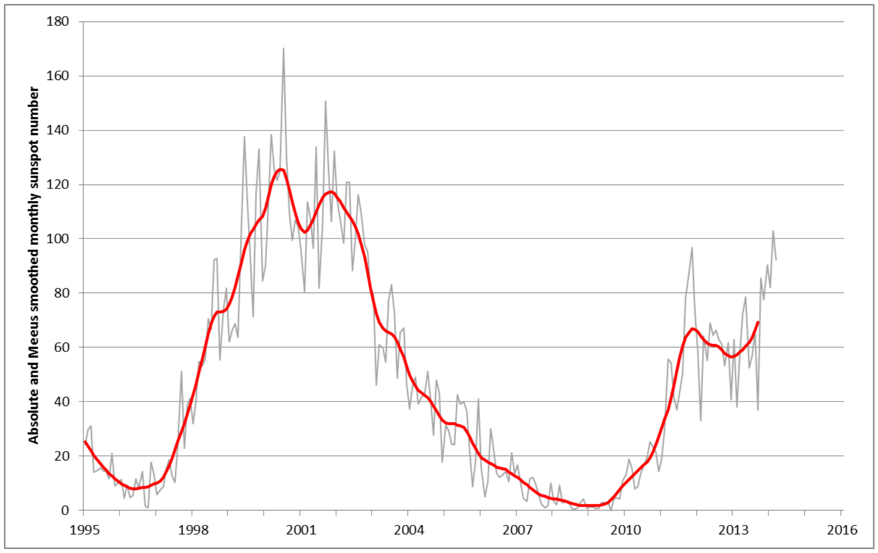

Figure 3: The evolution of the monthly and monthly smoothed SSN (1995-2013). Starting in the second half of 2013, a clear rise to a new and stronger maximum for SC24 can be seen, driven essentially by the increased activity on the southern hemisphere.

The official annual sunspot number (SSN) for 2013, as determined by the WDC-SILSO (World Data Center - Sunspot Index and Long-term Solar Observations), was 64.9. This is a 12% increase compared to the previous year.

The first nine months, long stretches of solar inactivity alternated with brief spurts of high flaring activity levels. Indeed, despite a brief outburst of active groups in April and May, the overall evolution was steady to a gradual decline, with rock-bottom in September when there was almost a spotless day on 10 September and an unusual long period of 10 days without a single solar flare (C-class or stronger). Then, driven by the southern solar hemisphere, sunspot activity quickly picked up with monthly sunspot numbers reaching the highest levels in two years. It is clear that solar cycle 24 (SC24) is heading for a new maximum, stronger than the one late 2011, and that most probably will be reached early 2014.

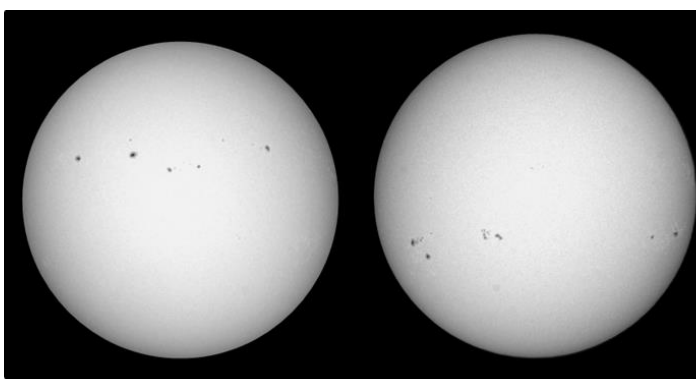

Figure 4: The above pictures were taken using the white light telescope from the Uccle Solar Equatorial Table (USET), on 14 March (left) and 29 October (right) respectively. Over this time-interval, solar activity clearly switched hemispheres.

The year opened immediately with the largest sunspot group that would be visible in 2013, NOAA 1654. According to the NOAA data, it reached its maximum sunspot area on 11 January, when it was more than 6 times as large as the surface of the Earth. Despite its size and its complex outlook, this sunspot group produced only 2 medium flares during its solar transit (on 11 January). The reason for this relatively meager flaring activity was that the opposite magnetic fields were nicely separated from each other, thus preventing the reconnections necessary to produce strong flares.

Most months of 2013 featured several filament and prominence eruptions, and on the average nearly half a dozen of coronal mass ejections (CMEs) every day. In particular the eruptions near the solar limb were truly spectacular. On several occasions they were featured in the STCE Newsletter (e.g. on 7 March, 31 July and 3 October). A few of the highlights are displayed in Figure 5. Note that due to their position close to the solar limb, Earth was hardly or not impacted at all.

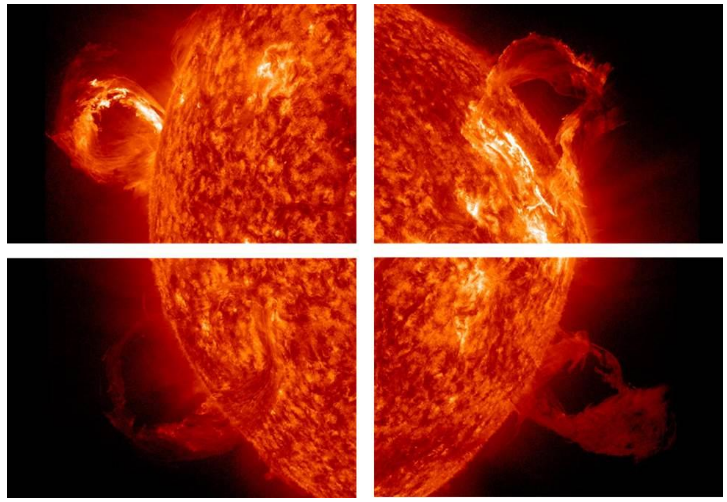

Figure 5: Some of the finest filament and prominence eruptions in 2013. Top left: 1 May, top right: 16 March, bottom left: 31 January, and bottom right: 27 February.

The first spurt of high flaring activity occurred near mid-May, when in a time-span of only 48 hours NOAA 1748 managed to produce 4 X-class solar flares. This sunspot region was relatively small (4-5 times smaller than the aforementioned NOAA 1654), but was magnetically very complex. The first X-flare occurred when NOAA 1748 was still behind the east limb, and the 2 subsequent X-class events were actually white light flares (WLF) as seen by SDO's telescopes in visible light. During the last flare early on 15 May, NOAA 1748 had already rotated far enough onto the solar disk such that the associated CME became geo-effective on 18 May, sparking a minor geomagnetic storm.

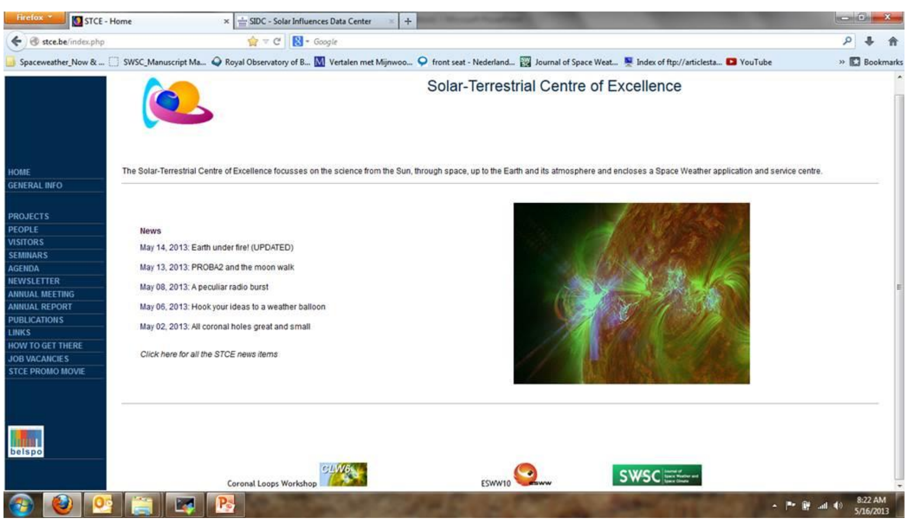

*Figure 6: The X-class flares from NOAA 1748 were prominently featured and updated in near real-time on the STCE website (**14-15 May 2013** and **21 May 2013** , as well as in the **STCE Newsletter**).*

One week later, on 22 May, an M5 flare took place in NOAA 1745 which was associated to the strongest proton event in 2013 (see STCE News item of 29 May 2013). These protons can be seen as numerous white dots and stripes on the imagery from SOHO's coronagraphs. The event was 4 times less intense than the strongest proton event so far this solar cycle (March 2012).

The year 2013 saw the transit of numerous, large and persistent coronal holes (CH) over the solar disk. One of the more impressive ones was visible in mid-July. This CH had an area equivalent to more than

300 times the surface area of the Earth (see STCE News item of 25 July 2013). It managed to survive 8 solar rotations, with the first central meridian passage around 23 May, and the last one on 30 November (8 transits). It sparked geomagnetically active to minor storm conditions during the first 5 transits. The high-speed stream (700 km/s) also brought a whole bunch of high-energy electrons with it, and satellite operators noted a significant increase in anomalies during these periods, thought to be due to repeated electrostatic discharges. Fortunately, none of the spacecraft was permanently damaged. During its October and November transits, the CH had become too small to have a significant space weather impact (see STCE News item of 23 October 2013).

Figure 7: The national Sun observing day (7 July) in Belgium enjoyed sunny weather and the presence of a fine sunspot group (NOAA 1785). No wonder that the public observatories and local solar observing posts got a lot of visitors and media attention!

Late on 29 September, a long and solid filament in the Sun's northwest quadrant erupted in a spectacular way. The modest C1-flare (a so-called "Hyder" or "spotless" flare) lasted for more than 3 hours, and was also a moderate proton event. This long duration event (LDE) was accompanied by a CME shaped like a whip, and it definitely stirred the geomagnetic field. Indeed, this CME delivered a glancing blow to the Earth on 2 October, resulting in a strong geomagnetic storm (locally attaining even severe levels). Together with the storms of 17 March and 1 June, it belonged to the strongest geomagnetic disturbances of 2013 (see STCE News item of 3 October 2013).

A trio of complex sunspot groups significantly beefed up the flaring activity during the last week of October. From 22 till 29 October, no less than 26 M- and 4 X-class flares took place over the solar surface, making it one of the most flare intense periods so far this solar cycle. Responsible active regions NOAA 1875, 1877 and 1882 also destroyed a million km long solar filament in the process, and NOAA 1875

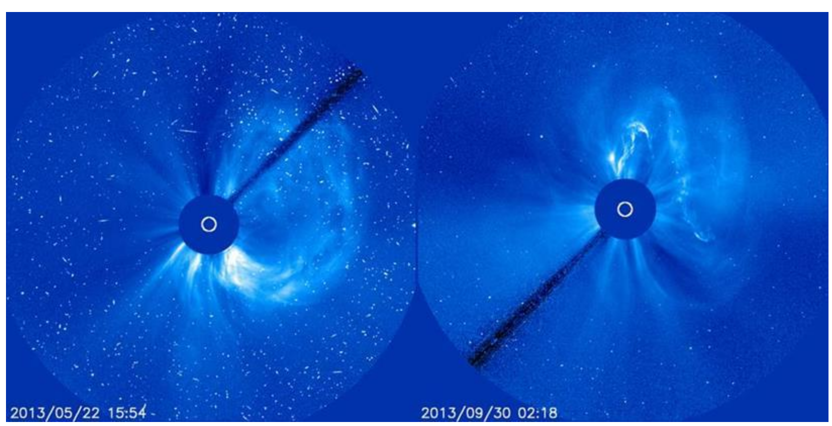

Figure 8: On the left the CME associated to the proton event on 22 May, and on the right the whip-like shaped CME associated to the filament eruption of 29 September.

would stay very active during its subsequent backside transit of the Sun, as nicely recorded by the two STEREO-spacecraft.

On 5 November, NOAA 1890 produced an X3.3 flare, the strongest of the year and the number 3 -so far- in solar cycle 24. NOAA 1890 was a big sunspot group with a magnetically complex trailing part, and would produce another 2 X-class solar flares during its passage over the solar disk. All three were impulsive flares lasting 10 minutes or less, but they were each associated to a non-Earth directed CME. In total, there were 12 X-class flares in 2013, almost as many as 2011 and 2012 combined, and bringing the total for SC24 on 27. Yet, only 5 sunspot regions were responsible for these extreme explosions on the Sun. Meanwhile, the magnetic field near the northern solar pole (finally) completed its reversal, whereas this magnetic flip is still ongoing at the southern pole. These reversals testify we're close to the maximum of SC24. It remains to be seen how many ups and down this moderate solar cycle will show.

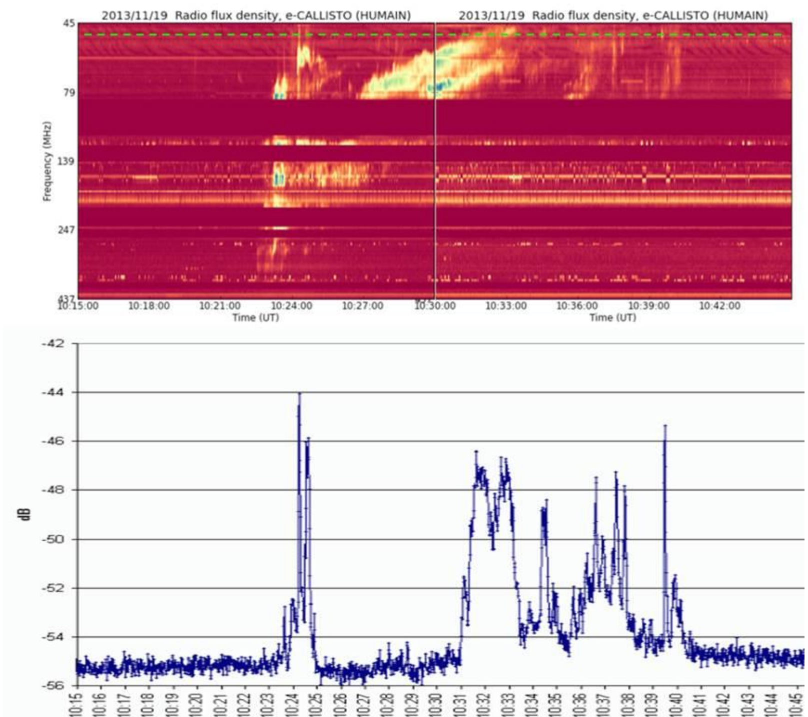

Figure 9: Radio observers from the BRAMS-network observed the X-class flare from NOAA 1893 at their frequency of 49.99 MHz on 19 November 2013 (bottom, and green dashed line on radio-spectrogram on top). The radio-spectrogram made by the Humain Solar Radio Observatory shows the full extent of the strong radio disturbance.

CLW6 and ESWW10: Two successful international conferences

During the course of the last few years, the STCE's Local Organizing Committee (LOC) has gained quite a reputation when it comes to efficiently organizing international conferences. In 2013, two such events were successfully handled by just a handful of people: the sixth Coronal Loops Workshop (CLW6) and the tenth European Space Weather Week (ESWW10).

The 6th Coronal Loops Workshop

The sixth Coronal Loops Workshop (CLW6) took place in La Roche-en-Ardenne (Belgium) from 25 till 27 June. Organized by the Solar-Terrestrial Centre of Excellence (STCE), it gathered more than 60 scientists from all over the world discussing the latest in coronal loops research. Understanding the fine-structure and evolution of these loops is of fundamental importance in our knowledge on solar eruptions and on the million degree hot corona, thus providing key elements on space weather itself.

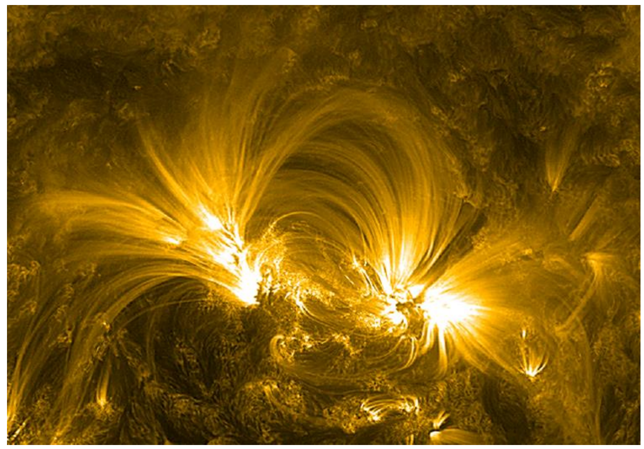

Figure 10: In the above SDO/AIA 171 image, fine coronal loops can be seen over an active region.

The 36 oral presentations and 33 posters focused on the 4 main topics of the workshop. These concerned the temporal and spatial resolution of the images and data, the energy release in the corona, insights in the way the different layers of the solar atmosphere are coupled, and the tools that are required to observe the various features and their key characteristics. Despite the different points of views, the discussions were courteous, constructive and inspiring. No wonder that in some cases the Q&A-session lasted longer than the presentation itself!

Figure 11: The 36 presentations were well attended and discussed by 60+ international scientists.

Another interesting aspect was that data and imagery of many solar observing satellites were used. So, aside the obvious SDO, SOHO and STEREO, satellites such as Hinode, Coronas-F and RHESSI were regularly mentioned too. Quite a few talks featured also the latest results from the High-Resolution Coronal Imager (Hi-C). This EUV-telescope was launched on 11 July 2012 aboard a NASA sounding rocket and gathered only for about 5 minutes worth of imagery.

However, its resolution was 5 times better than the current SDO-images, and the results obtained so far excite the entire coronal loops research community.

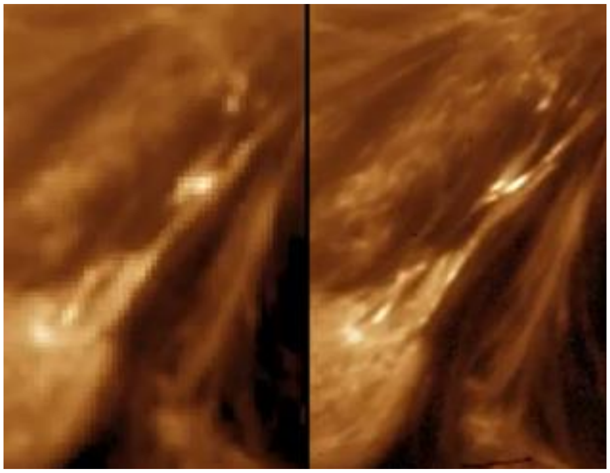

Figure 12: Hi-C's resolution is five times better compared to SDO's.

The participants also cheered the successful launch of IRIS (Interface Region Imaging Spectrograph). This satellite will study the interface region of the solar atmosphere and will hopefully shed more light on how the Sun manages in just a few kilometers to increase the temperature of her atmosphere by a factor of 100. The mission should last 2 years, and will probably give the researchers a lot to talk about during CLW7. This workshop would be due in 2015, and the venue is expected to be somewhere warmer and drier than the scenic but rainy La Roche-en-Ardenne.

The 10th European Space Weather Week

390 scientists, satellite and network operators from 36 countries worldwide gathered in Antwerp from 18 till 22 November to discuss the theme Space Weather during the tenth edition of the European Space Weather Week (ESWW). During this international congress, they addressed the question how vulnerable and at the same time how resilient the society is during severe space weather. Research into the causes of solar storms, the strategic organization of the data charts of the Sun, space, the Earth and its environment, as well as the continuous space weather monitoring should help them in finding an appropriate answer on the threat and impact of space weather.

Figure 13: The logo of the ESWW10.

This edition of the ESWW highlighted the space weather milestones reached in the past decennia and supported the outline for a future space weather strategy. Three medals were awarded during a formal ceremony for outstanding achievements in the field of space weather. The advanced course “Space Weather for Engineers” (SW4E), given just prior to the ESWW, aimed to make all involved in space weather and in particular engineers aware of the solar or spatial origin of disturbances and disruptions that are witnessed in ground based and spatial technological systems.

The Wall of Peace in front of the imposing railway station of Antwerp displayed the definition of space weather in more than 25 languages to emphasize that science is a universal language passing cultural and country borders. Space weather is universal and as such, Europe set up scientific initiatives to understand, cope and anticipate on space weather impacting our society, visualized in a time line going all the way back to 1859, the year of the famous Carrington event.

ESWW offers and continues to offer a full swing space weather recipe to learn, discuss and plan.

Figure 14: During the 10th edition of the ESWW, several special activities were offered to the participants such as the tutorial, a live and online wise scientist quiz, the time line, the wall of peace, an online classroom. New this year was that at the beginning of the fair, all stand-holders could orally introduce ("sell") their product with a 1-minute presentation.

Public Outreach

The Space Pole opens its doors!

In the context of the 100th anniversary of the Royal Meteorological Institute (RMI), an Open Door was organized on the premises of the Space Pole. This open door took place during the weekend of 25-26 May 2013, and attracted over 7000 visitors. The spotlight was certainly on the RMI which got the centroid of activities (movie). The STCE participation was intense with various events in the solar-terrestrial domain.

Figure 15: After a brief introduction on Sun and space weather in the SIDC corridor, the visitors got a guided tour of the telescopes in the solar dome.

One of the highlights was certainly a visit to the ***Solar Dome***. A small introductory presentation was first given in the corridor of the SIDC. Skilled observers and space weather forecasters explained in laymen terminology what sunspots are, how they are observed, why these observations are so important, and how solar eruptions affect us and our technology. Then, the small groups of 10-15 people were guided via more than 40 stairs towards the top of the solar dome. There, the various solar telescopes were shown and their specific applications discussed. Weather permitting, the visitors could also make solar observations using a projected solar image from the white light solar telescope. During and after the visit, there was plenty of opportunity to ask questions to the guides.

A much appreciated activity was the series of presentations that were given in the ***STCE-tent***. The presentations were short (15-20 minutes), and followed by 5-10 minutes for questions from the audience. Then there were 5 minutes to get the tent ready for the next group. The topics were various and included, aside the presentations on solar activity and space weather, also earthquakes, gravitational constant, astrophotography, the planet Mercury, atomic clocks, living on Mars, and research from Antarctica. A total of 26 (!) presentations were given, and they became the best-rated activity of the Open Door.

Figure 16: A dozen of short presentations on various topics were given each day in the STCE tent.

Figure 17: A view on the activities in the Kids' tent.

In the ***kids-tent***, the STCE teamed up with the Planetarium to present activities which were most suited for families with children. Aside a series of fun and didactic activities, also a small introduction on space weather and polar light was given, tailored to children's level of course, and there was also a color corner having as main theme "The Sun". The teenagers could test their knowledge on space weather at the quiz table. This quiz, consisting of about 20 multiple choice questions, could also be accessed online with a QR-code.

In the SSCC-room, the newly inaugurated European space weather coordination centre (***SSCC***) was co-located with the Proba2 Science Centre (***P2SC***). Visitors got an overview of the tasks of the SSCC and how these were realized (see pp. 41). People from the P2SC explained how they operate the PROBA2 satellite, which was in part constructed by scientists from the STCE. It was the place-to-be for gadgets and posters on this fine solar satellite, and the full-scale model of PROBA2 impressed many visitors.

The STCE ***Planeterrella***, based on a concept by Jean Lilensten (IPAG/CNRS), got completed just in time for the Open Door. This is an experiment which helps in understanding the mechanism of the polar lights. It consists of an electron gun and a conductive sphere placed in a vacuum chamber. The main advantage of the STCE Planeterrella is that it can be used for both scientific and educational purposes. The planeterrella was built by technicians from BISA with financial support from the STCE and was on display during the Open Door, the STCE Annual meeting and other visits. As it required a dark room to fully appreciate the subtle plasma hues, the planeterrella was placed in the cellar of the BISA.

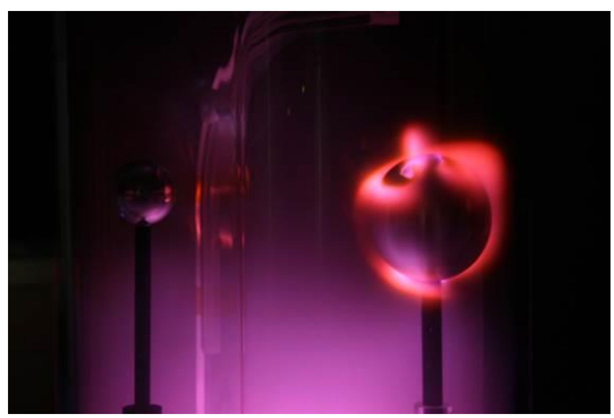

Figure 18: The planeterrella in action!

The Open Door would not have been possible without the enthusiastic support of the entire Space Pole community. Scientists, IT-personnel, logisticians, general support,… all contributed significantly to the successful organization of this major event. An “encore” performance will be required, as in the framework of the 50th anniversary of the BISA, another open door will be organized in October 2014.

Figure 19: The Open Door in full swing!

The STCE Annual Meeting

Since 2008, the STCE organizes an annual meeting for its members. This event consists of a morning session with easy-going lectures and discussions on solar-terrestrial topics, followed by a lunch that lasts well into the afternoon. The practicalities are taken care of by the same people who organize the space weather week and other conferences, spearheaded by their mastermind Petra Vanlommel.

Figure 20: The Meridian room at the ROB was well filled for the STCE Annual Meeting.

The 6th STCE annual meeting took place on 7 June 2013 in the ROB’s Meridian room. About 60 people were welcomed by Ronald Van der Linden, the STCE’s general coordinator, and Martine De Mazière, the Director General of BISA. Michel Kruglanski then gave a short talk on the SSCC, the first European SSA Space weather Coordination Centre. This centre was officially inaugurated just 2 months before (3 April), and had gathered a lot of media attention.

The summary reports from the workshops constitute the main body of the annual meeting. These workshops are organized by scientists in their respective field of research prior to the annual meeting. They sometimes last longer than 1 day, and usually have attendees and speakers from universities and institutions outside the Space Pole and Belgium. Hence, these meetings are valuable gatherings for the interested to get the latest in their area of expertise. As these are technical meetings, a non-specialist is assigned to assist to each of these workshops, in order to get a short and easy-to-understand summary at the annual meeting.

Figure 21: The beautiful RMI meeting room hosted the workshop on the automatic detection of events in radio data on 31 May.

In advance of the 2013 annual meeting, 6 (six!) workshops were organized:

- Solar EUV Irradiance Working Group: Inter-calibration and degradation of EUV instruments (15-18 April 2013), organized by Marie Dominique, and presented by Steven De Witte

- Automatic detection of events in radio data (31 May 2013), organized by Hervé Lamy and Christophe Marqué, and presented by David Berghmans

- Water Vapor, Meteorology and Climate (26 November 2012), organized by Eric Pottiaux, and presented by Roeland Van Malderen

- Alfven Waves and Turbulence in Solar and Space Plasmas (30 May 2013), organized by Yuriy Voitenko and Andrei Zhukov, and presented by Jesse Andries

- EPN Local Analysis Centres Workshop (15-16 May 2013), organized and presented by Carine Bruyninx

- Ionosphere: monitoring, research, services (14 May 2013), organized by Stan Stankov and Nicolas Bergeot, and presented by Stan Stankov

Figure 22: The space weather briefing during the pause was well appreciated by the audience.

The program scheduled a short coffee break after the first two workshop reports. During this pause, participants could watch the space weather briefing live on the big screen. This was a last minute idea that was quickly and efficiently organized by Marc De Knijf and David Berghmans, and presented from the SSCC-room by the space weather forecaster on duty Jasmina Magdalenic. This intermezzo was very well appreciated by the audience.

During lunch, the participants had the opportunity to visit the recently finished Planeterrella. This is an aurora simulator which main purposes are both educational (public outreach) and scientific (e.g. study of polarization of auroral light,…). Eddy Equeter and Johan De Keyser provided the enthusiastic crowd with a word of explanation near BISA's Green room.

By the end of the year, actions were already taken to start up the series of workshops for next year's annual meeting.

Fundamental Research

The SIDC-SILSO Sunspot Number: an end-to-end revision

A key service activity of the SIDC is the production of the sunspot number, which is the unique reference for the long-term solar activity over multiple centuries. As such, it is used worldwide in a wide range of scientific applications, from solar cycle modeling and predictions to climate change studies. Recent advances in those fields as well as the anomalous and unexpected evolution from solar cycle 23 to the current cycle 24 have brought a strong motivation to revisit and improve this unique time series that is maintained at the ROB since 1981, when the World Data Center for the International Sunspot Number was transferred from Zürich to Brussels. In this context, since 2011, the software and databases of the World Data Center (SILSO) have been intensively revised, expanded and improved. This process involved a stringent control of the consistency of the new calculation with the official sunspot number still produced by the heritage FORTRAN programs. 2013 marked a new step in this process: the production of the official sunspot index was moved to a new server running the new validated software.

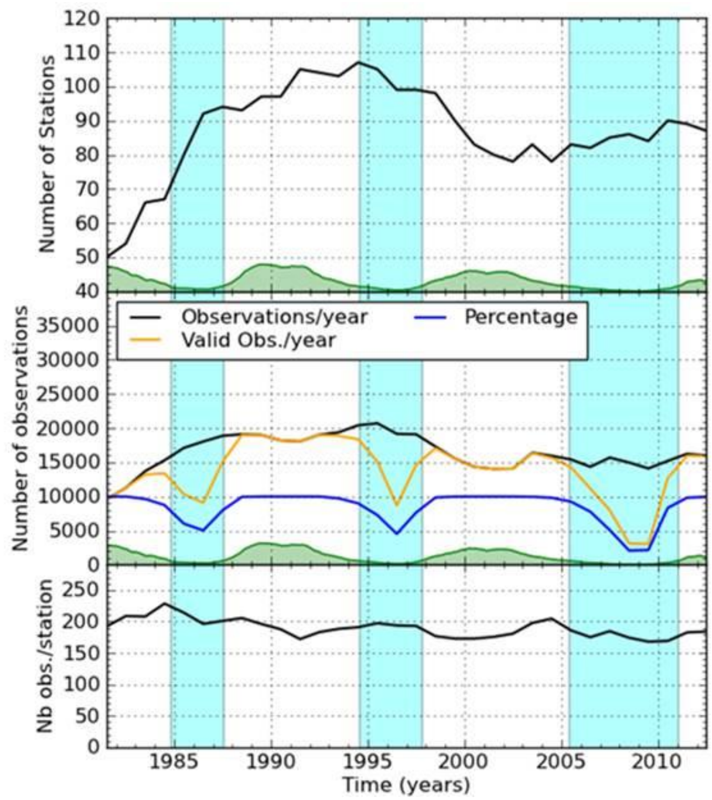

Figure 23: Evolution of the worldwide sunspot network: number of contributing stations (top panel), annual number of collected observations (middle panel) and average number of observations per station per year (lower panel). The solar cycles (shaded green) and minima intervals (shaded blue) are overlaid as time reference. In the middle panels, valid observations are days when both a given station and the reference pilot station give a non-zero Wolf number (i.e. when a personal k coefficient can be established).

This transition also opened entirely new possibilities, in particular for the implementation of a global quality control of the basic data collected by the worldwide SILSO network (currently 80 active stations). Indeed, all individual raw observations collected since 1981 (i.e. 34 years) are fully preserved and now accessible through a MySQL database, which now contains more than 540.000 observations from 269 stations in 39 different countries. Figure 23 retraces the evolution of the yearly contributions from the network. Based on such an extensive data set, it is possible to build global statistics in order to check the stability of reported sunspot numbers from each station over the last 3 solar cycles. In particular, we first investigated the stability of the pilot station of the network, namely the Specola Solare Ticinese Observatory (Locarno, Switzerland). This station played a key role to ensure the continuity with the past series built by the Zürich Observatory for all years before 1981, back to the 17th century.

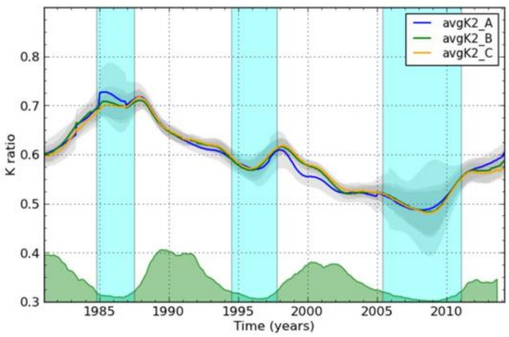

Figure 24: Plot of three different multi-station average k ratios. Three subsets of stations have been chosen, starting with the most reliable and long-duration stations (set A; 9 stations, in blue) and then adding more stations of shorter duration and lower stability (set B, 37 stations, in green; set C: 79 stations in orange). The gray shading gives the standard error of the average k ratio, which increases at cycle minima (blue shading). Although all three sets are very different, all curves display the same drifts and reversals, including local features.

Our study actually revealed a rather large and variable drift in the scale of the Locarno numbers that caused a corresponding bias in the scale of the sunspot number published over the past decades. This drift was established by computing the scale ratio k, also called the "personal coefficient", of each station of the network relative to the pilot station. By averaging over many stations and comparing between different network subsets, we derived an accurate mean ratio as a function of time as shown in Figure 24. The diagnosed variations reached up to 20% with steady trends reversing around 1987 and 2008. This first result illustrates the potential of the new software and its associated huge data collection. The network-wide mean ratio determined in 2013 can now be used as a correction to restore a uniform absolute scale for the past sunspot number, bringing the first major recalibration of this reference time series since its creation.

Moreover, the corrected series already addresses recent solar issues, like the unprecedented deviation between various parallel indices of solar activity since 2000. Figure 25 shows the relation between the sunspot number and the $F_{10.7cm}$ radio flux, before and after applying the above correction. While the corrected sunspot number definitely provides a better overall match with the $F_{10.7}$ proxy before 2000, a significant deviation still persists after 2003. This disagreement is confirmed by other index comparisons and thus points at an actual change in the source of solar magnetic activity. Therefore, new investigations will be required in coming months and years and our improved sunspot number series will definitely help researchers to get a cleaner picture of actual changes now happening on the Sun, in what seems to be the weakest solar cycle of the last

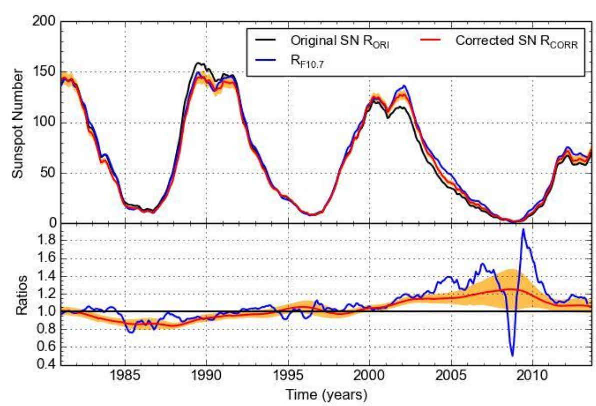

Figure 25: Comparison of the original sunspot number series (R_{ori}, black, upper panel) with the new corrected series (R_{corr}, red) and the $F_{10.7}$-based proxy (blue) over the last 3 solar cycles. Lower panel: the ratios R_{corr}/R_{ori} (red) and $F_{10.7}/R_{ori}$ (blue), with the standard error in the corrected sunspot number (orange shading). They show a better agreement between $F_{10.7}$ and the sunspot number after the correction, but still with a significant though reduced divergence after 2002.

100 years. Our work continues and additional improvements spanning the full 400-years of the sunspot record will follow in 2014.

PROBA2: 4 years in orbit

PROBA2 is the second satellite in the European Space Agency's series of PRoject for OnBoard Autonomy (PROBA) missions. In 2013, PROBA2 reached the milestone of 4 years in orbit, which oversaw the period of solar maximum. It also produced its 750.000th image of the Sun and over 1500 GB of data. 2013 also saw the release of the PROBA2 topical issue (see Figure 26).

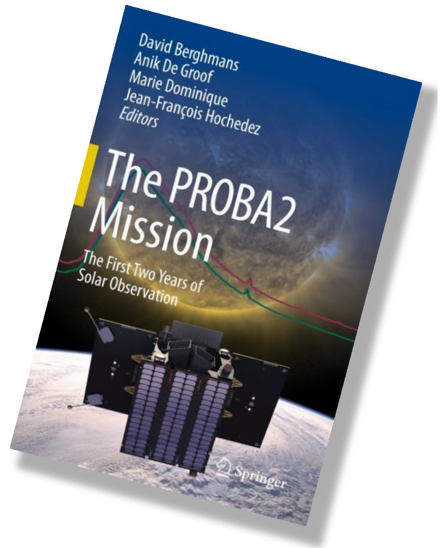

Figure 26: The PROBA2 special edition, containing several articles based around the PROBA2 mission, its observations and several research topics.

The PROBA2 topical issue covers four broad sections, containing a collection of previously published articles in book form. These cover several aspects of the engineering and calibration involved in the satellite platform and the instruments on board. The book also covers several research highlights in different areas of research, some of which are discussed below.

Jets and outflows on the Sun come in various forms, they often originate lower down in the Sun's atmosphere (the corona) before flowing out into the interplanetary medium.

Chandrashekhar and colleagues used PROBA2/SWAP data together with Solar Dynamics Observatory (SDO) observations to show that "bright points" observed on the Sun in the Extreme UltraViolet (EUV) wavelength range (observations around 500.000 degrees) are associated with the emergence of new magnetic flux from below. This suggests that the emerging flux interacts with existing magnetic fields in the Sun's atmosphere, whereby energy is released in a process known as "magnetic reconnection". This release of energy creates the bright points seen on the Sun.

The members from Filippov's team also used SWAP and SDO data to look at magnetic configurations on the Sun. However, they used SWAP's extremely large field of view to look for the connectivity of coronal structures with outer coronal (the outer solar atmosphere) features that were imaged with the Large Angle Spectrometric Coronagraph (LASCO) on the Solar and Heliospheric Observatory (SOHO). A coronagraph is a type of telescope that blocks the bright solar disk in order to see the comparatively less bright surrounding solar atmosphere. The data-sets revealed an Eiffel-tower shaped jet configuration extending into a narrow jet in the outer corona. An example image of the structure can be seen in Figure 27. The configuration provides a possibility for the plasma to escape along the open field lines into the outer corona, forming the white-light jet.

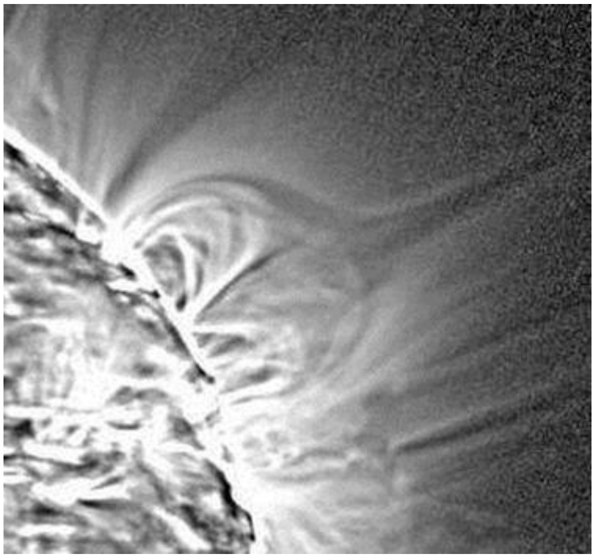

Figure 27: A filtered SWAP image showing a hyperbolic cavity forming to a large distance from the solar limb. The extended white-light jet is the long outward extension of the 'Eiffel-tower' structure.

A ***flare*** is a sudden brightening observed over the Sun's surface. The brightening is a signature of a large energy release on the Sun, and is often associated with the ejection of hot plasma. ***Eruptions*** on the Sun don't necessarily have to be associated with a flare, but they often occur together. In the PROBA2 special edition, Bonte and her team discuss new techniques to automatically detect solar flares with the PROBA2/SWAP imager, where they introduce the 'Solar Flare Automated Search Tool' (SoFAST), which will also be implemented on future solar missions.

Kretzschmar and his colleagues made use of the unique capabilities of the PROBA2/LYRA instrument to observe flares in a wavelength known as 'Lyman alpha', which is the strongest line of the solar spectrum. They observed several flares, and studied one in detail, which was a powerful 'M2' flare that occurred on 8 February 2010. For this flare, the flux in the LYRA Lyman-alpha channel increased by 0.6 %, which represents about twice the energy radiated and observed in X-ray channels. However, it was found that the Lyman-alpha emission represents only a minor part of the total radiated energy of this flare.

A phenomenon often associated with solar flares is a EUV wave. These are huge waves that flow through the solar atmosphere, having an appearance like a ripple on the surface of water when a stone is dropped into it. Kienreich and collaborators used PROBA2/SWAP images together with observations from the Solar TErrestrial RElations Observatory-A (STEREO-A) satellite to observe EUV waves on the Sun from different angles. In total, they recorded three such waves and observed them reflecting off different structures in the solar atmosphere.

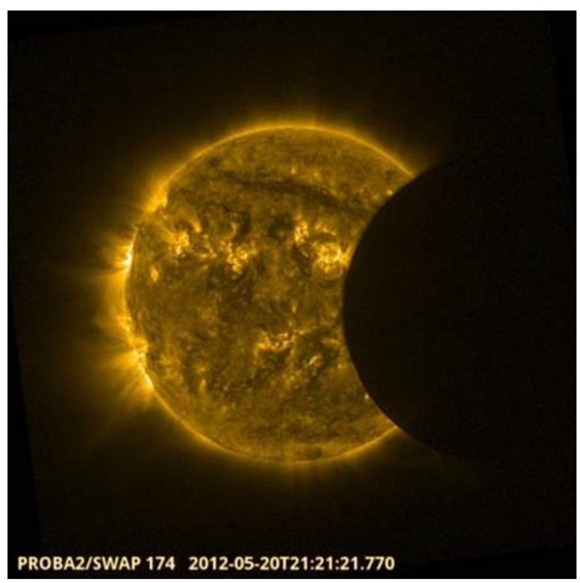

Figure 28: A SWAP image of a solar eclipse.

Solar prominences are large loop like structures observed on the Sun, extending thousands of kilometers outwards into the solar corona. Prominences can become unstable and erupt in an event known as a "prominence eruption". Mierla and her team made 3D reconstructions of such an event using PROBA2/SWAP and STEREO data showing its acceleration increased smoothly with height and concluded that the prominence is not accelerated immediately by local magnetic reconnection (energy releases) but rather is swept away as part of a large-scale relaxation of the coronal magnetic field.

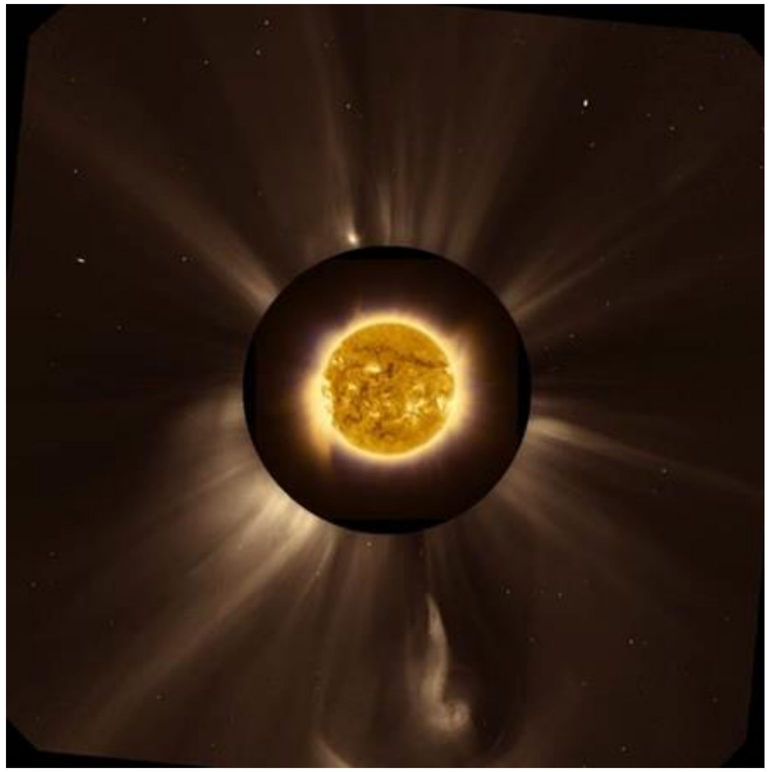

Figure 29: NASA picture of the day. An active Sun during a total eclipse. Image credit & copyright: D. Seaton (ROB), A. Davis & J. M. Pasachoff (Williams College Eclipse Expedition), NRL, ESA, NASA, NatGeo

The last section of the PROBA2 special edition focused on ***irradiance and spectral analyses***. Such studies focus on power per unit area produced by the Sun in the form of electromagnetic radiation and are important in understanding the total energy output of the Sun and how this might impact upon the Earth. Shapiro and colleagues used solar eclipse observations using PROBA2/LYRA to measure solar centre to solar limb variations in solar brightness. An image of a solar eclipse seen by PROBA2/SWAP is shown in Figure 28. In a separate paper they also used PROBA2/LYRA to analyze the variability of the spectral solar irradiance over a period from 7 till 20 January 2010, and developed an algorithm to extract solar variability from the LYRA data. Finally, a team led by Bazin used eclipse data to study prominence cavity regions using PROBA2/SWAP imagery and simultaneous ground based eclipse flash spectra observations from the 11 July 2010 eclipse.

In a separate article, PROBA2/SWAP images were once again used with ground based eclipse observations, but this time it made the NASA Astronomy Picture of the Day (APOD), see Figure 29. In this composite image we see the Sun in several wavelengths, using several different observatories. The central image of the Sun is imaged using SWAP, showing the Sun in the EUV wavelength range. This is surrounded by a ground-based eclipse image, reproduced in blue, taken from Gabon. Outside this we see the outer solar atmosphere, taken by the LASCO instrument aboard the Sun-orbiting SOHO spacecraft.

Sensing the ionosphere from above

The vertical incidence sounding of the ionosphere from the ground remains one of the most accurate and important ionosphere-monitoring techniques. In this technique, low- and high-frequency radio waves are transmitted upward and reflected in the ionosphere at the height where the refractive index becomes zero for vertical incidence.

The standard piece of equipment employed for the purpose is called "ionospheric sounder" (ionosonde), in which a transmitter and a receiver are swept synchronously in frequency, and the propagation time t_g (or the corresponding virtual height $h' = c \cdot t_g / 2$, with c the speed of light) of the reflected signal recorded for each of the transmitted frequencies. Thus, the resulting ionogram is an instantaneous record of the ionospheric conditions (above the location of the sounder) indicated by the relationship between the frequency of the radio pulse emitted upwards and the virtual heights of echoes reflected from the ionosphere (Figure 30). In a typical ionogram, the frequency range covers the interval 1-20 MHz and the height range covers 0-1000 km.

The original sounding method has been improved substantially during the years. For example, digitization was introduced. Also, with precise timing available, the transmitter and the receiver can be separated and thus sounding can be performed over oblique paths. Strength and direction of the echo can now be measured. Furthermore, automated scaling of ionograms was developed, broadening the digital ionosonde applications and immensely helping the user and the ionospheric/space weather research and services in general.

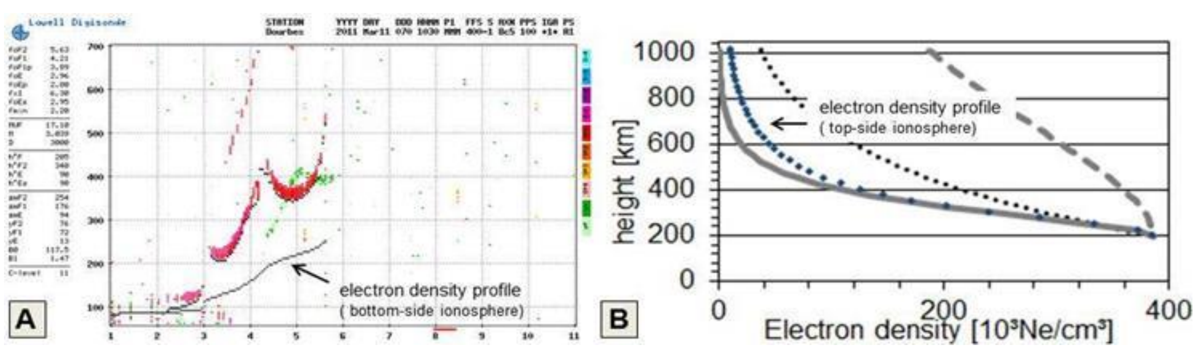

Figure 30: Ionospheric electron density profiles (EDP) deduced from ionospheric sounders. Left: ground-based sounding of the bottom side ionosphere, an ionogram and the corresponding electron density profile. Right: space-based (topside) sounding, the measured topside electron density profile (blue diamonds) together with analytical model fits (Exponential – dotted line, α-Chapman - solid line).

However, the ionospheric sounders installed on the ground are capable of providing information on the bottom of the ionosphere only, up to the height of the ionospheric peak electron density. Consequently, topside sounders were developed and placed onboard satellites, thus allowing for probing the ionosphere from above. There is currently a renewed interest in topside sounder measurements. Developments are currently under way in USA (Figure 31) and Poland to place advanced digital sounders (similar to the one operated here in Belgium) onboard several satellites which will allow regular high-quality measurements of the topside ionospheric plasma density on a global scale, something that is not possible to be done with the ionosondes on the ground. The project would further improve our understanding of the ionospheric dynamics and the ionosphere-plasmasphere coupling. Moreover, the intention is to provide these measurements in real time which, coupled with the ever-expanding ground network of sounders, would allow for the development of reliable ionospheric nowcast and forecast services that are needed by the scientists, radio communications engineers, GNSS service providers, and the space weather community as a whole.

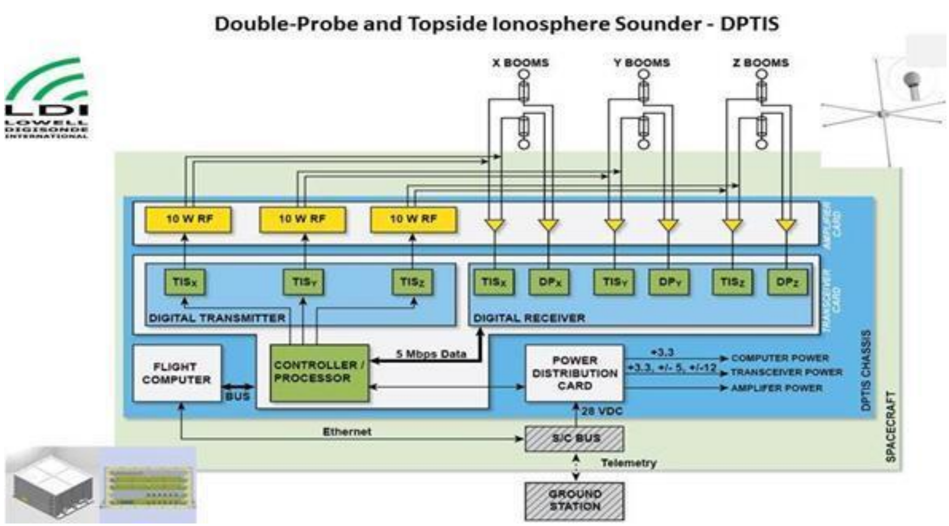

Figure 31: Concept for the Double-Probe and Topside Ionosphere Sounder (DPTIS). Courtesy / Copyright: B. Reinisch, Lowell Digisonde International.

In preparation for these new developments, we have revisited the older topside sounder datasets collected during the missions of the Canadian Alouette and the Japanese ISIS. The objective was to evaluate the analytical ionospheric models that have been used for the topside profiles in our operational system LIEDR.

LIEDR (Local Ionospheric Electron Density profile Reconstruction) has been developed and installed at the RMI Geophysical Center in Dourbes. At a given location, the entire vertical electron density profile (EDP) is deduced from local ground-based measurements of the total electron content (TEC), ionospheric vertical incidence soundings, and empirically-obtained values of the upper ion transition height/level (UTL). The retrieval of the corresponding vertical electron density distribution is performed in two main stages: construction of the bottom electron profile (below the ionospheric F_2-layer peak density height, h_mF_2) and construction of the topside profiles (above h_mF_2). The topside profile is allowed to take one of several forms: Exponential, α-Chapman, β-Chapman, or Epstein. The system acquires and promptly processes the incoming measurements, computes the full-height ionospheric electron density profile, and displays the resulting profilograms.

The Alouette and ISIS satellites flew from 1962 until 1995 and carried, among other instruments, ionosondes used to take soundings of the topside ionosphere. Part of the data obtained from these soundings has been converted to a digital format. The accumulated topside sounder database proved to be a valuable source of information when investigating the composition and complex dynamics of the upper ionosphere over several solar cycles. However, special attention had to be paid to proper data screening and pre-processing of the database. It has been established that, in order to adequately model the topside ionospheric plasma distribution with the help of these profilers, it is necessary to use different scale heights for the different profile shapes in use.

Evaluation of the above-mentioned forms of top-side profilers is needed in order to find out which of them provides the best representation of the current ionospheric conditions. Every measured profile has been fitted with each of the theoretical ionospheric profilers and the corresponding approximation errors were calculated. The aim of the current work was to find the appropriate topside profiler for given conditions, rather than a profile that fits best on average.

Since both the solar and magnetic activity are known to heavily influence the ionosphere, it was expected that the indices F10.7, K_p and D_{st} can be used to select an appropriate topside profiler, depending on the solar and magnetic conditions. For low solar activity, defined as F10.7 < 120 sfu, 76% of the profiles have an exponential shape while for high solar activity, F10.7 ≥ 180 sfu, this is only 66%. Thus, while the expected influence of the solar activity can indeed be seen in the available data, the correlation between the shape of the topside profile and the F10.7 index is not sufficient to be used for the selection of an appropriate profiler. There also seems to be a very slight trend towards profiles of non-exponential shapes during disturbed magnetic conditions ($K_p \geq 3$), although this trend, too, is not clear enough to be useful in the prediction of the topside profile shape.

In continuation to our previous work, we tried to further clarify the relation between the peak characteristics and the shape of the topside profile. One very important finding was that the best indication for selection of a profiler comes from the ionospheric density peak characteristics, rather than from “external” parameters such as solar/geomagnetic indices, season, local time, etc. Figure 32 shows the average integrated errors for the four profilers in relation to the F_2 peak density (N_mF_2) and height (h_mF_2). It is clear that both N_mF_2 and h_mF_2 can be used to select an appropriate profiler.

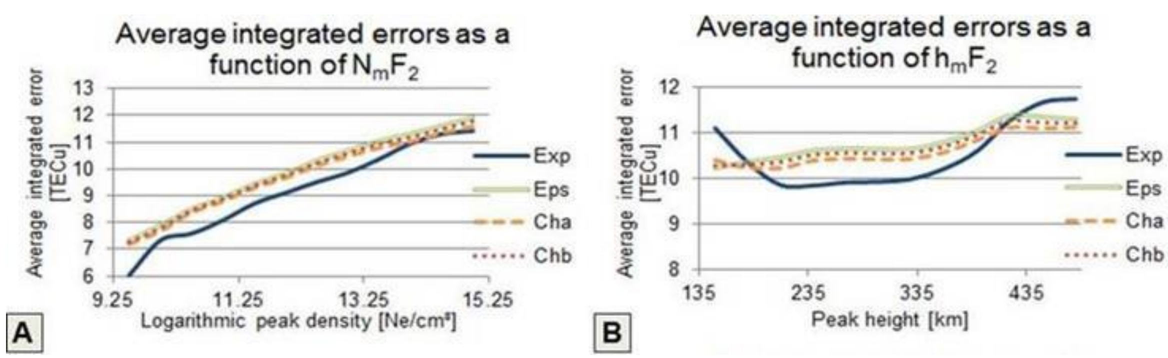

Figure 32: Average integrated error for the best fit obtained using each of the four considered profilers. The error obtained with the Exponential profiler (Exp) is indicated by a solid line, the one obtained using the Epstein curve (Eps) by a double line and the ones obtained using α-Chapman and β-Chapman functions (Cha and Chb) by dashed lines. Panel A: the relation between the average integrated errors and the peak density, N_mF_2. Panel B: the relation with the height of the F_2 peak density, h_mF_2.

For values of h_mF_2 between about 190 km and 400 km the error when using the exponential profiler is an order of magnitude lower than for any of the other three. However, for higher or lower values of the peak height the α-Chapman profiler is much better. In fact, the errors associated with the exponential profiler quickly become an order of magnitude larger than those of all three other profilers. For extremely low values of the peak height the Epstein profiler gives an even better fit than the α-Chapman, but the differences in errors between these two is never very large and there are relatively few profiles with such small h_mF_2, so this seems to be not significant. Regarding the peak density, it is obvious that the average errors become equal for all profiles with high densities.

The analysis shows that in almost 75% of the cases, the best fit is provided by the exponential profiler, and in the rest of the cases the best fit is mainly by the α-Chapman profiler. For real-time applications, such as LIEDR, these are very useful results because the peak characteristics can be measured locally and provided immediately by a ground-based ionosonde.

A new value for the solar constant

In November 2013, we celebrated the 30th anniversary of our first space instrument Solcon on Spacelab-1 for the measurement of the Total Solar Irradiance. The Total Solar Irradiance (TSI) quantifies the amount of energy that the Earth receives from the Sun and is of fundamental importance for the climate on Earth. Since 1983, we have made in total 11 space flights with 6 different instruments for the measurement of TSI. Figure 33 shows the Columbus module on the ISS launched in 2008 carrying our DIARAD/SOVIM instrument.

Figure 33: The Columbus module installed on the ISS.

Since the launch of the American TIM/SORCE instrument in 2003, the absolute value of the TSI, also known as the Solar Constant, is a matter of debate. TIM/SORCE measures a value around 1361 W/m^2 while the older radiometers measured a value around 1366 W/m^2. This led us to a critical examination of our own radiometer data evaluation and we now find a best estimate of the Solar Constant of solar minimum of 1363 +/- 1 W/m^2. In May/June 2013 we conducted a laboratory comparison at the TSI Radiometer Facility (TRF) in Boulder. During this laboratory campaign, we confirmed our value and we identified an underestimation of scattering and diffraction on the TIM side which can explain why they measure a too low value.

Figure 34 shows our TSI composite with the new absolute value which is available in near real-time from our website. This composite is internationally recognized and is used by the NASA's CERES project as input to calculate the EBAF Earth Radiation Budget product, which is widely used by the climate research community.

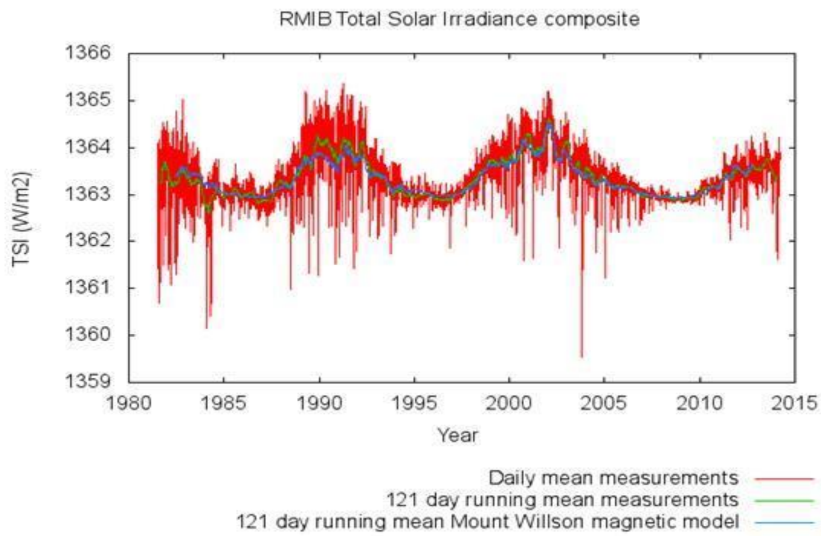

Figure 34: TSI composite as derived by RMIB since the early 1980's.

Figure 35: Verifying the laws of gravity during the Team Building Day…

Instrumentation and experiments

International Ozonesonde Data Quality Assessment

Worldwide, vertical profiles of the ozone concentrations are gathered by means of ozonesondes attached to weather balloons. An ozonesonde consists of two half cells, containing different concentrations of a solution, and of a miniature piston pump taking air into the cathode chamber at a constant rate. During operation, the ozonesonde is put in a Styrofoam isolating box. The ozone molecules present in the ambient air will then interact with the solution in the cells, generating an electric current, which can be related to the amount of ozone molecules in the atmosphere. Hence, the concept is very simple, but different additional corrections are needed, e.g. to account for the decreasing efficiency of the pump with decreasing pressure. Furthermore, every ozonesonde is a unique instrument, but time series of ozonesonde measurements at a given site of several decades have been built up. To be used in climate and trend analysis studies, these time series should be homogeneous.

On the other hand, the homogeneity of the ozonesonde time series all over the world is an important issue, as ozonesonde measurements are frequently used for the validation of both model output and satellite retrievals of ozone. It is true that, not only between those different stations, but also at a given station, different operation procedures, different solutions strengths, different amounts of solutions, different ozonesonde types and different corrections have been used. To this end, several international bodies initiated a working group to assess the ozonesonde data quality (O3SDQA, for Ozonesonde Data Quality Assessment). The main aims of this working group were (i) to come up with standard operating procedures and standard correction methods, (ii) to analyze and estimate the accuracies and uncertainties of the measurements, (iii) to develop transfer functions to convert all measurements to the standards set in (i).

Figure 36: Photograph of the Electrochemical Concentration Cell (ECC) ozonesonde used at the Royal Meteorological Institute

In 2013, this working group, in which we participated, finished their guidelines and assigned “coaches” to support the ozonesonde Principal Investigators in implementing these at their station. In Uccle, which has a long tradition in ozonesonde launches (since 1969), a dataset compliant with these recommendations and corrected with the standard correction algorithms has been created in mid-2013, being one of the first stations. As a matter of fact, at Uccle, the same operating procedure, ECC ozonesonde type, solution strength and amount have always been used, but an alternative, more complex, correction algorithm was developed some years ago. We look forward to investigate the differences between this standardized and in-house corrected datasets and to elaborate on their impact on the calculated trends in ozone.

Solar Orbiter Science Working Team meeting and EUI engineering model

Figure 37: The EUI engineering model displayed at the laboratory at the Centre Spatial de Liège, surrounded by the EUI team. This team consists of scientists and engineers from Belgium (ROB), France, Germany, the UK, and Switzerland.

Solar Orbiter is the next ESA flagship for studying our closest star, the Sun. It is currently scheduled for launch in 2017. By approaching as close as 0.28 AU (astronomical unit; 1 AU is nearly 150 million km), Solar Orbiter will view the Sun with high spatial resolution and combine this with in-situ measurements of the surrounding heliosphere. Thanks to its unique orbit, Solar Orbiter will deliver images and data of the unexplored Sun's polar regions and the side of the Sun not visible from Earth. Scientists expect that this satellite will provide important new insights into our Sun and its influence on the inner Solar System.

Solar physicists at STCE/ROB have a leading role in the EUI (Extreme Ultraviolet Imagers) instrument onboard Solar Orbiter. The instrument concept was conceived at the Solar Physics group of STCE/ROB including the use of some of its key technologies (APS detectors, compression,…). EUI is now being built by an international consortium under the leadership of Pierre Rochus from the Centre Spatial de Liège (CSL). A group of about 10 researchers at STCE/ROB is actively supporting this development. In the operational phase of the mission (post 2017), the EUI instrument will be operated from the EUI Data Center at STCE/ROB.

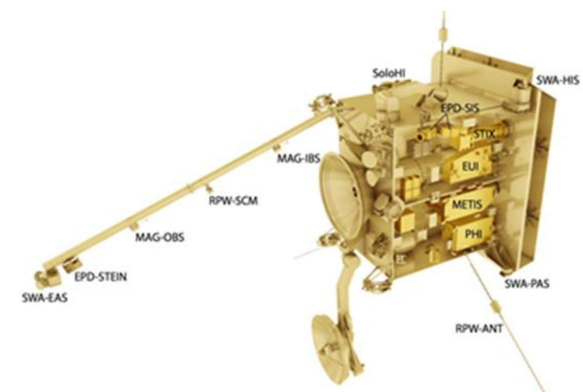

Figure 38: Solar Orbiter and its suite of remote sensing and in-situ instruments. Note in particular the heat shield in the back, the deployable high gain antenna at the bottom and the in-situ boom on the left. Belgium is a leading partner in the international consortium that is building the EUI instrument (EUI = Extreme Ultraviolet Imagers; Principal Investigator (PI): Pierre Rochus, from CSL).

Late November 2013, the engineering model of EUI was completed at CSL. This is an exact copy of EUI without all optical and electrical components (which are state-of-the-art and still being developed). The model will be tested thoroughly for its mechanical, thermal, and thermo-elastic stability to make sure that the instrument can handle the harsh conditions close to the Sun.

In order to prepare the science of Solar Orbiter, the STCE/ROB organized the Solar Orbiter Science Working Team meeting from 24-26 September 2013. Fifty-four scientists gathered there to discuss how science can best profit from the unique opportunities offered by Solar Orbiter, which is a partnership between ESA and NASA. The scientific synergy of Solar Orbiter with Solar Probe Plus and other missions was also highlighted. Progress was made on data analysis and the collaboration between the various instruments in joint science campaigns. To ensure a successful mission, the status and work ahead for the Solar Orbiter spacecraft and the different instruments onboard were followed up.

Figure 39: This photograph was taken during the Solar Orbiter Cleanliness Meeting at ROB on 23 September 2013. This satellite meeting immediately preceded the Solar Orbiter Science Working Team meeting.

Many STCE/ROB scientists participated actively in the talks and discussions. The meeting was chaired by Daniel Mueller (Project Scientist of Solar Orbiter, at ESA) and local organization was taken care of by the well-trained STCE team including Anne Vandersyppe, Jan Janssens, David Berghmans, Sarah Willems, Petra Vanlommel, Bram Bourgoignie, and Olivier Boulvin.

The degradation and inter-calibration of solar instruments

Investigating and analyzing the degradation of space instruments are crucial to achieve their scientific goals. Remote-sensing instrumentation exposed to the space environment usually degrades due to the harsh environment in which the instruments operate. Solar instruments (telescopes, spectrographs and radiometers) are particularly vulnerable because their optical elements are exposed to unshielded solar radiation.

For example, the Large Yield Radiometer (LYRA) onboard PROBA2 has strongly suffered substantial degradation due to a combination of ultraviolet (UV) solar irradiation and instrumental contamination that can cause polymerization of organic material and, subsequently, irreversible deposition of this material on the instruments' optical surfaces (Figure 40).

Different methods and approaches have been used to assess and monitor the evolution of these instruments' degradation (Figures 41 and 42). To reach a better understanding of how to both monitor and study this degradation, the Solar Terrestrial Centre of Excellence (STCE) at the Royal Observatory of Belgium organized a workshop on this subject on 3 May 2012 in Brussels, Belgium. Representatives from several active space-based solar instruments contributed to this workshop.

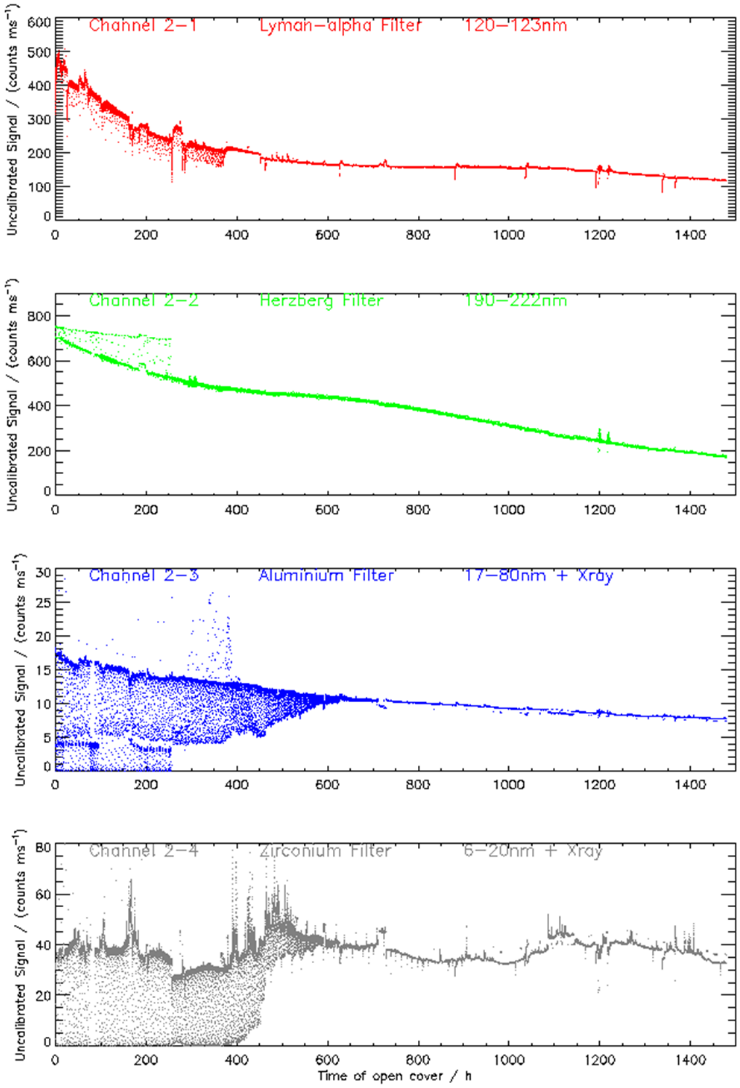

Figure 40: Temporal degradation of the PROBA2/LYRA instrument (unit 2, channel 1 to 4) over the first 1500 hours of operation.

The aim of this workshop was to bring up open discussions related to the degradation observed in Sun-observing instruments exposed to the effects of the space environment. The outcome of this meeting and discussions, together with the written contributions of the different mission teams, resulted in a Solar Physics article (BenMoussa et al., 2013) focusing on the major lessons learned about in-orbit degradation of solar instruments. This article also provided a summary of the recommendations for best practices with the hope that this information will help scientists and engineers to prevent -or cope with- degradation of active and future space-based solar instruments.

It should be mentioned that the degradation of space instruments can be complex; their causes and mechanisms are, in many instances, difficult to understand, since they are often the result of the combination of several independent degradation processes. Once a spacecraft is in orbit, the stability of calibration can be monitored by carefully planned observations. Alternatively, it is possible to track instrumental calibration by inter-calibration using observations from occasional rocket underflights using similar instruments that can be carefully calibrated on the ground both before and after the flight. Another option for establishing absolute calibration using in-flight observations is the use of invariant sources - assuming they are accessible by the instrument- such as observations of celestial standard sources, of the centre of the solar disk during quiet periods, or by inter-calibration of identical variable sources using different instruments with similar, corresponding wavelength sensitivities. Furthermore, qualified personnel and external expertise are often useful in the interpretation of the data obtained, both on the ground and in-flight, in order to accurately assess the evolution of the degradation of a space-based solar instrument.

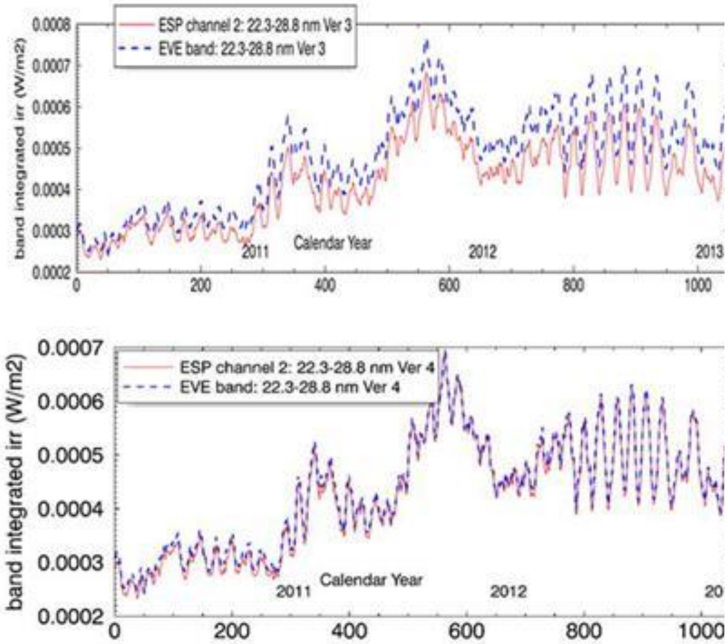

Figure 41: Comparison between SDO/ESP channel 2 and its reconstruction based on SDO/EVE-MEGS A spectra before and after the release of EVE level 4 data.

In this context and after the first degradation workshop in 2012, two workshops in 2013 and 2014 were organized by the STCE gathering a small group of experts specifically interested in the degradation and inter-instrument comparison of radiometers and spectrometers observing the Sun in the X-rays and the extreme UV (EUV) ranges. These events resulted in a much deeper understanding of the differences between the instruments and were even at the origin of a review of the calibration procedure for some of them.

In conclusion, there are several approaches to assess and monitor the degradation of spaced-based solar instruments that give good results. A prime conclusion is that there is no single best method, but rather that a combination of methods must be critically selected, taking into account the applicability of the methods given both the mission targets and instrumental design itself. It is therefore important to continue to share regular and open information about what is working and what is not, in order to learn from the community's shared experiences. Prevention is far better and much cheaper than cure.

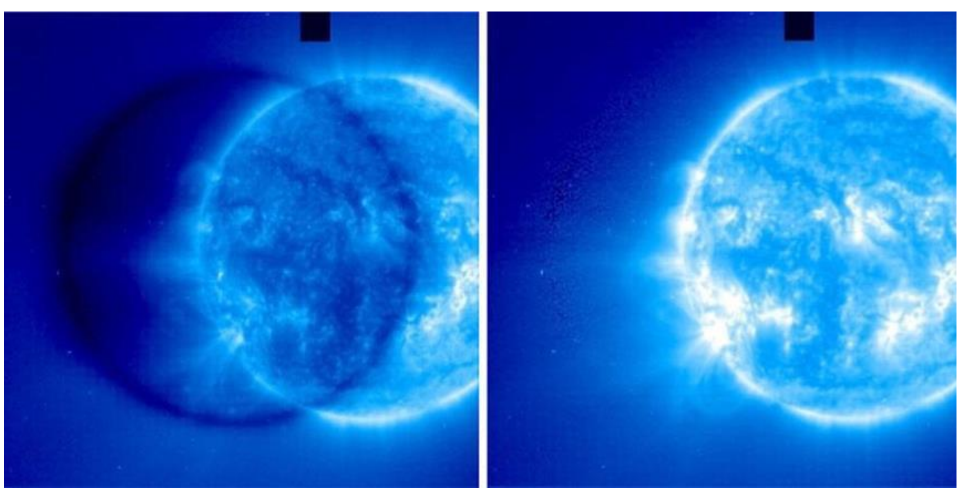

Figure 42: EIT (Extreme Ultraviolet Imager) onboard SOHO 17.1 nm images taken during an off-point maneuver before and after correction.

BRAMS: development of the network and calibration of antennas

BRAMS, the Belgian RAdio Meteor Stations, is a network of 25 radio receiving stations installed in Belgium to detect and characterize meteors using forward scattering techniques. The transmitter is located in Dourbes at the "Centre de Géophysique du Globe" and is emitting a purely sinusoidal wave at a frequency of 49.97 MHz with 150 Watt power towards zenith. All receiving stations are equipped with a GPS receiver allowing for time synchronization between the stations. In 2013, the network has been extended with new receiving stations in Gent and in Seneffe. A lot of effort has been also devoted to the development of the radio interferometer in Humain. Extensive simulations have been performed to determine the best location for the new container that hosts all the electronics of the interferometer to minimize its impact on the received signal. After its installation, very low-loss cables were connected (see Figure 43).

Figure 43: new container installed in Humain and trenches to install the new low-loss cables.

Two of the primary goals of the BRAMS project are the computation of meteoroid fluxes and determination of trajectories of individual meteoroids. Both of these goals require a good knowledge of the full radiation patterns of the transmitting and receiving antennas since meteor echoes can appear anywhere in the sky. These radiation patterns can be obtained by using numerical simulations or by conducting in situ measurements, or by a combination of both. In 2013 numerical simulations have been carried out using the NEC (Numerical Electromagnetic Code) software package. The antennas used for the transmitter in Dourbes (crossed dipole antenna with an 8 meter x 8 meter metallic grid acting as reflector), our receiving station in Uccle (one 3-element Yagi antenna and a cross 3-element Yagi antenna), and the interferometer in Humain (four 3-element Yagi antenna and one cross 3-element Yagi antenna) were modeled using a number of segments where currents are calculated using the method of moments. The characteristics of the material used for the antennas as well as the properties of the ground, such as its permittivity and electric conductivity, were also taken into account. An example of the results of these simulations is given in Figure 44.

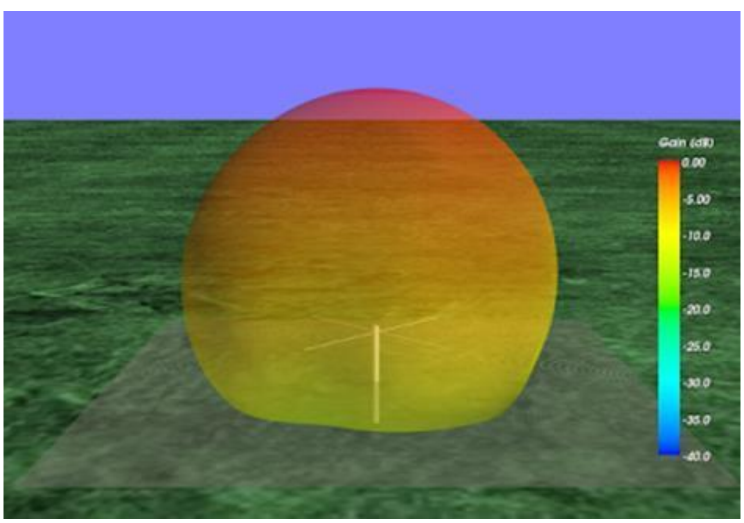

Figure 44: Antenna radiation pattern of the BRAMS transmitter located in Dourbes obtained using numerical simulations (crossed-dipole antenna and reflective plane).

In order to validate the results of these simulations, in situ measurements must also be considered to estimate the impact of real conditions - such as metallic pieces in the surroundings of the antenna, or different soil properties (e.g. when the ground is wet) - on the simulation results. Various options were considered. The final choice was to fly an Unmanned Aerial Vehicle (UAV) equipped with a dedicated transmitter developed at BIRA-IASB in the far-field of the antenna. The chosen UAV is an Okto-XL ARF-Mikrokopter (see Figure 45). Measurements will be done next year.

Figure 45: Picture of the Okto-XL ARF-Mikrokopter flying over Dourbes. This UAV will be equipped with a transmitter developed at BIRA-IASB so as to act as a known radio source in the far field of the antennas.

Electronic design for the Scanning Langmuir Probe on PICASSO

In 2013 one of the tasks specifically sponsored in the framework of the STCE was the design of the electronics hardware for the Scanning Langmuir Probe (SLP) instrument that is part of the PICASSO CubeSat. A Langmuir probe is an electrical conductor immersed in a plasma (the ionosphere in this case) that is brought to a specific potential relative to its environment. From the current-voltage characteristic one can then recover electron density and temperature.

The SLP on PICASSO consists of 4 identical probes mounted at the extremes of the deployable solar panels. The system therefore needs 4 independent channels, each connected to a probe, that each can measure currents with a total resolution of 50 pA, while sweeping the probe potentials from -10 V to +10 V relative to the spacecraft, with a resolution of 1 mV. The instrument also has to be able to autonomously perform some data processing and storage.

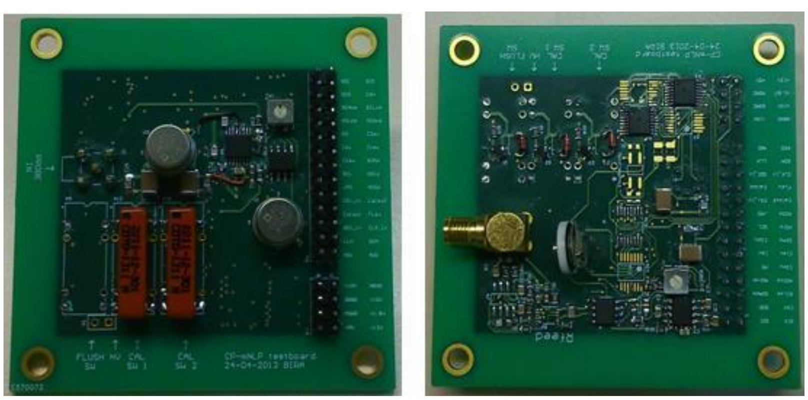

Figure 46: Pictures of the capacitive feedback electrometer prototype board (1 channel)

The first activities consisted of a study to investigate how to do this kind of measurements. A literature study concluded that an electrometer was the only feasible solution. However, there are two kinds of electrometers: one with a capacitor as feedback element (which is also known as a Coulomb meter) and one with a purely resistive feedback element. To select which one would be best suited for the SLP setup, a lot of schematic simulations were done.

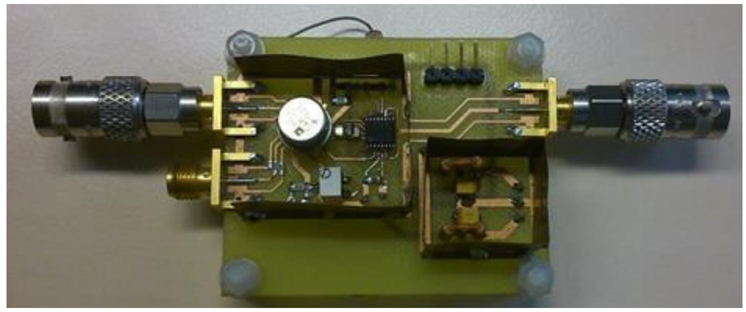

Figure 47: Picture of the resistive feedback electrometer prototype board (electrometer + switch only)

It soon became clear that the Coulomb meter offered better results than the resistive electrometer. However, its control and timing mechanisms were much more complicated. After tackling this problem, a first prototype was made, and was tested in the lab. The meter functioned as expected above the 1 nA region. However, below the 1 nA region it started to behave differently. It turned out that this system would never be able to work properly because of parasitic capacitive effects.

The decision was then made to try a resistive feedback electrometer. After building a first prototype, the solution appeared to work quite well: We could reach a current resolution of 10 pA.

The instrument control was implemented via a Field-Programmable Gate Array (FPGA), and the VHDL code to describe the internal hardware configuration was written. In the meanwhile also a Graphical User Interface (GUI) was developed to handle the prototype.

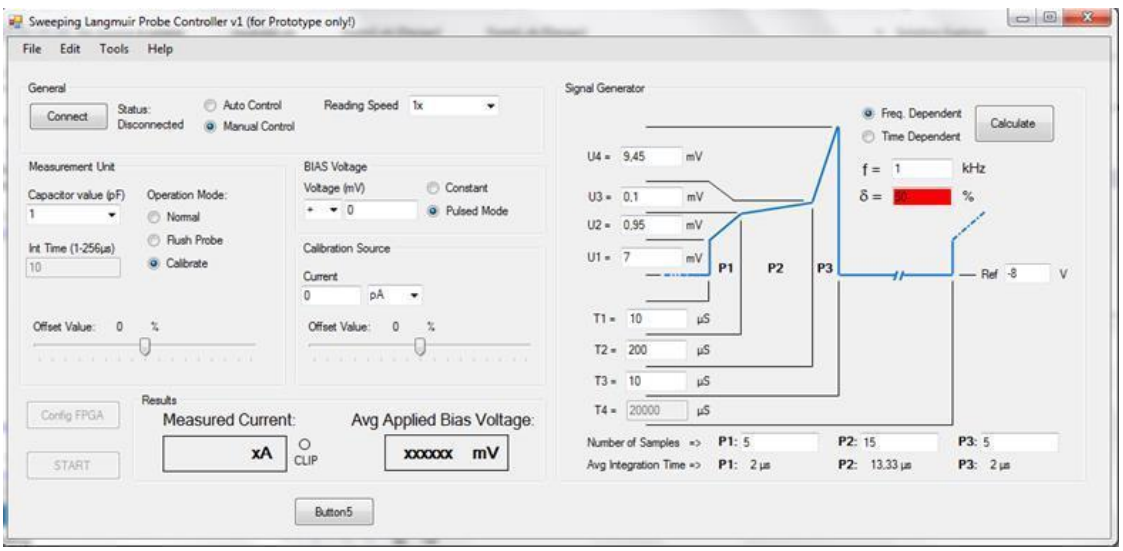

Figure 48: Screenshot of the control Graphical User Interface

Future steps will be to implement a complete channel with the resistive feedback method onto a single PCB and have everything controlled by an FPGA with a soft processor. If the results from this design are satisfactory, a full design will be made including all four channels, the FPGA, and the required memory.

Absolute spectrophotometry of the Sun using the SOLAR SOLSPEC instrument

The electromagnetic emission of the Sun covers a large spectral range, from the X-rays to the radio waves. Being a variable star, the Sun presents also a wide range of periodicities of its energy flux, ranging from minutes to decades with amplitudes strongly dependent on the wavelength. The periodicities generally increase for decreasing wavelengths. Solar Spectral Irradiance (SSI) variability comes from the magnetic activity of the Sun with its 11-year periodicity.

The scientific community has an interest in measuring the SSI above the atmosphere from the EUV to the IR. Knowledge of the SSI is a prerequisite for the study of the photochemistry of the Earth's atmosphere and for climate modeling because the composition, the thermal structure, and the dynamics of the atmosphere are dependent on the incoming solar flux, its spectral distribution and variability. Solar atmospheric models are developed for computation of the spectral lines and the continuum of the solar spectrum. Measurements of the SSI are required for parameter adjustments and validation of such semi-empirical models.

SSI measurements are performed on board of the International Space Station (ISS) by the SOLAR SOLSPEC instrument. The SOLSPEC (for SOLar SPECtrum) project was initiated in the seventies by the CNRS (France, currently the LATMOS-CNRS) and supervised by the CNES (France), with major collaborations from BIRA-IASB and the Observatory of Heidelberg (Germany). SOLSPEC is equipped with 3 coupled spectrometers that use concave gratings, covering simultaneously the UV-VIS and IR spectral ranges. The current version of this instrument (SOLAR SOLSPEC) has been built to measure the SSI from 166 to 2900 nm as part of the long-term SOLAR mission from ISS between 2008 and 2017. SOLAR SOLSPEC was developed thanks to the excellence of BIRA-IASB in space applications under the auspices of the BElgian Science Policy Office (BELSPO) and in close collaboration with the LATMOS.

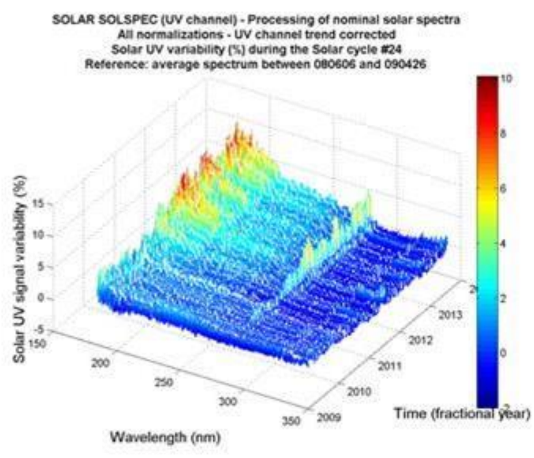

Figure 49: On the left, the SOLAR payload stowed on the COLUMBUS European module on ISS since February 2008. On the right, the UV SSI relative change during the solar cycle 24 as measured by SOLAR SOLSPEC.

The ***SOLAR SOLSPEC*** mission is organized in Sun Visibility Windows (SVW) due to alternation of scientific activities on ISS, with an average of 10 days of measurements per month. The objective is to provide a database of solar UV spectra and their variability during the course of solar cycle 24. Then, a comparison can be performed with other instruments such as SOLSTICE (SOLar STEllar Irradiance Comparison Experiment) on SORCE (Solar Radiation and Climate Experiment). Due to the severe space environment, UV spectroradiometers are subject to changes in their responsivity due to deposition of contaminants on optical surfaces or a decrease of detector sensitivity, for example.

For SOLAR SOLSPEC, the degradation of the UV channel response has been monitored during the 6 year campaign. A degradation correction was applied to all solar measurements. This allowed extracting the UV SSI variability as measured by SOLAR SOLSPEC. An average intercycle (quiet Sun) spectrum was defined from June 2008 to April 2009. With respect to this time interval, we calculated the SSI relative UV change (%), as a function of time and wavelength. The results are shown in Figure 49 (right).

As an example, we obtained the SSI temporal variability at 205 nm -a key quantity for ozone due to the deep penetration of this wavelength through the atmosphere and the role it plays for ozone photochemistry- shown in Figure 50 (left). The MgII index is a proxy for the Middle-UV (MUV, 170-400 nm) variability. This is a physical parameter related to the core-to-wing change of the MgII line (at 280 nm) during the solar cycle and it provides an accurate representation of chromospheric emission. As the MgII index is measured by SOLSPEC, we calculated the relation between MgII and SOLAR SOLSPEC UV SSI variabilities. It is expressed as a scaling factor that represents the UV change (%) for 1 % change of MgII index as a function of the wavelength. The scaling factors from SBUV (Solar Backscatter UltraViolet) and SOLAR SOLSPEC are compared in Figure 50 (right), showing that both instruments provide nearly the same relation between MgII index and SSI variabilities.

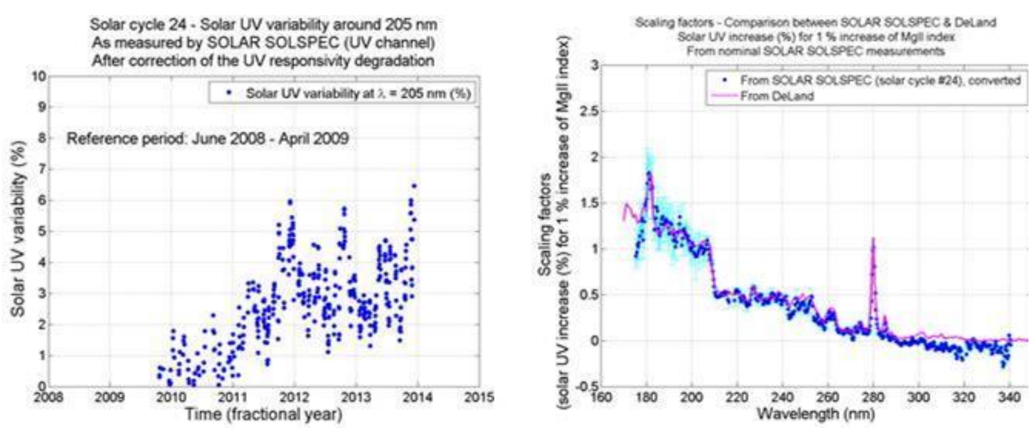

Figure 50: On the left, the UV SSI relative change at 205 nm during solar cycle 24 as measured by SOLAR SOLSPEC. On the right, comparison between the scaling factors from SOLAR SOLSPEC and SBUV.

It can be concluded that, after 6 years of mission, SOLAR SOLSPEC appears to be a robust and well-monitored instrument with limited aging of its UV channel. This is also the result of the full radiometric characterization and absolute calibration performed before the flight under the lead of BIRA-IASB. SOLAR SOLSPEC is ready to continue its measurements until the end of the SOLAR mission (extended until February 2017) and to provide the solar UV changes during solar cycle 24. Through European collaborations, the data set of solar spectra measured by SOLAR SOLSPEC will be provided to the science community.

Figure 51: The men's restrooms at the ESWW10 Conference Centre: checking out the instrumentation…

Applications and Modeling

SSCC: Providing support to ESA during spacecraft launch

ESA has set up a Space Situational Awareness (SSA) program dedicated to space weather, with the purpose to establish and provide access to a network of European space weather products for end users. The products include ESA owned applications, as well as, space weather products provided by different European expert groups. In the context of the SSA program, the SSCC (SSA Space Weather Coordination Centre) is the focal point for space weather user support.

The SSCC was officially inaugurated on 3 April 2013 during a dedicated event at the Space Pole, attended by key personnel of ESA, the SSA program and the collaborating partners of the project. The program included Philippe Mettens, Chairman of the Belgian Science Policy Office, ESA Director Thomas Reiter, SSA Program Manager Nicolas Bobrinsky, SSA Space Weather Segment Manager Juha-Pekka Luntama, and Michel Kruglanski, project manager leading the consortium responsible for implementing the SSCC.

Figure 52: The official inauguration of the SSCC took place on 3 April.

In coordination and collaboration with ESA, the local coordination team took care of the entire organization of the SSCC ***inauguration*** and turned it into a very successful media event. This involved the set-up of a program that was agreed upon by all, the compilation of a press-, VIP- and users-list, the timely mailing of two announcements, the automatic management of the subscriptions, and the distribution of the press text. A space weather movie was shown and a digital press map was provided. The attendance of and coverage by the media was very satisfying, and media interest continued for the rest of the week. Event Support and the local IT-team provided the technical support for projection of the presentation, and assured that the event was livestreamed. A movie of the event is still available on YouTube, and images are at the SIDC-website and in this STCE News item.

The SSCC is monitoring the space weather services ensuring their availability to the users and their nominal performance. It also provides the first level user support for all those services. Located at the Space Pole premises in Brussels, its activities are gradually expanding as more services become online and users increasingly interact with the SSCC. The SSCC functions as a relay between the users and the European space weather products.

GAIA is an ESA satellite constructed to produce the largest three-dimensional map of our galaxy. To that end, the spacecraft is observing one percent of all 100 billion stars of our galaxy. The satellite was launched on 19 December 2013 with a Soyuz-rocket from the launch basis of Kourou, French Guyana. In the period from 6 to 14 January 2014, the spacecraft did maneuver to its final destination.

The SSCC and the forecast team of the Regional Warning Center (RWC) in Belgium provided support on the days before, during and after the launch of the GAIA spacecraft. During the launch window, seven space weather bulletins were delivered, while six ones were sent during the spacecraft maneuvers. The bulletins provided a description of the current space weather activity and predictions for any activity that could result in increased risks for the spacecraft.

Figure 53: Launch of the GAIA satellite on 19 December 2013

Specific attention was paid to the risks for increased amounts of energetic particles, during which protons are accelerated to very high energies by a solar flare or by the interplanetary shock wave associated with a coronal mass ejection (CME). Monitoring the solar activity (by observing and classifying the sunspot groups) allows for the forecast of the flaring activity. The solar flares are categorized in classes based on their peak burst X-ray emission. A CME could occur during a long duration flare or during the eruption of a solar filament. Major solar proton events could result from the acceleration of solar wind particles by an interplanetary shock wave of an Earth-directed CME.

An increased flux from energetic particles might for example result in damage of the spacecraft's instruments. A special bulletin was provided to the GAIA team during the rising phase of an energetic particle event on 6 January 2014 to inform them on the increased risks for radiation exposure to the spacecraft.

Near real-time monitoring of the European ionosphere using GNSS

The ionizing action of the Sun's radiation on the Earth's upper atmosphere produces free electrons by photo-ionization. In the ionosphere, from about 60km above the Earth's surface, the number of these free electrons is sufficient to affect the propagation of electromagnetic waves. Nowadays, various scientific applications and services increasingly demand to monitor in real-time the electron content in the Earth's ionosphere. This is particularly the case for applications requiring radio-signals reflecting on, or propagating through, the ionosphere. In that frame, the STCE is monitoring in near real-time (NRT) since 2012 the electron content over Europe and provides publicly several derived products.

By combining GNSS (Global Navigation Satellite Systems, e.g., GPS, GLONASS, GALILEO) measurements on two separate frequencies, the ionospheric delay between a ground receiver and a satellite can be determined. This delay is function of the integrated number of electrons encountered in the ionosphere along the ray path called the Total Electron Content (TEC with 1 TECu = 10^{16}e-.m^{-2}). It is thus possible to build ionospheric maps representing the vertical TEC (vTEC, i.e. above a given point on the Earth's surface) as a function of latitude, longitude and time using a network of GNSS stations.

The STCE is involved in the daily management of the EUREF Permanent GNSS Network (EPN) and takes advantage of these dense GNSS observations to monitor the ionosphere over Europe from the measured delays in the GNSS signals. For that, we developed a software called ROB-IONO which analyses the GNSS data from ~110 stations of the EPN providing real-time data streams. The ROB-IONO software delivers in NRT vTEC maps and their variability over Europe. The maps are updated every 15 minutes on a 0.5°x0.5° grid extended from -15° to 25° in longitude and 35° to 62° in latitude. The maps are available online with a latency of ~3 minutes at ftp://gnss.oma.be as ASCII data files and interactive web pages are displayed at www.gnss.be

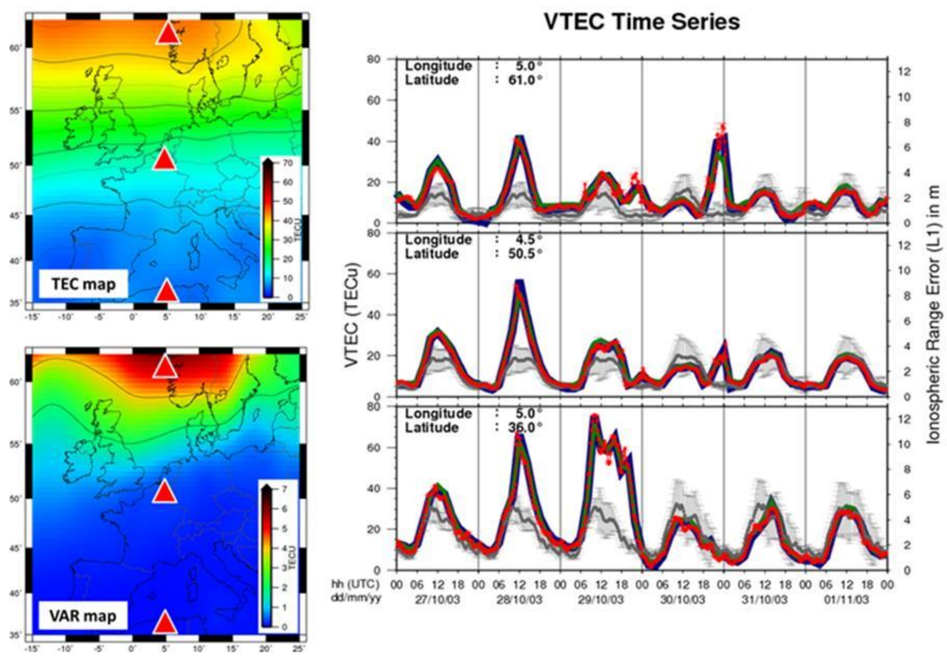

Figure 54: NRT ROB-TEC maps during the 2003 Halloween storm. Left: ROB-TEC maps estimated between 22:15 and 23:00 UTC for 30 October 2003. Left top: ROB-TEC map estimated in NRT. Left bottom: ROB-TEC variability map during the 15-minutes time span. Right: 6-day vTEC time series extracted from ROB-TEC maps at three different geographic locations represented by the red triangle on the maps (top: northern part of the maps; middle: above Brussels, bottom: southern part of the maps). The red dots are the vTEC time series estimated in NRT. The grey dots represent the expected ionospheric behavior based on the vTEC median and its standard deviation from the 15 previous days. The green and blue lines are the interpolated values from the IGS and CODE final products respectively.

To test the capability of the ROB-IONO software to detect in NRT abnormal ionospheric activity due to space weather events, we focused on the results obtained during an identified geomagnetic storm. For that, the ROB-IONO software was applied on the EPN data gathered during the Halloween storm of 28-30 October 2003 considered as a major geomagnetic storm which affected the Earth upper atmosphere and communications systems.

Figure 54 shows the estimated ROB-TEC map above Europe between 22:15 and 23:00 UTC on 30 October 2003. vTEC values reach up to 47 TECu in the northern part of the map, whereas during quiet ionospheric activity vTEC values below 7 TECu are expected (time-series in grey on Figure 54, right). The variability map in Figure 54 highlights also large TEC variations in the Northern region. This is in accordance with extreme TEC gradients occurring at mid-latitudes due to plasma increase during such an event. This assesses the capability of the ROB-IONO software to detect abnormal ionospheric behavior in NRT over Europe. The comparison with post-processed (i.e. available a few days after the day of interest) global ionospheric maps from the International GNSS Service (IGS) and the Center for Orbit Determination in Europe (CODE), considered as the reference for many ionospheric and geophysical studies, demonstrate negligible differences. However, maximum differences (>10 TECu) occur during the major phase of the storm. These differences are due to the low resolution in time and space of the IGS and CODE maps compared to the ROB-TEC maps.

ROB is now maintaining a public data base with identified ionospheric events since 2012. Consequently, ROB-TEC together with variability maps estimated in NRT permit to follow the ionospheric behavior in more details, bringing valuable information during a disturbed period. Presently, more than 25 events of abnormal ionospheric activity have been reported at the www.gnss.be for the period 2012-2013. The Space Weather origin of each event is provided in collaboration with other STCE members. For the period 2012-2013, the ionospheric perturbations are associated with coronal mass ejections (~70% of the time), not well established origin of active geomagnetic conditions (~20% of the time) or unidentified phenomena (10% of the time).

N. Bergeot (ROB) received the price for the “Concours Annuel 2013, Groupe II – Astronomie-Physique” from the Académie royale de Belgique.

GNSS for Severe Weather and Climate: STCE contribution to COST Action ES1206

Figure 55: The logo created for the COST Action ES1206

Since 15 years, the Royal Observatory of Belgium (ROB) and then the Solar-Terrestrial Centre of Excellence (STCE) are involved in GNSS meteorology projects such as the EUMETNET EIG GNSS water VApor Program (E-GVAP). After a 2-year elaboration phase, STCE and institutes from 7 other European countries co-founded in 2013 the COST Action ES1206 on “Advanced Global Navigation Satellite Systems Tropospheric Products For Monitoring Severe Weather Events And Climate” (GNSS4SWEC) in order to bring the contribution of GNSS to meteorology and climate at the next level. COST (European COoperation in Science and Technology) is an intergovernmental framework, supporting cooperation among scientists and researchers across Europe and the coordination of nationally-funded research on a European level. GNSS4SWEC ensures the follow-up and enlargement of current STCE activities as well as its integration at the international level.

Global Navigation Satellite Systems (GNSS) is now an established atmospheric observing system which can accurately sense water vapor, the most abundant greenhouse gas, accounting for 60-70% of the atmospheric warming. Severe weather forecasting is challenging, in part due to the high temporal and spatial variations of atmospheric water vapor. Water vapor is under-sampled in the current meteorological and climate observing systems, hence obtaining and exploiting more high-quality humidity observations is essential to weather forecasting and climate monitoring. In both cases, i.e. nowcasting severe weather and monitoring climate, GNSS can play a key role!

The COST Action GNSS4SWEC addresses new and improved capabilities from concurrent developments in both the GNSS and meteorological communities. For the first time, the synergy of the three GNSS systems (i.e. the US GPS, the Russian GLONASS and the EU Galileo) will be used to develop new, advanced tropospheric products, exploiting the full potential of multi-GNSS water vapor estimates on a wide range of temporal and spatial scales, from real-time monitoring and forecasting of severe weather, to climate research. Furthermore, improved modelling of the atmospheric influence can contribute to the speed and precision of GNSS positioning, navigation, and timing services, making the collaboration between the geodetic and atmospheric communities mutually beneficial.

Figure 56: A picture from the kick-off meeting in Brussels on 17 May 2013

To achieve its goals, GNSS4SWEC is organized into three Working Groups (WGs):

- WG1 “Advanced GNSS processing techniques” focuses on the development of new/advanced GNSS processing techniques and products;
- WG2 “GNSS tropospheric products for high-resolution, rapid-update Numerical Weather Prediction (NWP) and severe weather forecasting” focuses on the application/development of new GNSS tropospheric products for severe weather;
- WG3 “GNSS tropospheric products for climate monitoring” aims at the evaluation of existing and forthcoming GNSS tropospheric products and assesses their potential for climate research.

Having clear interdependence and common topics of interest, the 3 WGs will work in close collaboration to achieve their goals.

GNSS4SWEC officially started with its kick-off meeting being held in Brussels on 17 May 2013 and STCE was nominated to co-chair WG2. During the first Action year, several members of the STCE (from ROB, RMI and BISA) joined and accepted the coordination-ship of major work packages within GNSS4SWEC such as the development of new GNSS processing techniques (e.g. atmospheric asymmetry models and slant delays) and the development of GNSS products for severe weather (IWV maps, gradients, fluxes…).

Indeed, several existing STCE research projects such as the “Advanced Multi-GNSS Troposphere Modelling for Improved Monitoring and Forecasting of Severe Weather” *(awarded at the gfg² summer* *school*), the “GPS assimilation in the ALARO weather forecast model” and the “multi-site inter-comparison of Integrated Water Vapor (IWV) observations for climate change analysis” (published in AMTD) are naturally aligned with the objectives of the COST Action.

STCE also plays an important role in WG3. Indeed, the use of GNSS tropospheric products in climate science has been advertised for several years, but they are still not widely used, despite the excellent time stability of the observing system. This is in clear contrast to the advances of GNSS meteorology. One STCE outcome is to contribute to the exploitation of 15+ years of homogeneously reprocessed GNSS tropospheric products to detect climatic signals and to evaluate independent climate data records of IWV, which is recognized as an essential climate variable by the Global Climate Observing System (GCOS). This contribution started already with the above-mentioned IWV inter-technique comparison.

Finally, GNSS4SWEC also benefits STCE by facilitating the collaboration at the international level and the exchange of knowledge. As an example, a PhD student from Geodetic Observatory Pecný (GOP), Czech Republic, visited ROB in the framework of a 1-month COST Short-Term Scientific Mission (STSM) in order to start a collaboration on real-time GNSS data processing. The collaboration focuses today on GNSS meteorology but might also be extended on long-term reprocessing activities for Regional Climate Modelling (RCM). In the next years, STCE might benefit of additional STSMs.

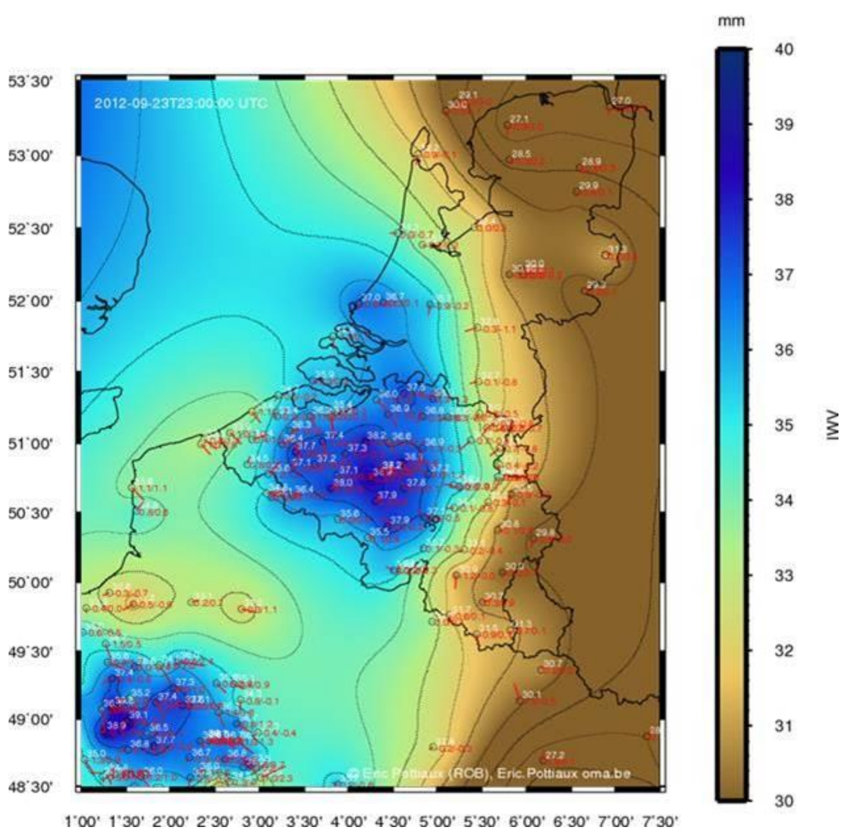

Figure 57: Water vapor map built by the STCE team for nowcasting application

To conclude, GNSS4SWEC is definitely paving the way for future European GNSS meteorology and climate services and STCE is actively contributing to these developments!

More details about the COST Action ES1206 can be found in its memorandum of understanding and on the GNSS4SWEC website.

COMESEP: forecasting the space weather impact

The development of the COMESEP (COronal Mass Ejections and Solar Energetic Particles) Alert System was funded by a three-year EU FP7 grant (European Union Seventh Framework Program) that concluded in January 2014. The project was led by BIRA-IASB and consisted of a collaboration with KSB-ORB and 5 other European Institutes. Tools for forecasting geomagnetic storms and solar energetic particle (SEP) radiation storms were developed, validated and implemented into an operational space weather alert system that runs without human intervention. The COMESEP Alert System is triggered by the observation of solar phenomena such as CMEs (Coronal Mass Ejections) and solar flares. After the automatic detection in solar data of any of these transients, the different modules of the system communicate in order to exchange information. The system produces a series of coherent alerts that are then displayed online and sent via email to subscribed users. In this way, COMESEP provides automatic notifications for the space weather community.

Arrival of CME / Likelihood of occurrence						
Ongoing (100%)	L	M	H	H	E	E
Very likely (90-100%)	L	M	H	H	E	E
Likely (70-90%)	L	M	M	H	H	E
Possible (40-70%)	L	L	M	M	H	E
Unlikely (10-40%)	L	L	M	M	H	H
Very Unlikely (0-10%)	L	L	L	M	M	H
Storm Level	None	Minor	Moderate	Strong	Severe	Extreme
Geomagnetic |Dst| in nT	<50	50-100	100-200	200-300	300-400	>400
SEP peak flux > 10 MeV in $s^{-1}sr^{-1}cm^{-2}$	$<10^1$	10^1-10^2	10^2-10^3	10^3-10^4	10^4-10^5	$>10^5$
SEP peak flux > 60 MeV in $s^{-1}sr^{-1}cm^{-2}$	$<7.9\times10^{-2}$	7.9×10^{-2} - 1.4	1.4 - 2.5×10^1	2.5×10^1 - 4.5×10^2	4.5×10^2 - 7.9×10^3	$>7.9\times10^3$
Kp	<5	5	6	7	8	9

Figure 58: The COMESEP risk matrix. The rows represent the probabilities of arrival of a CME or an SEP event. The columns indicate the impact calculated for the corresponding geomagnetic or SEP radiation storm (in two energy ranges). The combination of these two parameters provide the risk level: low (L, green), medium (M, yellow), high (H, orange) and extreme (E, red).

The COMESEP Alert System can be found online at http://comesep.eu/alert/ , with a general description of the system available at http://comesep.eu/ The alerts are based on the COMESEP definition of risk that combines the likelihood of occurrence of the predicted event with its estimated impact at the Earth. This information, derived internally by the system, is then used to obtain the corresponding risk level for a particular event according to the COMESEP risk matrix (Figure 58).

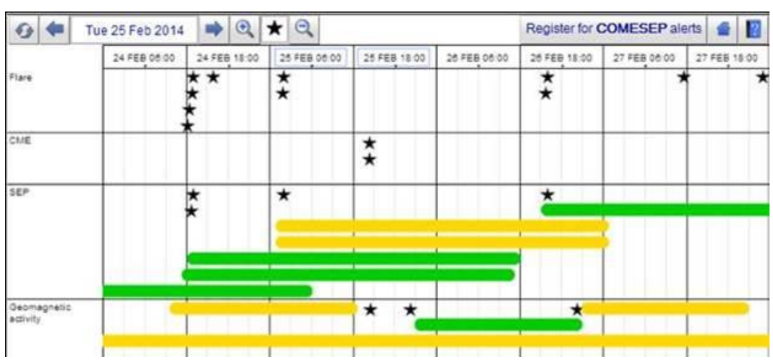

Figure 59: Status of the COMESEP Alert System for the period 24-27 February 2014. The first row shows the occurrence of solar flares (stars). The second row marks the eruption of CMEs (stars). The third row shows the prediction for SEP radiation storms. The last row displays the expected geomagnetic storms. The length of the bars in the last two rows is an indication of the expected duration of the corresponding SEP radiation or geomagnetic storm, while the color represents the derived risk level (see Figure 58).

As an example, Figure 59 shows the status of the COMESEP Alert System for the time period 24-27 February 2014. During that time, several flares and a CME occurred and were detected by the system (stars in the first two rows of the figure). The corresponding geomagnetic storm and SEP radiation storm predictions are shown in the last rows. The SEP radiation storm with moderate risk predicted for 25 February actually arrived at Earth and was measured by the GOES13 satellite (Figure 60). This occurred as a consequence of an X4.9 flare peaking at 00:49 UT, the COMESEP Alert System dispatched the following e-mail alert correspondingly *(edited here for brevity)*:

SEP Forecast Alerts from COMESEP has issued the following SEP alert with impact risk evaluated as medium.
Details on the above alert can be found hereafter.

Best Regards,

COMESEP Alert system.

=== Comesep Alert Info ===
Alert id: 20140225_014002_b740be01f7@SEPForecast.oma.be
Status:normal
AlertIdAction: update
Emitter: SEP Forecast Alerts from COMESEP
Emitter HRef: http://www.comesep.eu/sepforecast
Emitter Version: 0.0.0
Subject: Forecast for a SEP radiation storm following a X4.9 flare with peak at 2014-02-25 00:49UT (protons > 10 MeV: MODERATE, POSSIBLE; protons > 60 MeV: MODERATE, POSSIBLE).
SubjectTopic: SEP

== DISCLAIMER ==
COMESEP makes no warranties or representations as to its accuracy and COMESEP specifically disclaims any liability or responsibility for any errors or omissions in the content on the website, as well as the alerts that are sent out. Neither COMESEP nor any other party involved in creating, producing, or delivering information that is used in the COMESEP alert system is liable for any direct, incidental, consequential, indirect, or punitive damages arising out of your access to, or use of, or inability to use or access, the website and/or the alerts that are sent out.

This file has been generated on 25-02-2014 01:46 by Comesep dispatcher at www.comesep.eu/alert

This example above shows how an automated system can provide helpful aid to human forecasters in real time. The COMESEP Alert System runs continuously 24/7.

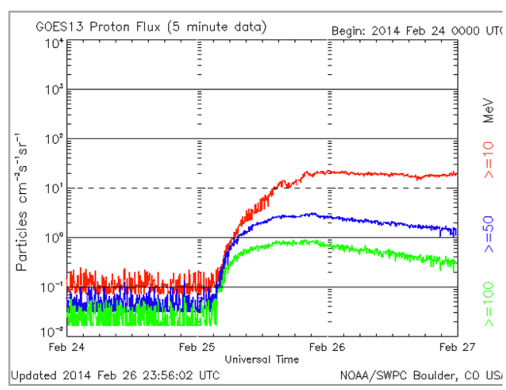

Figure 60: Time profile of the GOES 13 proton flux showing the SEP radiation storm starting on 25 February 2014.

The LIDAR ceilometer at Uccle

In May 2011, RMI installed a LIDAR ceilometer (LIght Detection And Ranging) at Uccle that offers the opportunity to monitor the vertical profile of aerosols and the mixing layer height (MLH) on a continuous temporal scale.

Support to the monitoring of the air pollution dispersion

LIDAR ceilometers were primarily designed for cloud base height (CBH) detection (for air traffic safety and weather forecasting). They greatly improved over the last years and now offer the opportunity to monitor the vertical profile of aerosols and the MLH on a continuous temporal scale. The knowledge of MLH can improve the forecasting of the dispersion of trace gases and aerosols in the lowest layers of the atmosphere and can also improve the accuracy of the greenhouse gas concentration budgets highly depending on MLH. In this frame, up to 2013, several tools to monitor in real-time the vertical profile of aerosols, the MLH with a control on its measurement accuracy and the CBH have been developing by RMI.

Support to the forecaster's work

In 2013, some atmospheric phenomena such as radiative fog, stratus build-down fog, warm frontal passage, virga, and the ignition of convection were studied with the LIDAR measurements and detailed with others measurements such as the radio-sounding when the data were available. This study wants to develop and to improve the use of the LIDAR data in the diagnosis of the weather forecasters and their prognosis for some specific atmospheric conditions.

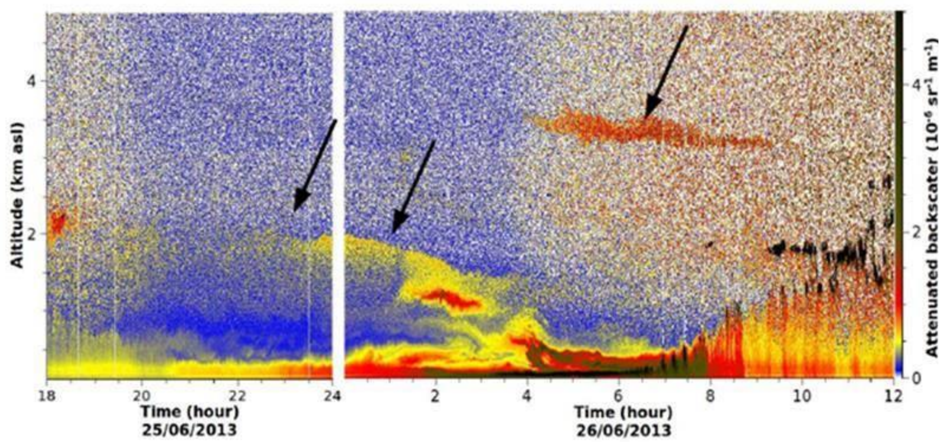

Figure 61: LIDAR observations from Uccle on 25 and 26 June 2013 showing the position of the smoke plume (below arrows).

Support to the monitoring of the aerosol clouds

At the end of 25 June and during the morning of 26 June 2013, the LIDAR of Uccle showed (Figure 61) a clear layer of aerosol at an altitude of around 3000-4000 meters. This layer of aerosol originated from biomass burning aerosol released by intense wildfires in North America. The transport of these aerosols over Europe was due to the production of pyrocumulonimbus clouds by these wildfires that injected the aerosols at the top of the troposphere where the configuration of the Jet Stream was suitable for blowing the aerosols across the North Atlantic.

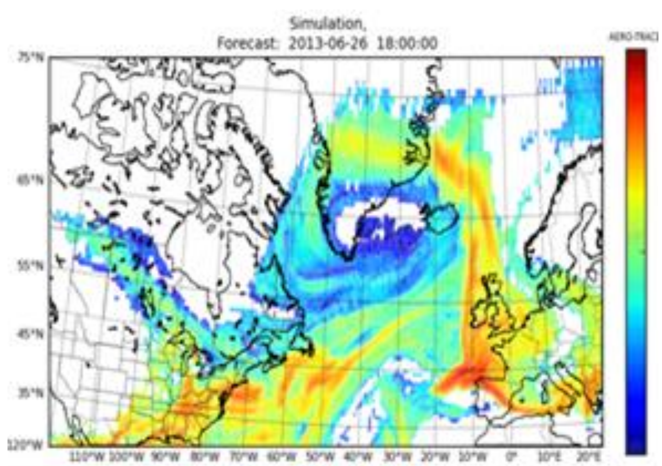

Figure 62: Snapshot of the simulation (computed by RMI) of the dispersion plume coming from Colorado and Quebec wildfires. The color scale is in arbitrary units.

The observation of this intercontinental smoke transport event by the LIDAR of Uccle (and with the LIDAR network of MetOffice) illustrates the ambiguity that can happen if one type of remote sensor instrument is used to monitor smoke plumes. Indeed, during this event, some remote sensing scientists claimed that the origin of the observed plume over Europe came from Colorado wildfires (United States) and others claimed that the smoke plume came from Quebec wildfires (Canada), more than 2000 km from Colorado! In this case, a dispersion model was used (Figure 62) and its output was compared with the LIDAR measurements to discriminate which wildfires contributed mainly to the smoke plume over Europe. The dispersion model suggested that much of the smoke came from Quebec wildfires, with a remarkable agreement between the LIDAR observations and the dispersion model.

This intercontinental smoke transport event is a remarkable case study to illustrate that a LIDAR network is more sensitive and more precise (spatially and temporally) than satellite data to monitor a smoke plume. The monitoring of wildfire smoke plumes by LIDAR network can help to validate and to improve the dispersion models for the forecast of various pollution events including aerosol plumes dangerous for aviation and health.

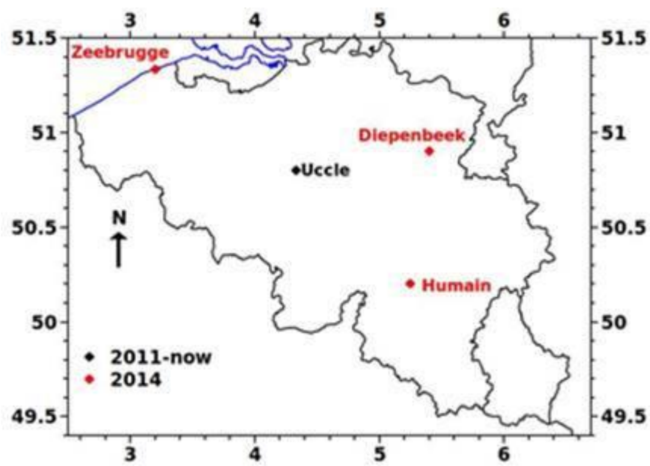

Figure 63: Map of Belgium with the locations of future LIDAR at Zeebrugge, at Diepenbeek and at Humain in addition to the one already installed at Uccle.

LIDAR network in Belgium

In 2013, the data acquisition system for the three new LIDAR (Vaisala CL51) purchased at the end of 2012 was produced and tested at Uccle close to the LIDAR already in place. They will be installed and become operational in 2014 in the synoptic stations of Zeebrugge, Diepenbeek and Humain, (Figure 63).

National and international collaboration

In the frame of the objectives of AGACC-II (Research project SD/CS/07A funded by BELSPO with BISA, ULg, ULB and RMI as partners), the LIDAR ceilometer increases the Belgian expertise in the field of aerosol remote sensing, can determine additional optical parameters of the aerosols, provides information on their vertical distribution, and measures the MLH. The AGACC-II data will be very useful for the verification of global and regional chemistry climate models. The latter are used to understand atmospheric processes and biogeochemical cycles, and to predict the future state of the atmosphere and climate. In addition, field data will be delivered to international databases such as NDACC (Network for the Detection of Atmospheric Composition Change).

In the frame of the development of a coordinated system for the LIDAR observation in Europe, RMI is involved in two major European projects with the goal to make available the measurements of its future LIDAR ceilometers network to the European meteorological community in near real time. In EUMENET, RMI (as a member) participates in the E-PROFILE program (started in January 2013) to develop an operational LIDAR ceilometer network by the exchange of LIDAR ceilometer backscatter data in a standard format and the maintenance of an archive of communicated data and metadata for all systems connected to the networks.

RMI also participates in a COST Action: TOPROF. The aim of this action (started in October 2013) is to co-ordinate the operation of many ceilometers installed across Europe, so that they can be networked and provide quality controlled and calibrated observations of aerosols in the lowest few kilometers of the atmosphere to national meteorological services in near real-time. In this Action, the data will be used to evaluate the backscatter profiles predicted by the prognostic aerosol schemes within the next generation of European forecast models for forecasting air quality. A monitoring system will be set up for the observation of the spatial distribution, height and density of aerosols plumes (e.g. volcanic ash, biomass burning,...) over Europe, which are key information for air traffic safety. The same system will monitor the MLH over Europe, a key factor for pollutant concentration predictions.

Figure 64: The local TGV brought the CLW6 participants to the conference dinner…

Publications

This overview of publications consists of three lists: the peer-reviewed articles, the presentations and posters at conferences, and the public outreach talks and publications for the general public. It does not include non-refereed articles, press releases, the daily, weekly and monthly bulletins that are part of our public services, … These data are available at the STCE-website http://stce.be/index.php or upon request.

Authors belonging to the STCE have been highlighted in the list of peer reviewed articles.

Peer reviewed articles

1. **Q. Baire, C. Bruyninx, J. Legrand, E. Pottiaux E, W. Aerts, P. Defraigne, N. Bergeot, J.-M. Chevalier**
Influence of different GPS receiver antenna calibration models on geodetic positioning
GPS Solutions, 22 November 2013, DOI: 10.1007/s10291-013-0349-1

2. **A. BenMoussa, B. Giordanengo, S. Gissot**, G. Meynants, X. Wang, B. Wolfs, J. Bogaerts, U. Schuehle, G. Berger, A. Gottwald, C. Laubis, U. Kroth, F. Scholze
Characterization of backside-illuminated CMOS APS prototypes for the Extreme Ultraviolet Imager on-board Solar Orbiter
IEEE Transactions on Electron Devices, 60, pp.1701-1708

3. **A. BenMoussa, S. Gissot, B. Giordanengo**, G. Meynants, X. Wang, B. Wolfs, J. Bogaerts, U. Schuehle, G. Berger, A. Gottwald, C. Laubis, U. Kroth, F. Scholze, A. Soltani, T. Saito
Irradiation Damage Tests on Backside-Illuminated CMOS APS Prototypes for the Extreme Ultraviolet Imager On-Board Solar Orbiter
IEEE Transactions on Nuclear Science, 60, Issue 5, pp.3907-3914

4. **A. BenMoussa, S. Gissot**, U. Schuehle, F. Auchere**, D.B. Seaton, I.E. Dammasch, D. Berghmans, M. Dominique, B. Giordanengo**, M. Kretzschmar, **B. Nicula**, + 39 coauthors
On-Orbit Degradation of Solar Instruments
Solar Physics, 288, Issue 1, pp.389-434, 2013, DOI: 10.107/10.1007/s11207-013-0290-z

5. **A. BenMoussa**, A. Soltani, J.-C. Gerbedoen, T. Saito, S. Averin, **S. Gissot, B. Giordanengo**, G. Berger, U. Kroth, J.-C. De Jaeger, A. Gottwald
Developments, characterization and proton irradiation damage tests of AlN detectors for VUV Solar Observations
Nuclear Instruments & Methods in Physics Research section B : Beam interactions with Materials and Atoms, 312, pp.48-53

6. **N. Bergeot**, I. Tsagouri, **C. Bruyninx, J. Legrand, J.-M. Chevalier, P. Defraigne, Q. Baire, E. Pottiaux**
The Influence of Space Weather on Ionospheric Total Electron Content during the 23rd Solar Cycle
Journal of Space Weather Space Climate, 3, A25, 2013, DOI: 10.1051/swsc/2013047

7. **D. Berghmans, A. De Groof, M. Dominique**, J.-F. Hochedez, J.W. Leibacher
Preface
Solar Physics, 286, pp.1-3

8. **K. Bonte, D. Berghmans, A. De Groof**, K. Steed, S. Poedts
SoFAST: Automated Flare Detection with the PROBA2/SWAP EUV Imager
Solar Physics, 286, pp.185-199

9. **H. Brenot, J. Neméghaire, L. Delobbe, N. Clerbaux, P. De Meutter, A. Deckmyn, A. Delcloo, L. Frappez, M. Van Roozendael**
Preliminary signs of the initiation of deep convection by GNSS
Atmospheric Chemistry and Physics, 2013, 13:5425-5449, DOI: 10.5194/acp-13-5425-2013

10. **S. Calders, H. Lamy, E. Gamby, S. Ranvier**
Recent developments in the BRAMS project
Proceedings of the International Meteor Conference, 22-25 August 2013, Poznan, Poland, 2014

11. S. Calders, C. Verbeeck, H. Lamy, S. Ranvier, E. Gamby
Results of Draconid 2011 observations from the BRAMS network
Proceedings of the International Meteor Conference, La Palma, Canary Islands, Spain, 20-23 September 2012, ISBN 978-2-87355-024-4, pp. 84-87, 2013

12. K. Chandrashekhar, S.K. Prasad, D. Banerjee, B. Ravindra, **D.B. Seaton**

Dynamics of Coronal Bright Points as seen by SWAP, AIA, and HMI
Solar Physics, 286, pp.125-142

13. E.W. Cliver, **F. Clette**, L. Svalgaard
Recalibrating the Sunspot Number (SSN): the SSN Workshops
Central European Astrophysical Bulletin, 37 (2), pp.401-416

14. E. De Schrijver, **R. Van Malderen**
ASGARD-II, III and III-b balloon flights: growing a worldwide hand-on space education project for secondary school students
Proceedings "21st ESA Symposium European Rocket & Balloon Programmes and Related Research", pp.597-601, 9-13 June 2013, Thun, Switzerland (ESA SP-721, October 2013)

15. **M. Dominique, J.-F. Hochedez**, W. Schmutz, **I.E. Dammasch**, A.I. Shapiro, M. Kretzschmar, **A.N. Zhukov**, D. Gillotay, Y. Stockman, **A. BenMoussa**
The LYRA instrument onboard PROBA2: description and in-flight performance
Solar Physics, 286, pp.21-42

16. L. Feng, B. Inhester, **M. Mierla**
Comparisons of CME Morphological Characteristics Derived from Five 3D Reconstruction Methods
Solar Physics, 282, pp.221-238

17. T.G. Forbes, E.R. Priest, **D.B. Seaton**, Y.E. Litvinenko
Indeterminacy and instability in Petschek reconnection
Physics of Plasmas, 20, 052902, 2013, DOI: http://dx.doi.org/10.1063/1.4804337

18. C. Guennou, F. Auchere, J.A. Klimchuk, K. Bocchialini, **S. Parenti**
Can the Differential Emission Measure constrain the timescale of energy deposition in the corona?
Astrophysical Journal, 774, pp.31

19. **H. Gunell, J. De Keyser, E. Gamby,** I. Mann
Vlasov simulations of parallel potential drops in auroral flux tubes
Annales Geophysicae, 31, pp.1227-1240, 2013

20. **H. Gunell, J. De Keyser**, I. Mann
Numerical and laboratory simulations of auroral acceleration
Physics of Plasmas, 20, 102901, 2013, DOI: 10.1063/1.4824453

21. J.P. Halain, **D. Berghmans, D.B. Seaton, B. Nicula, A. De Groof, M. Mierla**, A. Mazzoli, J.-M. Defise, P. Rochus
The SWAP EUV Imaging Telescope. Part II: In-flight Performance and Calibration
Solar Physics, 286, pp.67-91

22. T. Hurtig, N. Brenning, **H. Gunell**
Relativistic Magnetic Flux Amplification
Pulsed Power Conference, 19th IEEE, ISSN 2158-4915, 2013, DOI: 10.1109/PPC.2013.6627640

23. I.W. Kienreich, N. Muhr, A.M. Veronig, **D. Berghmans, A. De Groof**, M. Temmer, B. Vrsnak, **D.B. Seaton**
Solar TErrestrial Relations Observatory-A (STEREO-A) and PRoject for On-Board Autonomy 2 (PROBA2) Quadrature Observations of Reflections of Three EUV Waves from a Coronal Hole
Solar Physics, 286, pp.125-142

24. E. Kilpua, A. Isavnin, A. Vourlidas, H. E. J. Koskinen, **L. Rodriguez**
On the relationship between interplanetary coronal mass ejections and magnetic clouds
Annales Geophysicae, 31, pp.1251-1265

25. M. Kretzschmar, **M. Dominique, I.E. Dammasch**
Sun-as-a-Star Observation of Flares in Lyman alpha by the PROBA2/LYRA Radiometer
Solar Physics, 286, pp.221-239

26. H. Lamy, E. Gamby, S. Ranvier, Y. Geunes, S. Calders, J. De Keyser
The BRAMS viewer: an online tool to access the BRAMS data
Proceedings of the International Meteor Conference (IMC2012), La Palma, Canary Islands, Spain, 20-23 September 2012, International Meteor Organisation, pp.48-50, 2013

27. J. Lilensten, M. Barthélémy, P.-O. Amblard, **H. Lamy, C.S. Wedlund**, V. Bommier, J. Moen, H. Rothkaehl, J. Eymard, J. Ribot
The thermospheric auroral red line polarization: confirmation of detection and first quantitative analysis
Journal of Space Weather and Space Climate, Volume 3, A01, 12 pp., 2013, DOI: 10.1051/swsc/2012023

28. O. Malandraki, **A. Devos**, M. Dumbovic, **L. Rodriguez, E. Robbrecht**, B. Vrsnak, + 20 authors
Statistical analysis of geomagnetic storms, coronal mass ejections and solar energetic particle events in the framework of the COMESEP project
EGU General Assembly, EGU2013-10389

29. **M. Mierla, D.B. Seaton, D. Berghmans**, I. Chifu, **A. De Groof**, B. Inhester, **L. Rodriguez**, G. Stenborg, **A.N. Zhukov**
Study of a Prominence Eruption using SWAP/PROBA2 and EUVI/STEREO Data

Solar Physics, 286, pp.241-253

30. P.M. Miller, M.E. Koepke, **H. Gunell**
Quasiperiodic mode hopping in competing ionization waves
Plasma Physics and Controlled Fusion, 56, 015003, 2014, DOI: 10.1088/0741-3335/56/1/015003

31. C. Munteanu, S. Haaland, B. Mailyan, **M. Echim**, K. Mursula
Propagation delay of solar wind discontinuities: Comparing different methods and evaluating the effect of wavelet denoising
Journal of Geophysical Research: Space Physics, Volume 118, Issue 7, pp.3985-3994, 2013

32. V. Pierrard, Y. Voitenko
Modification of the proton velocity distributions by Alfvénic turbulence in the solar wind
Solar Physics, 288, Issue 1, pp.355-368, 2013, DOI: 10.1007/s11207-013-0294-8

33. R. Pinto, R. Grappin, M. Velli, **A. Verdini**
Coupling the solar surface and the corona: coronal rotation, Alfvén wave-driven polar plumes
SOLAR WIND 13: Proceedings of the Thirteenth International Solar Wind Conference, AIP Conference Proceedings, 1539, pp.74-77

34. **L.A. Rachmeler**, S.E. Gibson, J. Dove, C.R. DeVore, Y. Fan
Polarimetric Properties of Flux-Ropes and Sheared Arcades in Coronal Prominence Cavities
Solar Physics, 288, pp.617-636

35. C.L. Raftery, D.S. Bloomfield, P.T. Gallagher, **D.B. Seaton, D. Berghmans, A. De Groof**
Temperature Response of EUV Imagers
Solar Physics, 286, pp.111-124

36. S. Ranvier, M. Anciaux, H. Lamy, J. De Keyser, S. Calders, E. Gamby
Radio polarization measurement of meteor trail echoes during the 2012 Perseids
Proceedings of the International Meteor Conference (IMC2012), La Palma, Canary Islands, Spain, 20-23 September 2012, International Meteor Organization, p. 51-55, 2013

37. N. Romanova, **N.B. Crosby**, V.A. Pilipenko
Relationship of World-Wide Rocket Launch Crashes with Geophysical Parameters
International Journal of Geophysics, Volume 2013, Article ID 297310

38. **D.B. Seaton, D. Berghmans, B. Nicula**, J.P. Halain, **A. De Groof**, T. Thibert, D.S. Bloomfield, C.L. Raftery, P.T. Gallagher, F. Auchere, J.-M. Defise, **E. D'Huys**, J.H. Lecat, E. Mazy, P. Rochus, L. Rossi, U. Schuehle, V.A. Slemzin, M.S. Yalim, J. Zender
The SWAP EUV Imaging Telescope Part I: Instrument Overview and Pre-Flight Testing
Solar Physics, 286, pp.43-65

39. D.B. Seaton, A. De Groof, P. Shearer**, D. Berghmans, B. Nicula**
SWAP Observations of the Long-Term, Large-Scale Evolution of the EUV Solar Corona
Astrophysical Journal, 777, pp.72

40. A.I. Shapiro, W. Schmutz, **M. Dominique**, A.V. Shapiro
Eclipses Observed by Large Yield RAdiometer (LYRA) - A Sensitive Tool to Test Models for the Solar Irradiance
Solar Physics, 286, pp.271-287

41. A.V. Shapiro, A. I. Shapiro, **M. Dominique, I.E. Dammasch**, C. Wehrli, E. Rozanov, W. Schmutz
Detection of Solar Rotational Variability in the Large Yield RAdiometer (LYRA) 190 - 222 nm Spectral Band
Solar Physics, 286, pp.289-301

42. V.A. Slemzin, L. K. Harra, Alexander Urnov, S.V. Kuzin, Farid Goryaev, **D. Berghmans**
Signatures of Slow Solar Wind Streams from Active Regions in the Inner Corona
Solar Physics, 286, pp.157-184

43. I. Tsagouri, A. Belehaki, **N. Bergeot**, C. Cid, **V. Delouille**, T. Egorova, N. Jakowski, L. Kutiev, A. Mikhailov, M. Nunez, M. Pietrella, A. Potapov, R. Qahwaji, Y. Tulunay, P. Velinov, A. Viljanen, J. Watermann
Progress in space weather modeling in an operational environment
Journal of Space Weather and Space Climate, 3, A17, 2013, DOI: 10.1051/swsc/2013037

44. Y. Tulunay, **N.B. Crosby**, E. Tulunay, **S. Calders**, A. Parnowski, D. Sulic
The COST Example for International Collaborative Outreach to the General Public: I Love My Sun
Journal of Space Weather and Space Climate, 3, 2013

45. **A. Verdini**, R. Grappin, R. Pinto, M. Velli
Building small scales in MHD turbulence
SOLAR WIND 13: Proceedings of the Thirteenth International Solar Wind Conference, AIP Conference Proceedings, 1539, pp.58-61

46. T. Verhulst, S.M. Stankov
The topside sounder database - data screening and systematic biases

Advances in Space Research, 51, Nr.11, pp.2010-2017, 2013, DOI: 10.1016/j.asr.2012.12.023

47. Y. Voitenko, V. Pierrard
Velocity-space proton diffusion in the solar wind turbulence
Solar Physics, 288, issue 1, pp.369-387, 2013, DOI: 10.1007/s11207-013-0296-6

48. **C. Simon Wedlund, H. Lamy**, B. Gustavsson, T. Sergienko, U. Brändström
Estimating energy spectra of electron precipitation above auroral arcs from ground-based observations with radar and optics
Journal of Geophysical Research: Space Physics, Volume 118, Issue 6, pp.3672-3691, 2013

49. J. Zender, **D. Berghmans**, D.S. Bloomfield, **C. Cabanas Parada, I.E. Dammasch, A. De Groof, E. D'Huys, M. Dominique**, P.T. Gallagher, **B. Giordanengo**, P. Higgins**, J.-F. Hochedez**, M.S. Yalim, **B. Nicula, E. Pylyser**, L. Sanchez-Duarte, G. Schwehm, **D.B. Seaton**, A. Stanger, **K. Stegen, S. Willems**
The Projects for Onboard Autonomy (PROBA2) Science Centre: Sun Watcher Using APS Detectors and Image Processing (SWAP) and Large-Yield Radiometer (LYRA) Science Operations and Data Products
Solar Physics, 286, pp.93-110

50. F. Zuccarello, L. Balmaceda, G. Cessateur, H. Cremades, S.L. Guglielmino, J. Lilensten, T. Dudok de Wit, M. Kretzschmar, F.M. Lopez, **M. Mierla, S. Parenti**, J. Pomoell, P. Romano, **L. Rodriguez**, N. Srivastava, R. Vainio, **M.J. West**, F.P. Zuccarello
Solar activity and its evolution across the corona
Journal of Space Weather and Space Climate, 3, A18

Presentations and posters at conferences

1. W. Aerts, Q. Baire, A. Bilich, C. Bruyninx, J. Legrand
On the Error Sources in Absolute Individual Antenna Calibrations
EGU General Assembly, Vienna, Austria, 7-12 April 2013

2. M. Barthelemy, H. Lamy
Can the thermospheric green line at 557nm be considered as a non-polarised standard?
EGU General Assembly 2013, Vienna, Austria, EGU2013-11350, 7-12 April 2013, (poster)

3. A. Belehaki, M. Hapgood, and the ESPAS Team
ESPAS, the near-Earth space data infrastructure for e-Science: architecture, data model and first release
EGU, 9th General Assembly, Vienna, Austria, 7-12 April 2013

4. A. Belehaki, I. Tsagouri, K. Tziotziou, I. Kutiev, P. Marinov, N. Bergeot, J.-M. Chevalier
Validation of the DIAS TEC Maps developed with the TaD Topside Profiler
ESWW10, Antwerp, Belgium, 18-22 November 2013 (poster)

5. R.D. Bentley, J. Aboudarham, D. Berghmans
Creating a Collaborative Environment for Space Weather
ESWW10, Session 7: "Data and Model Infrastructures for the Advancement of Space Weather Science and Services", Antwerp, Belgium, 18-22 November 2013 (poster)

6. R.D. Bentley, D. Berghmans, J. Aboudarham, and the CASSIS-Team
Using Standards to Make Data and Services in Solar system Science more Interoperable
Science Operations 2013 (SCIOPS 2013), "Working Together in Support of Science", ESA/ESO Conference at ESAC Madrid, Spain, 10-13 September 2013

7. R.D. Bentley, D. Berghmans, and the CASSIS Team
CASSIS
ESWW10, Splinter Session on "FP7 Projects", Antwerp, Belgium, 18-22 November 2013

8. J. Berckmans, E. Pottiaux
Advanced Multi-GNSS Troposphere Modelling for Improved Monitoring and Forecasting of Severe Weather
GfG2 Summer School 2013, Potsdam, Germany, 1-3 July 2013 (poster)

9. N. Bergeot, J.-M. Chevalier, C. Bruyninx, E. Pottiaux, Q. Baire, J. Legrand, P. Defraigne, W. Aerts
Ionospheric monitoring based on GNSS data - recent developments at ROB
STCE Workshop - Ionosphere: monitoring, research, services, Dourbes, Belgium, 14 May 2013

10. N. Bergeot, J.-M. Chevalier, C. Bruyninx, E. Pottiaux, Q. Baire, J. Legrand, P. Defraigne, W. Aerts
Space Weather products and studies based on EPN GNSS data at ROB
EPN Local Analysis Centres Workshop, Brussels, Belgium, 15-16 May 2013

11. N. Bergeot, I. Tsagouri, C. Bruyninx, J.-M. Chevalier
The Influence of Space Weather on Ionospheric Total Electron Content during the 23rd Solar Cycle
Beacon Satellite Symposium, Bath, UK, 8-12 July, 2013 (poster)

12. D. Berghmans, J. Andries, B. Nicula, P. Gallagher, B. Bentley
Making Solar FITS files interoperable
ESWW10, Antwerp, Belgium, 18-22 November 2013 (poster)

13. F.M. Boler, S. Wier, N. D'Agostino, R.M. Fernandes, A. Ganas, C. Bruyninx
New Collaboration Among Geodesy Data Centers in Europe and the US Facilitates Data Discovery and Access
AGU Fall Meeting, San Francisco, CA, USA, 9-13 December 2013 (poster)

14. C. Bruyninx, Q. Baire, J. Legrand, E. Pottiaux
The EUREF Permanent Network: Status and Strategy
EUREF 2013 Symposium, Budapest, Hungary, 6-8 June 2013

15. C. Bruyninx
The EUREF Permanent GNSS Network and its relation to EPOS
41st Workshop of the International School of Geophysics "A Roadmap for Earth Science in Europe: The next generation of Geophysical Research Infrastructures", Erice, Italy, 26 August - 4 September 2013 (invited)

16. S. Calders
Belgian RAdio Meteor Stations (BRAMS)
IMC 2013, Poznan, Poland, 2013 (poster)

17. J.-M. Chevalier, N. Bergeot, C. Bruyninx, J. Legrand, E. Pottiaux, Q. Baire, P. Defraigne, W. Aerts
Near-Real Time Ionospheric Products from the EUREF Permanent Network GPS data
Beacon Satellite Symposium, Bath, UK, 8-12 July 2013 (poster)

18. C. Cid, B. Schmieder, L. Rodriguez, and the ISSI International Team
Can a halo CME from the limb be geoeffective?
Nature of Prominences and their role in Space Weather Workshop, Paris, France, 10-14 June 2013

19. F. Clette
SSN 3 Workshop highlights: a summary
3rd SSN workshop, Tucson, AZ, USA, 21-25 January 2013

20. F. Clette, L. Lefèvre
Long-term variations in the sunspot number and sunspot properties
AGU Chapman Conference "Causes and Consequences of the Extended Solar Minimum between Solar Cycles 23 and 24 (4CESM)", Key Largo, FL, USA, 8-12 April 2013 (invited)

21. F. Clette, L. Lefèvre, L. Wauters
The International Sunspot Number revisited: from SIDC to SILSO
ESWW10, Antwerp, Belgium, 18-22 November 2013 (poster)

22. F. Clette, L. Wauters, L. Lefèvre
The stability of the Sunspot Number: reconstructions and lessons from the last 30 years
3rd SSN workshop, Tucson, USA, 21-25 January 2013

23. F. Clette, L. Wauters, L. Lefèvre
Revisiting the long-term calibration of the International Sunspot Number
Space Climate 5 meeting, Oulu, Finland, 15-19 June 2013

24. F. Clette, L. Wauters, L. Lefèvre
Long-term solar indices: current progresses and perspectives
TOSCA meeting, Prague, Czech Republic, 30 September - 4 October 2013

25. N.B. Crosby, A. Veronig, E. Robbrecht, L. Rodriguez, B. Vrsnak, S. Vennerstrom, O. Malandraki, S. Dalla, N. Srivastava, M. Hesse, D. Odstrcil
The COMESEP Alert System
ESWW10, Antwerp, Belgium, 18-22 November 2013 (poster)

26. N.B. Crosby, A. Veronig, E. Robbrecht, B. Vrsnak, S. Vennerstrom, O. Malandraki, S. Dalla, N. Srivastava, M. Hesse, D. Odstrcil
COMESEP: a new type of space weather alert system
EGU General Assembly 2013 meeting, Vienna, Austria, 7-12 April 2013

27. N.B. Crosby, D. Heynderickx, P. Jiggens, A. Aran, B. Sanahuja, S. Poedts, P. Truscott, F. Lei, S. Gabriel, I. Sandberg, A. Glover, A. Hilgers
The Updated Solar Energetic Particle Environment Modelling Tool
ESWW10, Antwerp, Belgium, 18-22 November 2013

28. Csillaghy, J. Aboudarham, D. Berghmans, C. Jacquey
An open platform for promoting interoperability in solar system sciences
EGU General Assembly 2013, ST5.1: "Space Weather and its Effects on Terrestrial and Geo-Space Environments: Science and Applications", Vienna, Austria, 7-12 April 2013 (poster)

29. I.E. Dammasch, M. Dominique
Correlation of solar flares with long-term irradiance and sunspot levels
ESWW10, Antwerp, Belgium, 18-22 November 2013 (poster)

30. I.E. Dammasch, L. Lefèvre
Correlation between sunspot numbers and EUV irradiance as observed by LYRA on PROBA2
ROB/SIDC, Brussels, Belgium, July 2013

31. F. Darrouzet, S. Ranvier, J. De Keyser, H. Lamy, J. Lichtenberger, P. Décréau
Detection of whistlers by the Belgian VLF antenna: Statistical analysis and comparison with Cluster data
EGU General Assembly, Vienna, Austria, 7-12 April 2013

32. H. De Backer, R. Van Malderen, A. Mangold
Ozone, UV, and aerosol observations in Uccle (Belgium) and Utsteinen (Antarctica)
WMO GAW Symposium 2013, Geneva, Switzerland, 18-20 March 2013 (poster)

33. J. De Keyser, E. Gamby, M. Kruglanski, S. Poedts, G. Lapenta, A. Lani, H. Deconinck D. Heynderickx
Why would a modeller take the trouble to comply with a shared modelling framework?
ESWW10, Session on Data and Model Infrastructures for the Advancement of Space Weather Science and Services, Antwerp, Belgium, 18-22 November 2013 (invited)

34. J. De Keyser, H. Lamy
Ionospheric studies at BISA: ionosphere-magnetosphere coupling in the auroral zone and the impact of meteors on the ionosphere
STCE Workshop on the Ionosphere, Brussels, Belgium, 14 May 2013

35. J. De Keyser, Y. Voitenko, M. Echim
The effects of plasma turbulence on the structure of discontinuities: application to aurora
Cluster 23rd workshop, Tromsø, Norway, 16-20 September 2013

36. V. Delouille
Visualization tools at ROB

SOLID Kick off meeting, Davos, Switzerland, 12-14 February 2013

37. V. Delouille, B. Mampaey, K. Stegen, R. Vansintjan
SDO Data center in Belgium
SOLARNET Kick-off meeting, Brussels, Belgium, 7-10 April 2013

38. R. De Visscher, V. Delouille
Predicting Flaring Activity through Supervised Classification on Predictor Variables
ESWW10, Antwerpen, Belgium, 18-22 November 2013

39. R. De Visscher, V. Delouille, P. Dupont
Preliminary Study on Predicting Flaring Activity
ESWW10, Antwerpen, Belgium, 18-22 November 2013 (poster)

40. A. Devos
Alert system for arrival and geo-effectiveness of CMEs
ISEST Workshop, Hvar, Croatia, 17-20 June 2013

41. A. Devos, M. Dumbović, L. Rodriguez, B. Vrsnak, S. Davor, D. Ruzdjak, E. Robbrecht, K. Leer, S. Vennerstrom, A. Veronig
Statistical Model for Predicting Arrival and Geoeffectiveness of CMEs Based on near Real-Time Remote Solar Observations
ESWW10, Antwerp, Belgium, 18-22 November 2013 (poster)

42. A. Devos, K. Stegen, R. Vansintjan, M.J. West, B. Mampaey, V. Delouille
The 'ideal' Collection of Data Sets for Space Weather Forecasting
ESWW10, Antwerp, Belgium, 18-22 November 2013

43. A. Devos, C. Verbeeck
Forecast verification of our space weather predictions
SIDC internal seminar, Brussels, Belgium, 9 October 2013

44. A. Devos, C. Verbeeck, E. Robbrecht
A Critical View on the Space Weather Forecasts at the Regional Warning Center in Belgium
ESWW10, Antwerp, Belgium, 18-22 November 2013

45. A. Devos, C. Verbeeck, E. Robbrecht, P. Vanlommel
Verification Analysis of space weather forecasts at the Regional Warning Center in Belgium
Second General Meeting of AFFECTS, Brussels, Belgium, 26-27 February 2013

46. A. Devos, M.J. West, K. Stegen, C. Marqué, C. Verbeeck, L. Rodriguez
The 'ideal' Collection of Data Sets for Space Weather Forecasting
Royal Astronomical Society Specialist Discussion Meeting "Space weather: a dialogue between scientists and forecasters", London, UK, 13 December 2013 (poster)

47. E. D'Huys, D.B. Seaton, K. Bonte, S.Poedts
Properties and Initiation Mechanisms for CMEs without distinct coronal signatures
ESWW10, Antwerp, Belgium, 18-22 November 2013 (poster)

48. M. Dierckxsens, I. Patsou, K. Tziotziou, M. Marsh, N. Lygeros, N.B. Crosby, S. Dalla, O. Malandraki
Statistical analysis of solar energetic particle events and related solar activity
EGU General Assembly 2013, Vienna, Austria, 7-12 April 2013

49. L. Dolla
Analysing spectral line profiles in the solar corona
Royal Observatory of Belgium, Uccle, 6 November 2013

50. L. Dolla, A.N. Zhukov
Non-Gaussian coronal spectral lines profiles in active region cores
CLW6, La-Roche-en-Ardenne, Belgium, 25-27 June 2013

51. M. Dominique, I.E. Dammasch, T. Katsiyannis, L. Wauters
The LYRA radiometer onboard PROBA2 as a detector of solar flares
ESWW10, Antwerp, Belgium, 18-22 November 2013 (poster)

52. M. Dominique, I.E. Dammasch, L. Wauters, T. Katsiyannis
LYRA status update
ESWW10, PROBA2 splinter, Antwerp, Belgium, 18-22 November 2013

53. M. Dominique, L. Wauters, I.E. Dammasch, T. Katsiyannis
How can PROBA2/LYRA contribute to the SOLID project (or to any other attempt to model the solar irradiance in the EUV)?
ESWW10, Antwerp, Belgium, 18-22 November 2013

54. Y. Dong, A. Verdini, R. Grappin
From 1AU solar wind turbulence backward to coronal turbulence: an inverse problem
EGU 2013, Vienna, Austria, 7-12 April 2013 (poster)

55. R. Fernandes, L. Bastos, C. Bruyninx, N. D'Agostino, J. Dousa, A. Ganas, M. Lidberg, J.-M. Nocquet
Current status of the EPOS WG4 - GNSS and Other Geodetic Data
EGU General Assembly, Vienna, Austria, 7–12 April 2013

56. C. Guennu, F. Auchère, J.A. Klimchuk, K. Bocchialini, S. Parenti
Exploring the Network of SDO Science
LWS-Solar Dynamics Observatory Science Workshop, MD, USA, 3-8 March 2013

57. G. Guerova, J. Jones, J. Dousa, G. Dick, S. De Haan, E. Pottiaux, O. Bock, R. Pacione, G. Elgered, H. Vedel
Advanced Global Navigation Satellite Systems tropospheric products for monitoring severe weather events and climate (GNSS4SWEC)
4th International Colloquium Scientific and Fundamental Aspects of the Galileo Programme 2013, Prague, Czech Republic, 4-6 December 2013

58. Gulisano, S. Dasso, P. Demoulin, L. Rodriguez
The dynamical behavior of Magnetic Clouds: From 0.3 to 5.4 astronomical units
Nature of Prominences and their role in Space Weather Workshop, Paris, France, 10-14 June 2013

59. H. Gunell, J. De Keyser, I. Mann
Vlasov simulations of auroral flux tubes
EGU General Assembly 2013, Vienna, Austria, 7-12 April 2013 (poster)

60. H. Gunell, J. De Keyser, I. Mann
Vlasov simulations of auroral processes
Presentation at the AGU Fall Meeting, San Francisco, CA, USA, 9-13 December 2013

61. H. Gunell, J. De Keyser, I. Mann
Vlasov simulations of auroral flux tubes
12th International Workshop on the Interrelationship between Plasma Experiments in Laboratory and Space (IPELS), Nagano, Japan, 1-5 July 2013

62. H. Gunell, J. De Keyser, I. Mann
Vlasov simulation of auroral processes
Cluster 23rd Workshop, Tromsø, Norway, 16-20 September 2013

63. H. Gunell, R. Maggiolo, G. Stenberg, H. Nilsson, M. Hamrin, T. Karlsson, N. Brenning, M. André, J. De Keyser
Fast plasmoids striking the magnetopause
Cluster 23rd Workshop, Tromsø, Norway, 16-20 September, 2013

64. M. Haberreiter, J. Beer, V. Delouille, B. Mampaey, C. Verbeeck, W. Schmutz
Long-term reconstruction of the solar EUV for planetary science applications
ESWW10, Antwerp, 18-22 November 2013

65. M. Haberreiter, M. Dasi, V. Delouille (and 15 other collaborators)
A Collaborative FP7 Effort towards the First European Comprehensive SOLar Irradiance Data Exploitation (SOLID)
EGU General Assembly 2013, Vienna, Austria, 7-12 April 2013

66. M. Haberreiter, V. Delouille, B. Mampaey, C. Verbeeck, I. Ermolli, M. Kretzschmar, M. Dominique, S. Wieman, W. Schmutz
Reconstruction of the Solar EUV Irradiance as observed with SOHO/SEM and PROBA2/LYRA
AGU 2013, San Francisco, CA, 9-13 December 2013

67. M. Haberreiter, C. Verbeeck, V. Delouille, I. Ermolli
Modeling the variations of the solar EUV spectrum
EGU 2013, Vienna, Austria, 7-12 April 2013 (poster)

68. M. Hapgood, A. Belehaki, F. Darrouzet, L. Spogli, B. Zolesi, and the ESPAS team
ESPAS and Cluster
Cluster, 23rd Workshop, Tromsø, Norway, 16-20 September 2013

69. M. Hernandez-Pajares, A. Aragon-Angel, P. Defraigne, N. Bergeot, R. Prieto-Cerdeira, J. Sanz, A. Garcia-Rigo
Higher Order Ionospheric Delay Effects and Mitigation in GNSS Signals for High Precision Applications
Beacon Satellite Symposium, Bath, UK, 8-12 July 2013 (poster)

70. M. Hernandez-Pajares, A. Aragon-Angel, J. Sanz, P. Defraigne, N. Bergeot, R. Priero-Cerdeira
Impact of Higher Order Ionospheric Delay on Precise GNSS Computation
4th International Colloquium, Scientific and Fundamental Aspects of the Galileo Programme, Prague, Czech Republic, 4-6 December 2013

71. L. Hetey
SPENVIS Java Geometry Definition Tool
SPENVIS User Workshop, Brussels, Belgium, 22-24 May 2013

72. L. Hetey
SPENVIS4 Tutorial: Geant4 package
SPENVIS User Workshop, Brussels, Belgium, 22-24 May 2013

73. D. Hubert, T. Verhoelst, A. Keppens, J. Granville, J.-C. Lambert, M. Allaart, T. Deshler, B. Johnson, R. Kivi, F. Schmidlin, H. Smit, W. Steinbrecht, R. Stübi, D. Tarasick, A. Thompson, M. Tully, R. Van Malderen, P. von der Gathen
Assessment of the internal consistency of the NDACC ozonesonde network by comparison with the satellite system of ozone profilers
Atmospheric Composition Validation and Evolution (ACVE) Workshop, ESA-ESRIN, Frascati, 13-15 March 2013

74. T. Hurtig, N. Brenning, H. Gunell
Relativistic Magnetic Flux Amplification
IEEE Pulsed Power & Plasma Science, San Francisco, California, USA, 16-21 June 2013

75. J. Ihde, Z. Altamimi, E. Brockmann, C. Bruyninx, A. Caporali, R. Dach, J. Dousa, R. Fernandes, H. Habrich, A. Kenyeres, M. Lidberg, R. Pacione, M. Poutanen, W. Söhne, G. Stangl, J. Torres
EUREF's GNSS Infrastructure Real Time and Galileo Ready
IAG Scientific Assembly 2013, Potsdam, Germany, 1-6 September 2013 (poster)

76. J. Jones, G. Guerova, O. Bock, S. De Haan, G. Dick, J. Dousa, G. Elgered, R. Pacione, E. Pottiaux, H. Vedel
Advanced GNSS Tropospheric Products for monitoring Severe Weather Events and Climate (GNSS4SWEC)
COST ES1206 Kickoff Meeting, Brussels, Belgium, 17 May 2013

77. J. Jones, G. Guerova, J. Dousa, O. Bock, H. Vedel, E. Pottiaux, G. Dick, S. De Haan, R. Pacione
COST ES1206: Advanced GNSS Tropospheric Products for Monitoring Extreme Weather Events and Climate
EUREF Symposium 2013, Budapest, Hungary, 29-31 May 2013

78. J. Jones, G. Guerova, J. Dousa, S. De Haan, O. Bock, G. Dick, E. Pottiaux, R. Pacione, H. Vedel, G. Elgered
COST Action ES1206: Advanced GNSS Tropospheric Products for Monitoring Severe Weather and Climate
IAG Scientific Assembly 2013, Potsdam, Germany, 1-6 September 2013 (poster)

79. J. Jones, G. Guerova, J. Dousa, S. De Haan, O. Bock, G. Dick, E. Pottiaux, R. Pacione, H. Vedel, G. Elgered
COST Action ES 1206: Advanced Global Navigation Satellite Systems Tropospheric Products for Monitoring Severe Weather Events and Climate (GNSS4SWEC)
RMI Centenary Meeting, Brussels, Belgium, 26-27 September 2013 (poster)

80. O. Karatekin, J. De Keyser
PICASSO: A triple CubeSat mission for atmospheric and space science
Atelier: Quels débouchés pour les nanosatellites? Observatoire de Paris, Meudon, 25-26 November 2013

81. E. Kilpua, A. Isavin, A. Vourlidas, H. Koskinen, L. Rodriguez
On the relationship between interplanetary coronal mass ejections and magnetic clouds
EGU General Assembly 2013, Vienna, Austria, 7-12 April 2013

82. E. Kraaikamp, C. Verbeeck
Solar Demon: Dimming and EUV wave Monitor for Space Weather
ESWW10, Antwerp, Belgium, 18-22 November 2013

83. E. Kraaikamp, C. Verbeeck
Solar Demon: Dimming and EUV wave Monitor for Space Weather
ESWW10, Antwerp, Belgium, 18-22 November 2013 (poster & demo)

84. E. Kraaikamp, C. Verbeeck
Solar Demon: Near real-time dimming and EUV wave detection on SDO-AIA
Second AFFECTS General Meeting, Brussels, Belgium, 26-27 February 2013

85. E. Kraaikamp, C. Verbeeck
Solar Demon: Near real-time dimming and EUV wave detection on SDO-AIA
AFFECTS User Workshop, Brussels, Belgium, 28 February 2013

86. E. Kraaikamp, C. Verbeeck, and the AFFECTS team
Solar Demon: Dimming and EUV wave Monitor on SDO-AIA
Space Weather Workshop, Boulder, CO, USA, 16-19 April 2013 (poster)

87. M. Kretzschmar, M. Dominique, I.E. Dammasch
Solar EUV irradiance during solar cycle 24 as observed by PROBA2/LYRA and SDO/EVE
EGU General Assembly, Vienna, Austria, 7-12 April 2013

88. M. Kruglanski, A. Devos, L. Wauters, S. Chabanski, and the SN-IV Consortium
ESA SSA Space Weather Coordination Centre
ESWW10, Antwerp, Belgium, 18-22 November 2013 (demo)

89. M. Kruglanski, S. Chabanski, S. Calders, N. Messios, L. Hetey, S. Hallet, V. Pierrard, N.B. Crosby
Space weather activities at the Belgian Institute for Space Aeronomy
ESWW10, Antwerp, Belgium, 18-22 November 2013 (poster)

90. Q. Laffineur, H. De Backer, A. Delcloo, J. Nemeghaire, F. Debal
Quality control on the retrieval of mixing layer height by LIDAR-ceilometer
EGU General Assembly 2013, Vienna, 7-12 April 2013

91. Q. Laffineur, H. De Backer, J. Nemeghaire, F. Debal
Illustration of physical processes with LIDAR ceilometer measurements
Third Joint Meeting on meteorological applications and forecasts including warnings, Brussels, Belgium, 21-22 November 2013

92. L. Lefèvre
Detailed Sunspot Catalogs

SOLID Kick-off Meeting, Davos, Switzerland, February 2013

93. L. Lefèvre
Towards a reconstruction of detailed sunspot information over the last 150 years
EGU Meeting, Vienna, Austria, 7-12 April 2013

94. L. Lefèvre
Dissemination in the TOSCA project
TOSCA Meeting, GHOST group, Tromsø, Norway, August 2013

95. L. Lefèvre
Dissemination in the TOSCA project
TOSCA Meeting, Prague, Czech Republic, October 2013

96. L. Lefèvre, F. Clette
Sunspots behaviour during the recent Solar Minimum
Third Sunspot Workshop, Tucson, Arizona, USA, 22-25 January 2013

97. L. Lefèvre, F. Clette
A new Sunspot Number: Diagnostics of recent and past trends in Sunspot statistics
Asia-Oceania Space Weather Alliance (AOSWA) Workshop, Kunming, China, November 2013 (invited)

98. L. Lefèvre, M. Dumbovic, S. Vennerstrom, F. Clette
Historical Analysis of Sun-Earth Connections in the context of extreme Space Weather events
International Space Climate Symposium 5, Oulu, Finland, June 2013

99. L. Lefèvre, S. Vennerstrom, M. Dumbovic
Historical Analysis of Sun-Earth Connections in the context of extreme Space Weather events
ESWW10, Antwerp, Belgium, 18-22 November 2013 (poster)

100. J. Lemaire, M. Echim, O. Lie-Svendsen
On the kinetic and multi-fluid modeling of the supersonic solar wind expansion
IAGA 2013, XII Scientific Assembly Merida Yucatan Mexico, 26-31 August 2013

101. J. Lilensten, M. Barthelemy, H. Lamy, C. Simon, V. Bommier, P.-O. Amblard, J. Moen, H. Rothkaehl
The thermospheric auroral red line polarization: confirmation of detection and first quantitative analysis
EGU General Assembly 2013, Vienna, Austria, EGU2013-1170, 7-12 April 2013 (poster)

102. J. Magdalenić, V. Krupar, C. Marqué, M. Mierla, A.N. Zhukov, L. Rodriguez, M. Maksimović, B. Cecconi
The CME-driven shock wave on 05 March 2012
CESRA Workshop 2013 - New eyes looking at solar activity: Challenges for theory and simulations, Prague, Czech Republic, 24-29 June 2013

103. J. Magdalenić, V. Krupar, C. Marqué, M. Mierla, A.N. Zhukov, L. Rodriguez, M. Maksimović, B. Cecconi
Tracking the CME-driven shock wave on 05 March 2012
Kanzelhöhe Colloquium 2013 - Solar activity in the ascending phase of cycle 24, Kanzelhöhe, Austria, 8-10 October 2013

104. J. Magdalenić, R. Madden, C. Marqué
Characteristics of Multiple Type II Radio Bursts
CESRA workshop 2013 – New eyes looking at solar activity: Challenges for theory and simulations, Prague, Czech Republic, 24-29 June 2013 (poster)

105. J. Magdalenić, R. Madden, C. Marqué
Radio Signatures of Multiple Shock Waves
ESWW10, Antwerp, Belgium, 18-22 November 2013 (poster)

106. O. Malandraki, A. Devos, and the COMESEP Team
Statistical analysis of geomagnetic storms, coronal mass ejections and solar energetic particle events in the framework of the COMESEP project
EGU, Vienna, Austria, 7-12 April 2013 (poster)

107. V. Malisse, C. Verbeeck
STAFF: The Solar Timelines viewer for AFFects
Second AFFECTS General Meeting, Brussels, Belgium, 26-27 February 2013

108. V. Malisse, C. Verbeeck
STAFF: The Solar Timelines viewer for AFFects
AFFECTS User Workshop, Brussels, Belgium, 28 February 2013

109. V. Malisse, C. Verbeeck
The STAFF viewer: a powerful tool for space weather forecasters and researchers
NOAA-SWPC, Boulder, CO, USA, 25 July 2013

110. V. Malisse, C. Verbeeck
Online demo of the STAFF viewer: a powerful tool for space weather forecasters
ESWW10, Antwerp, Belgium, 18-22 November 2013 (demo at Fair)

111. V. Malisse, C. Verbeeck
The STAFF viewer: a powerful tool for space weather forecasters
ESWW10, AFFECTS splinter, Antwerp, Belgium, 18-22 November 2013

112. V. Malisse, C. Verbeeck
The STAFF viewer: a powerful tool for space weather forecasters and researchers
ESWW10, Antwerp, Belgium, 18-22 November 2013 (poster)

113. B. Mampaey, V. Delouille
Segmentation of EUV image in view of SSI reconstruction
First Annual Meeting SOLID, Orléans, France, 14-18 October 2013

114. N.Messios, L. Hetey, S. Calders, E. de Donder, M. Kruglanski
SPENVIS Interface to Geant4 based tools
Ninth Geant4 Space Users Workshop, Barcelona, Spain, 4-6 March 2013

115. M. Mierla, I. Chifu, B. Inhester, L. Rodriguez, A.N. Zhukov
Low polarized emission from the core of coronal mass ejections
IAU 300, Nature of Prominences and their role in Space Weather Workshop, Paris, France, 10-14 June 2013

116. M. Mierla, G. Dima, E. Moise, L. Rodriguez, D.B. Seaton
3D reconstruction of a sigmoidal active region
CLW6, La Roche, Belgium, 25-27 June 2013 (poster)

117. M. Mierla, E. Kilpua, L. Rodriguez, E. D'Huys, F.P. Zuccarello, A.N. Zhukov, D.B. Seaton
Study of stealth CMEs arriving at the Earth in the period 2009 – 2010
ESWW10, Antwerp, Belgium, 18-22 November 2013 (poster)

118. M. Mierla, D.B. Seaton, D. Berghmans, I. Chifu, A. De Groof, B. Inhester, L. Rodriguez, G. Stenborg, A.N. Zhukov
Study of a Prominence Eruption using PROBA2/SWAP and STEREO/EUVI Data
EGU General Assembly 2013, Vienna, Austria, 7-12 April 2013 (poster)

119. S. Parenti
Theory & modeling support/preparatory science: What do we need? How do we implement it?
12th Science Working Team, London, UK, 18-21 February 2013

120. S. Parenti
Community-driven Sun-Heliosphere: modeling efforts for science planning
3rd Science Operation Working Group, ESTEC, 10-11 April 2013

121. S. Parenti
SPICE collaborations with other instruments
SPICE consortium meeting, 23-24 May 2013

122. S. Parenti and the EUI team
An overview of the Extreme Ultraviolet Imager suite for Solar Orbiter
Meeting of the Italian Community in Solar and Heliospheric Physics, Catania, Italy, 4-6 September 2013

123. S. Parenti, J.-C. Vial
On the nature of the prominence-corona transition region
IAUS 300, Nature of Prominences and their role in Space Weather, Paris, France, 10-14 June 2013

124. S. Parenti, M.J. West
Comparing radiative signatures of cooling in coronal loops
International Space Science Institute (ISSI) meeting on "Coronal Heating: Using Observables", Bern, Switzerland. 27 February-1 March 2013

125. V. Pierrard
The kinetic approach to model the solar wind
Astronum 2013, Biarritz, France, 1-5 July 2013 (invited)

126. V. Pierrard
Kappa distributions in space plasmas: possible origin and consequences
AGU meeting, San Francisco, USA, 9-13 December 2013 (invited)
SOLID WP2 Workshop, Orléans, France, 14-15 October 2013

127. V.Pierrard, K. Borremans, F. Darrouzet, J. Lemaire
A 3D model of the plasmasphere to study its links with other regions of the magnetosphere
ESWW10, Antwerpen, Belgium, 18-22 November 2013 (invited)

128. V. Pierrard, M. Lazar
Kinetic models for space plasmas: the influence of suprathermal particles and the wave turbulence
16th Conference on Plasma Physics and Applications (CPPA2013), Magurele, Bucharest, Romania, 20-25 June 2013 (poster)

129. S. Poedts, G. Lapenta, A. Lani, H. Deconinck, B. Fontaine, J. Depauw, F. Diet, H.N. Diep, N. Mihalache, D. Heyndrickx, J. Dekeyser, N.B. Crosby, L. Rodriguez, R. Van der Linden
The ESA Virtual Space Weather Modelling Centre - Phase 1
ESWW10, Antwerp, Belgium, 18-22 November 2013

130. S. Poedts, G. Lapenta, H. Deconinck, A. Lani, B. Fontaine, J. Depauw, F. Diet, H.H. Diep, N. Mihalache, D. Heynderickx, J. De Keyser, N.B. Crosby, L. Rodriguez, R. Van der Linden
The ESA Virtual Space Weather Modelling Centre - Phase 1B
ESWW10, Antwerp, Belgium, 18-22 November 2013

131. E. Pottiaux
E-GVAP Activities at ROB in 2013

E-GVAP III Joint Expert Team Meeting 2013, Copenhagen, Denmark, 27-29 November 2013

132. E. Pottiaux, W. Aerts, Q. Baire, J. Berckmans, P. Defraigne, C. Bruyninx, J.-M. Chevalier, P. Defraigne, J. Legrand, D. Mesmaker, A. Moyaert
EPN-Related Activities and Research at ROB: Status and Challenges
EPN LAC Workshop 2013, Brussels, Belgium, 15-16 May 2013

133. E. Pottiaux, J. Berckmans, C. Bruyninx
Remote Sensing of Atmospheric Water Vapor using GNSS Signals: From Monitoring Severe Weather to Climate
RMI Centenary Meeting, Brussels, Belgium, 26-27 September 2013 (poster)

134. E. Pottiaux, J. Berckmans, C. Bruyninx
COST ES1206: Contribution of the Royal Observatory of Belgium to WG1 Activities
COST Action ES1206 - 1st WG Meeting, Valencia, Spain, 16-17 October 2013

135. E. Pottiaux, J. Berckmans, C. Bruyninx
COST ES1206: Contribution of the Royal Observatory of Belgium to WG2 Activities
COST Action ES1206 - 1st WG Meeting, Valencia, Spain, 16-17 October 2013

136. R. Qahwaji, P. Vanlommel, J. Lilensten
Promoting citizen science for space weather research and applications: splinter organization
ESWW10, Brussels, Belgium, 18-22 November 2013

137. L.A. Rachmeler, S.J. Platten, C.W. Bethge, D.B. Seaton, A.R. Yeates
From a double-helmet streamer to a pseudostreamer
Hinode 7 conference, Takayama, Japan, 12 November 2013

138. L.A. Rachmeler, S.J. Platten, A.R. Yeates, D.B. Seaton, C.W. Bethge
Magnetic properties of coronal pseudostreamers
IAUS 300, Nature of prominences and their role in space weather, Paris, France, 10 June 2013

139. S. Ranvier, P. Cardoen, J. De Keyser, D. Pieroux
A Novel Langmuir Probe Instrument for CubeSats
5th European CubeSat Symposium, Brussels, Belgium, June 2013

140. S. Ranvier, H. Lamy, M. Anciaux, J. De Keyser
Radio Polarization Measurements of Meteor Trail Echoes with BRAMS
IMC 2013, Poznan, Poland, August 2013

141. S. Ranvier, D. Pieroux, J. De Keyser, D. Fussen, P. Cardoen, M. Echim, H. Lamy, H. Gunell, I. Mann, A. Tjulin
Space weather investigation with PICASSO
ESWW10, Antwerp, Belgium, 18-22 November 2013

142. L. Rodriguez
ISEST WG 4, Campaign Event Group description
ISEST Workshop (International Study of Earth-Affecting Solar Transients), Hvar, Croatia, 17-20 June 2013

143. L. Rodriguez, A. Devos, B. Bourgoignie, E. Kraaikamp, B. Nicula, K. Bonte, C. Verbeeck, N.B. Crosby, M. Dierckxsens, S. Calders, M. Kruglanski, A. Veronig, T. Rotter, M. Temmer, B. Vrsnak, M. Dumbovic, T. Zic, J. Calogovic, S. Vennerstrom, K. Leer, O. Malandraki, K. Tziotziou, I. Patsou, N. Lygeros, S. Dalla, M. Marsh
The COMESEP space weather alert system
ESWW10, Antwerp, Belgium, 18-22 November 2013
Second AFFECTS General Meeting, Brussels, Belgium, 26-27 February 2013

144. L. Rodriguez, and the Solar Influences Data Analysis Center (SIDC) team
Space weather services at the Royal Observatory of Belgium
European Week of Astronomy and Space Science, Turku, Finland, 8-13 July 2013 (invited)

145. D. Sapundjiev, S.M. Stankov
A single-station F-layer critical frequency model from the Dourbes digisonde data
ESWW10, Antwerp,Belgium, 18-22 November 2013 (poster)

146. D. Sapundjiev, S.M. Stankov, J.C. Jodogne
Data analysis of Dourbes neutron monitor data for solar events forecast
ESWW10, Antwerp, Belgium, 18-22 November 2013 (poster)

147. D. Sapundjiev, S.M. Stankov, J.C. Jodogne
Monitoring of the cosmic rays intensity at the RMI
RMI Conference on Ionosphere and Space Weather, Brussels, Belgium, 4 December 2013

148. D. Sapundjiev, S.M. Stankov, T. Verhulst, J.C. Jodogne
Ionospheric and cosmic ray monitoring - recent developments at the RMI
STCE Workshop on Ionosphere, Dourbes, Belgium, 14 May 2013

149. B. Schmieder, S.Parenti, J. Dudik , G.Aulanier, P. Heinzel, L.Golub, M. Zapior, P. Schwartz, S. Gunar
Solar prominences in SDO/AIA channels and MHD model of bubbles
LWS-Solar Dynamics Observatory Science Workshop, MD, USA, 3-8 March 2013

150. D.B. Seaton, K.K. Reeves, T.G. Forbes

The role of magnetic reconnection in CME energetics: Lessons learned from analytical theory!
ESWW10, Antwerp, Belgium, 18-22 November 2013

151. P. Vanlommel
Dissemination and education
eHEROES First annual meeting, Leuven, Belgium, 6 February 2013

152. P. Vanlommel
Communication, dissemination and exploitation
EUI consortium meeting, Davos, Swiss, 3 March 2013

153. R. Van Malderen
Klimaatverandering en de broeikasgassen waterdamp en ozon
Colloquium 100 jaar KMI, Brussel, 29 September 2013

154. R. Van Malderen, H. Brenot, E. Pottiaux, S. Beirle, C. Hermans, M. De Mazière, T. Wagner, H. De Backer, C. Bruyninx
Evaluating satellite retrievals of Integrated Water Vapor (IWV) data by co-located ground-based devices for climate change analysis
Joint EUMETSAT/AMS Meteorological Satellite Conference, Vienna, Austria, 16-20 September 2013

155. R. Van Malderen, E. Pottiaux, H. Brenot
Water Vapor, Meteorology, and Climate
STCE Annual Meeting 2013, Brussels, Belgium, 7 June 2013

156. R. Van Malderen, E. Pottiaux, H. Brenot, S. Beirle, C. Hermans, M. De Mazière, T. Wagner, H. De Backer, C. Bruyninx
The Integrated Water Vapor project in Belgium: techniques intercomparison and time series analysis
COST Action ES1206 (GNSS4SWEC) - 1st WG Meeting, Valencia, Spain, 16-17 October 2013 (invited)

157. R. Van Malderen, E. Pottiaux, H. Brenot, S. Beirle, T. Wagner, C. Hermans, M. De Mazière, H. De Backer, C. Bruyninx
Techniques Intercomparison of Integrated Water Vapor Measurements for Climate Change Analysis
RMI Centenary Meeting, Brussels, Belgium, 26-27 September 2013 (poster)

158. S. Vennerstrom, L. Lefèvre, M. Dumbovic, N.B. Crosby, F. Clette, A. Veronig, B. Vrsnak, K. Leer
The 100 Largest Geomagnetic Storms in the Last 150 Years
ESWW10, Antwerp, Belgium, 18-22 November 2013

159. V. Ventouras, A. Belehaki, M. Hapgood, and the ESPAS Team
Accessing near-Earth space data through the ESPAS e-science platform: an overview of the system design and demonstration of the first working prototype
ESWW10, Antwerp, Belgium, 18-22 November 2013

160. C. Verbeeck, V. Delouille, R. De Visscher, B. Mampaey, M. Haberreiter
Determination of filling factors of Active Regions, Coronal Holes and Quiet Sun for the EIT archive 1997-2011
EGU General Assembly 2013, Vienna, Austria, 7-12 April 2013 (poster)

161. C. Verbeeck, V. Delouille, B. Mampaey, R. De Visscher
Automatic segmentation of EUV images for reconstruction of SSI
SOLID Kick-off Meeting, Davos, Switzerland, 12-14 February 2013

162. C. Verbeeck, V. Delouille, B. Mampaey, R. De Visscher
SPoCA: software for extraction, characterization, and tracking of Active Regions and Coronal Holes on EUV images
SIDC seminar, Brussels, Belgium, 3 May 2013

163. A. Verdini
Which kind of coronal turbulence? Constraints from heliospheric data, a numerical approach to the inverse problem.
Solar Probe Plus workshop, Pasadena, CA, USA, 27 March 2013

164. A. Verdini
Turbulence in the Expanding Solar Wind or How expansion affects anisotropy in MHD turbulence
First CHARM annual meeting, ROB, Brussels, Belgium, 18 April 2013

165. A. Verdini
Anisotropy of solar wind turbulence, the role of expansion
SoHe 2013, Catania, Italy, 4 September 2013

166. A. Verdini
MHD turbulence in the expanding solar wind
Arcetri Workshop on Plasma Astrophysics, Firenze, Italy, 14 October 2013

167. T. Verhulst, D. Sapundjiev, M. Nemry, S.M. Stankov
Improving the local ionospheric electron density reconstruction profile
International Beacon Satellite Symposium (BSS), Bath, UK, 8-12 July 2013

168. T. Verhulst, S.M. Stankov
Comparison of topside ionospheric profilers for use in modelling and monitoring applications
EGU General Assembly, Geophysical Research, Vienna, Austria, 7-12 April 2013

169. T. Verhulst, S.M. Stankov
The LIEDR model - recent and future improvements
RMI Conference on Ionosphere and Space Weather, Brussels, Belgium, 12 June 2013

170. T. Verhulst, S.M. Stankov
On improving the topside ionospheric modelling by selecting an optimal electron density profiler
International Reference Ionosphere (IRI) Workshop "IRI and GNSS", Olsztyn, Poland, 24-28 June 2013

171. G. Voitcu, M. Echim
Kinetic modeling and simulations of tangential discontinuities
16th International Conference on Plasma Physics and Applications, Magurele, Romania, 20-25 June 2013

172. G. Voitcu, M. Echim, R. Marchand
Forward and backward test-kinetic simulations of non-Maxwellian velocity distribution functions in space plasmas
EGU General Assembly, Vienna, Austria, 7-12 April 2013

173. G. Voitcu, M. Echim, R. Marchand
Forward and backward test-kinetic simulations of non-Maxwellian velocity distribution functions in space plasmas
16th International Conference on Plasma Physics and Applications, Magurele, Romania, 20-25 June 2013

174. G. Voitcu, M. Echim, R. Marchand
Kinetic simulations of plasma interfaces and discontinuities
11th International School/Symposium for Space Simulations, Jhongli, Taiwan, 19-29 July 2013

175. Y. Voitenko, J. De Keyser, V. Pierrard, J.S. Zhao, D.J. Wu
MHD-kinetic Transition in Alfvénic Turbulence and Particles
Second UK-Ukraine Meeting on Solar Physics and Space Science, 16-20 September 2013, Kyiv, Ukraine (invited)

176. Y. Voitenko, J. De Keyser, V. Pierrard, J.S. Zhao, D.J. Wu
What happens with MHD turbulence at the end of inertial range?
STORM-2013 Annual meeting, Graz, Austria, 25-26 November 2013

177. B. Vrsnak, T. Zic, M. Dumbovic, J. Calogovic, A. Veronig, M. Temmer, C. Moestl, T. Rollet, L. Rodriguez
Heliospheric propagation of ICMEs: The Drag-Based Model
ESWW10, Antwerp, Belgium, 18-22 November 2013 (poster)

178. M.J. West, L. Dolla, C. Marque, D.B. Seaton, T. Van Doorsselaere, M. Dominique, D. Berghmans , C. Cabanas, A. De Groof, W. Schmutz, A. Verdini, J. Zender, A.N. Zhukov
Quasi-Periodic Pulsations during the onset of solar flares: multi-instrumental comparison
LWS/SDO Science Workshop, Cambridge, MD, USA, 3-8 March 2013(poster)

179. M.J. West, D.B. Seaton, M. Dominique, D. Berghmans, B. Nicula, E. Pylyser, K. Stegen, J. De Keyser
Space Weather and Particle Effects on the Orbital Environment of PROBA2
EGU General Assembly, Vienna, Austria, 7-12 April 2013

180. M.J. West, D.B. Seaton, M. Dominique, D. Berghmans, J. Zender, K. Stegen, E. Pylyser
PROBA2 a Space Weather Monitor
ESWW10, Antwerp, Belgium, 18-22 November 2013

181. M.J. West, A.N. Zhukov, J. Klimchuk
Cross-sectional properties of coronal loops
CLW6, La-Roche-en-Ardenne, Belgium, 25-27 June 2013

182. A.N. Zhukov
How to choose the best target for the high-resolution payload of Solar Orbiter? Modeling perspective
Annual meeting of the IUAP network “CHARM”, Brussels, Belgium, 18-19 April 2013

183. A.N. Zhukov
How to choose the best target for the high-resolution payload of Solar Orbiter? A space weather forecaster’s perspective
Solar Orbiter/EUI Consortium meeting, Davos, Switzerland, 11-14 March 2013

184. F.P. Zuccarello, D.B. Seaton, M. Mierla, S. Poedts, L.A. Rachmeler, P. Romano, F. Zuccarello
Torus Instability as trigger mechanism for CMEs: the 2011 August 4 filament eruption
ESWW10, Antwerp, Belgium, 18-22 November 2013 (poster)

Public Outreach: Talks and publications for the general public

1. N. Bergeot
La Recherche en Antarctique
Open Doors Space Pole, Brussels, Belgium, 25 & 26 May 2013

2. N. Bergeot
GNSS based space weather applications
Visit French Defense Ministry (L. Birée) at Space Pole, Brussels, Belgium, 4 July 2013

3. N. Bergeot
Ionospheric products from ROB
Visit of KPN to SSCC, SSCC-room, Brussel, Belgium, 10 July 2013

4. N. Bergeot
Effet de l'activité solaire sur l'ionosphère et sur les mesures de positionnement en GNSS
Contribution for the 2013 contest of the royal academy, Group II - Astronomy - Physic b, 2013

5. C. Bruyninx, J. Legrand, D. Mesmaker, A. Moyaert, Q. Baire
Gestion du réseau GNSS permanent européen à l'Observatoire royal de Belgique
Revue XYZ, Association Française de la Topographie, Nr. 134, Mars 2013, ISSN 0290-9057, pp.37-44

6. F. Clette
Vers un Soleil plus actif ou un retour au calme? A surveiller de près…
Cercle Astronomique Mosan, Dinant, Belgium, 4 May 2013

7. F. Clette
Enfants du Soleil: évolution et influences de l'activité solaire
51ème Congrès pluraliste des Sciences, ULB, Brussels, Belgium, 22 July 2013

8. F.Clette
Du GPS au climat: l'emprise du Soleil sous haute surveillance
SEII, Société Européenne des Ingénieurs et des Industriels (SEII), Brussels, Belgium, 29 November 2013

9. N.B. Crosby
Introduction and chapter 1 of e-book "Self-Organized Criticality Systems"
Open Academic Press, Berlin, Warsaw, pp.1-22

10. F. Darrouzet, S. Ranvier, H. Lamy, J. De Keyser
Belgian Institute for Space Physics project to detect whistlers with VLF measurements
VERSIM Newsletter 28, December 2013

11. J. De Keyser, D. Pieroux, P. Cardoen
Science sensors and instruments for remote-sensing observations
VKI Lecture Series 2013 on CubeSat Technology and Applications, Von Karman Institute, Sint-Genesius-Rode, Belgium, 30 January 2013

12. J. De Keyser, D. Pieroux, P. Cardoen
Science sensors and instruments for remote-sensing observations
CubeSat Technology and Applications, R. Reinhard and C. O. Asma (eds.), VKI Lecture Series 2013-01, ISSN 0377-8312, pp.II.1-25, January 2013

13. V. Delouille
Les saisons du soleil et leur influence sur l'environnement terrestre
Open Doors Space Pole, Brussels, Belgium, 26 May 2013

14. E. D'Huys
Junior College Introductory Session
Kick-off meeting Junior College, KULeuven, Kortrijk, Belgium, 8 & 10 January 2013

15. E. D'Huys
PROBA2
PROBA2@school sessions for high school students, Klein Seminarie, Hoogstraten, Belgium, 26 March 2013

16. L. Dolla
Etudier la couronne solaire grâce aux techniques spectroscopiques
Visit of students of Université de Mons at ROB, Brussels, Belgium, 23 April 2013

17. M. Dominique
PROBA2 et l'activité solaire
Open Doors Space Pole, Brussels, Belgium, 25 May 2013

18. J. Janssens
Het voorspellen van zonnevlammen
PROBA2@school sessions for high school students, Klein Seminarie, Hoogstraten, Belgium, 26 March 2013

19. J. Janssens
Solar Cycle 24: een zonnecyclus op drift?
ASH Polaris, Herentals, Belgium, 5 April 2013

20. J. Janssens
De kunst van het zonnewaarnemen
RACA star party, Observatoire Centre Ardenne, Grapfontaine-Neufchateau, Belgium, 10 May 2013

21. J. Janssens
Zonnewaarnemingen
Public Observatory MIRA, Grimbergen, Belgium, 14 June 2013

22. J. Janssens
28 years of solar observations
Seminar at Space Pole, Brussels, Belgium, 25 October 2013

23. J. Janssens
Het Ruimteweer
Cosmodrome, Genk, Belgium, 14 November 2013

24. J. Janssens
Het Ruimteweer: stormachtige verhalen over onze ster
GALILEO, Heerlen, The Netherlands, 7 December 2013

25. E. Kraaikamp
Discussing AutoStakkert!2 lucky imaging software
Astrophotography meeting of Dutch speaking amateur astronomers, Oss, the Netherlands, 27 April 2013

26. E. Kraaikamp
*Astrofotografie van Zon, Maan, Planeten en Deeps*ky
Open Doors Space Pole, Brussels, Belgium, 25 & 26 May 2013

27. E. Kraaikamp
Lucky-imaging with AutoStakkert!2 and image processing techniques for amateur astronomers practicing planetary astrophotography
Workshop at the Norddeutsche Tagung der Planetenfotografen, Bremervörde, Germany, 5 October 2013

28. L. Lefèvre
De quelle façon mesure-t-on l'activité solaire?
Open Doors Space Pole, Brussels, Belgium, 25 & 26 May 2013

29. C. Marqué
La météorologie de l'espace
Open Doors Space Pole, Brussels, Belgium, 25 & 26 May 2013

30. D.B. Seaton
Effective scientific presentations
Space Science Training Week 2013, KULeuven, Leuven, Belgium, 16-19 September 2013

31. D.B. Seaton, L.A. Rachmeler
An introduction to contemporary solar imaging data
Space Science Training Week 2013, KULeuven, Leuven, Belgium, 16-19 September 2013

32. D.B. Seaton, L.A. Rachmeler
Elements of solar image processing
Space Science Training Week 2013, KULeuven, Leuven, Belgium, 16-19 September 2013

33. P. Vanlommel
De aarde in de greep van de zon
Kick-off meeting Junior College, KULeuven, Heverlee-Leuven, Belgium, 8 & 10 January 2013

34. P. Vanlommel
Ruimteweer
PROBA2@school sessions for high school students, Klein Seminarie, Hoogstraten, Belgium, 26 March 2013

35. P. Vanlommel
De snelheid van een plasma wolk berekenen
PROBA2@school sessions for high school students, Klein Seminarie, Hoogstraten, Belgium, 26 March 2013

36. P. Vanlommel
De Zon en PROBA2
VVS Ruimtevaartnamiddag, Public Observatory Armand Pien, Gent, Belgium, 25 May 2013

37. P. Vanlommel
Ruimteweer: de fysica en voorspellingen
Visit of KPN to SSCC, SSCC-room, Brussel, Belgium, 10 July 2013

38. P. Vanlommel
De Zon
Summerschool VVS, GroepT, Leuven, Belgium, 26 August 2013

39. P. Vanlommel
Ruimteweer en impact
KPN, Hilversum, Nederland, 10 September 2013

40. P. Vanlommel, L. Rodriguez
Interpreting the solar wind
eHEROES/CHARM summerschool, Leuven, Belgium, 19 September 2013

41. F. Verbeeck
Ruimteweer: De impact van zonnestormen op Aarde
Open Doors Space Pole, Brussels, Belgium, 25 May 2013

42. A.N. Zhukov
Coronal Mass Ejections and Space Weather
Visit of students of Université de Mons at ROB, Brussels, Belgium, 23 April 2013

List of abbreviations

3D	Three dimensional
4CESM	Chapman Conference on Causes and Consequences of the Extended Solar Minimum between Solar Cycles 23 and 24
4D	Four dimensional
A	Ampère
ACE	Advanced Composition Explorer
ACRIM	Active Cavity Radiometer Irradiance Monitor
ACVE	Atmospheric Composition Validation and Evolution
AFFECTS	Advanced Forecast For Ensuring Communications Through Space
AGACC	Advanced exploitation of Ground based measurements Atmospheric Chemistry and Climate applications
AGU	American Geophysical Union
AIA	Atmospheric Imaging Assembly (SDO)
AIP	American Institute of Physics
AIRS	Atmospheric Infra-Red Sounder
ALARO	Aire Limitée Adaptation/Application de la Recherche à l'Opérationnel
AlN	Aluminum Nitride
ALTIUS	Atmospheric Limb Tracker for Investigation of the Upcoming Stratosphere
AMS	American Meteorological Society
AMTD	Atmospheric Measurement Techniques Discussion
AOD	Aerosol Optical Depth
AOSWA	Asia-Oceania Space Weather Alliance
APOD	Astronomy Picture of the Day (NASA)
APS	Active Pixel Sensor
ASCII	American Standard Code for Information Interchange
ASGARD	An educational space program for schools (no acronym)
ASH	Amateur Sterrenkundigen van Herentals
ASL	Above Sea Level
ATLAS	ATmospheric Laboratory for Applications and Science
ATMOS	Advances in Atmospheric Science and Applications
AU	Astronomical Unit; about 150 million km
avg.	average
BELSPO	Belgian Science Policy Office
BIRA	Belgisch Instituut voor Ruimte-Aëronomie
BISA	Belgian Institute for Space Aeronomy
BRAMS	Belgian RAdio Meteor Stations
BSS	Beacon Satellite Symposium
BUSOC	Belgian User Support and Operation Center
c	Speed of light
CaII K	Singly ionized Calcium (K-line)
CACTus	Computer Aided CME Tracking software
CALLISTO	Compound Astronomical Low frequency Low cost Instrument for Spectroscopy and Transportable Observatory
CASSIS	Coordination Action for the integration of Solar System Infrastructures and Science
CBH	Cloud Base Height
CCD	Charge-Coupled Device
CERES	Clouds and Earth's Radiant Energy System (radiometer)
CESRA	Community of European Solar Radio Astronomers
CH	Coronal Hole
CHARM	Contemporary physical challenges in Heliospheric and AstRophysical Models
CLW	Coronal Loops Workshop
CME	Coronal Mass Ejection
CMOS	Complementary Metal Oxide Semiconductor
CNES	Centre National d'Etudes Spatiales
CNRS	Centre National de la Recherche Scientifique
CODE	Center for Orbit Determination

COMESEP	COronal Mass Ejections and Solar Energetic Particles
COPUOS	COmmittee on the Peaceful Uses of Outer Space (UN)
COSPAR	COmmittee on SPAce Research
COST	(European) COoperation in Space & Technology
CPPA	Conference on Plasma Physics and Applications
CSL	Centre Spatial de Liège
CubeSat	A small satellite measuring 10cm x 10cm x 10cm
dB	Decibel
DEM	Differential Emission Measure
DeMeLab	Detector Measurements Laboratory
DIARAD	DIfferential Absolute RADiometer
DIAS	Digital Upper Atmosphere Server
DLR	Deutsche Zentrum für Luft- und Raumfahrt
DMI	Danish Meteorological Institute
DOI	Digital Object Identifier
DOY	Day Of Year
DPD	Debrecen Photographic Data
DPTIS	Double-Probe and Topside Ionospheric Sounder
Dst	Disturbance Storm Time index
E-GVAP	EUMETNET EIG GNSS water VApor Program
EBAF	Energy Balanced And Filled
ECC	Electrochemical Concentration Cell
EDP	Electron Density Profile
EGNOS	European Geostationary Navigation Overlay Service
eds.	editors
EGU	European Geosciences Union
eHEROES	Environment for Human Exploration and RObotic Experimentation in Space
EIG	Economic Interest Grouping
EISCAT	European Incoherent SCATter scientific association
EIT	Extreme ultraviolet Imaging Telescope (SOHO)
ELF	Extremely Low Frequency
EPN	EUREF Permanent Network
EPOS	European Plate Observing System
ERB(S)	Earth Radiation Budget (Satellite)
ES	Earth System (Science and Environmental Management (COST)
ESA	European Space Agency
ESAC	European Space Astronomy Centre
ESC	Expert Service Centre
ESO	European Southern Observatory
ESP	EUV SpectroPhotometer (SDO/EVE)
ESPAS	European Strategy and Policy Analysis System (FP7)
ESRIN	European Space Research INstitute
ESTEC	European Space Research and Technology Centre
ESWP	European Space Weather Portal
ESWW	European Space Weather Week
EU	European Union
EUI	Extreme-Ultraviolet Imagers (Solar Orbiter)
EUMETNET	European Meteorological services Network
EUMETSAT	European Organisation for the Exploitation of Meteorological Satellites
EUREF	EUropean Reference Frame
EUV	Extreme Ultraviolet
EUVI	Extreme Ultraviolet Imager (STEREO/SECCHI)
EVE	Extreme ultraviolet Variability Experiment (SDO)
$F_{10.7\ cm}$	Solar radio flux at 10.7 cm wavelength
F_2	Main ionospheric layer
FeIX	8 times ionized iron
FITS	Flexible Image Transport System
FP7	Framework Program 7
FPGA	Field-Programmable Gate Array
G4SUW	Geant4 Space Users Workshop
Galileo	European GNSS
GB	gigabyte (10^9 bytes)

GCOS	Global Climate Observing System
GEANT4	GEometry ANd Tracking (4th version)
GEEO	Global Environmental Earth Observation
GEOSS	Global Earth Observation System of Systems
GERB	Geostationary Earth Radiation Budget (radiometer)
Gfg^2	GNSS for GEEO and GEOSS
GHOST	name of WG5 of the TOSCA project (no acronym)
GLONASS	GLObal NAvigation Satellite System (Russia)
GNSS	Global Navigation Satellite System
GNSS4SWEC	Advanced GNSS tropospheric products for the monitoring of Severe Weather Events and Climate
GOES	Geostationary Operational Environmental Satellite
GOP	Geodetic Observatory Pecný
GPS	Global Positioning System (USA)
GUI	Graphical User Interface
h’	virtual height
H-alpha	A red visible spectral line created by Hydrogen
Hi-C	High Resolution Coronal Imager
h_mF_2	peak density height of F_2-layer
HMI	Heliospheric and Magnetic Imager (SDO)
HQ	Headquarters
IAG	International Association of Geomorphologists
IAGA	International Association of Geomagnetism and Aeronomy
IAS(B)	Institut d’Aéronomie Spatiale de Belgique
IASI	Infrared Atmospheric Sounding Interferometer
IAU	International Astronomical Union
IAUS	IAU Symposium
ICME	Interplanetary CME
ICT	Information and Communication Technologies
IDL	Interactive Data Language
IEEE	Institute of Electrical and Electronics Engineers
IERS	International Earth Rotation Service
IGS	International GNSS Service
IMC	International Meteor Conference
IPAG	Institut de Planétologie et d'Astrophysique de Grenoble
IPELS	Interrelationship between Plasma Experiments in Laboratory and Space
IR	Infrared
IRI	International Reference Ionosphere
IRIS	Interface Region Imaging Spectrograph
Irr.	Irradiance
ISBN	International Standard Book Number
ISES	International Space Environment Service
ISEST	International Study of Earth-Affecting Solar Transients
ISIS	International Satellites for Ionospheric Studies
ISS	International Space Station
ISSI	International Space Science Institute
ISSN	International Standard Serial Number
IT	Information Technology
ITRF	IERS Terrestrial Reference Frame
IUAP	Intra-University Attraction Pole network
IWV	Integrated Water Vapor
JSWSC	Journal of Space Weather and Space Climate
K_p	A geomagnetic index, ranging from 0 (quiet) to 9 (extremely severe storm)
KPN	Koninklijke PTT Nederland NV
KSB	Koninklijke Sterrenwacht van België
KUL	Katholieke Universiteit Leuven
λ	wavelength
LAC	Local Analysis Centres (EPN)
LASCO	Large Angle Spectrometric Coronagraph (SOHO); small

	(C2) and wide (C3) field of view
LATMOS	Laboratoire Atmosphères, Milieux, Observations Spatiales
LDE	Long Duration Event
LIDAR	LIght Detection And Radar
LIEDR	Local Ionospheric Electron Density profile Reconstruction
LOC	Local Organizing Committee
LYRA	Lyman Alpha Radiometer (PROBA2)
LWS	Living With a Star
µm	micrometer (10^{-6} meter)
M-class flare	Medium x-ray flare
MEGS-A	Multiple EUV Grating Spectrograph A (SDO)
MEGS-B	Multiple EUV Grating Spectrograph B (SDO)
METIS	Multi Element Telescope for Imaging and Spectroscopy (Solar Orbiter)
MetOffice	Meteorological institute of the UK
MeV	Mega electronvolt ($10^6 . 1.6 . 10^{-19}$ Joule)
MgII	singly ionized Magnesium
MHD	Magneto-Hydro-Dynamic
MHz	Megahertz (10^6/s)
MLH	Mixing Layer Height
MOZAIC	Measurement of Ozone and Water Vapor by Airbus In-Service Aircraft
MSM	Metal-Semiconductor-Metal
MSSL	Mullard Space Science Laboratory
ms	millisecond (10^{-3} s)
MUV	Middle UltraViolet
mV	milliVolt (10^{-3} V)
mW	milliWatt (10^{-3} W)
MySQL	My Structured Query Language
N_2	Nitrogen (molecule)
NatGeo	National Geographic
NASA	National Aeronautics and Space Administration
NDACC	Network for the Detection of Atmospheric Composition Change
N_e	Number of electrons
NEC	Numerical Electromagnetic Code
NEMO	Novel EIT wave Machine Observing
NIR	Near InfraRed
nm	nanometer (10^{-9} meter)
nA	nano-Ampère (10^{-9} Ampère)
N_mF_2	peak density of F_2-layer
NOA	National Observatory of Athens
NOAA	National Oceanic and Atmospheric Administration (numbering of sunspots)
NRL	Naval Research Laboratory (US)
NRT	Near Real-Time
NSSDC	National Space Science Data Center
nT	nano-Tesla (10^{-9} Tesla)
NWP	Numerical Weather Prediction
O	Oxygen
O_3	Ozone
O3SDQA	Ozone Sonde Data Quality Assessment
ORB	Observatoire Royal de Belgique
P2SC	PROBA2 Science Centre
pA	pico-Ampère (10^{-12} Ampère)
PCA	Principal Component Analysis
PCB	Printed Circuit Board
PCO	Phase Center Offset
PhD	Doctor of Philosophy
PI	Principal Investigator
PICASSO	Pico-satellite for Atmospheric and Space Science Observations
PMOD	Physikalisch-Meteorologisches Observatorium Davos
PMT	Photo Multiplier Tube
ppm	parts per million
ppb	parts per billion
PROBA	PRoject for OnBoard Autonomy
PRODEX	PROgram for the Development of scientific Experiments
PTB	Physikalisch-Technische Bundesanstalt
Q&A	Questions and Answers
QB50	A network of 50 cubesats to be launched simultaneously (FP7)
QR-code	Quick Response code

RACA	Rencontre Astronomique Centre Ardenne
RCM	Regional Climate Modelling
RHESSI	Reuven Ramaty High Energy Solar Spectroscopic Imager
RMI(B)	Royal Meteorological Institute (of Belgium)
RMS	Root Mean Square
ROB	Royal Observatory of Belgium
RS	Radiosonde
RSTN	Radio Solar Telescope Network (USAF)
RWC	Regional Warning Center
σ	Standard deviation
S/N	Signal-to-Noise
SAA	South Atlantic Anomaly
SBUV	Solar Backscatter UltraViolet
SC24	Solar Cycle 24
SCIAMACHY	SCanning Imaging Absorption spectroMeter for Atmospheric CHartographY (ENVISAT)
SCIOPS	SCIence OPerationS
SDO	Solar Dynamics Observatory
SECCHI	Sun Earth Connection Coronal and Heliospheric Investigation (STEREO)
SEII	Société Européenne des Ingénieurs et des Industriels
SEP	Solar Energetic Particle
SFU, sfu	Solar Flux Unit (10^{-22} W m^{-2} Hz^{-1})
SIDC	Solar Influences Data analysis Center
SILSO	Sunspot Index and Long-term Solar Observations
SIMBA	Sun-earth IMBAlance radiometer
SLP	Scanning Langmuir Probe
SN	Space weather and Near-earth objects
SN	Sunspot Number
SOC	Scientific Organizing Committee
SoFAST	Solar Flare Automated Search Tool
SoHe	Meeting of the Italian Community in Solar and Heliospheric Physics
SOHO	SOlar & Heliospheric Observatory
SOLCON	SOLar CONstant radiometer
SOLID	SOLar Irradiance Data exploitation (FP7)
SolO	Solar Orbiter
SOLSPEC	SOLar SPECtrum
SOLSTICE	Solar Stellar Irradiance Comparison Experiment
SORCE	Solar Radiation and Climate Experiment
SOTERIA	SOlar-Terrestrial Investigations and Archives
SOVA	SOlar constant and VAriability
SOVAP	SOlar VAriability Picard
SOVAR	Refurbished SOVA1 radiometer
SOVIM	Solar Variations and Irradiance Monitor
SPENVIS	Space Environment Information System
SPICE	Spectral Imaging of the Coronal Environment (Solar Orbiter)
SPoCA	Spatial Possibilistic Clustering Algorithm
sr	steradian
SSA	Space Situational Awareness
SSCC	SSA Space Weather Coordination Centre
SSI	Solar Spectral Irradiance
SSN	SunSpot Number
SSN_{ori}	Original series of sunspot numbers
SSN_{corr}	Corrected series of sunspot numbers
STAFF	Solar Timelines viewer for AFFECTS
STCE	Solar-Terrestrial Centre of Excellence
STEREO	Solar-TErrestrial RElations Observatory
STORM	Solar system plasma Turbulence: Observations, inteRmittency and Multifractals
STSM	Short-Term Scientific Mission (COST)
SVW	Sun Visibility Window
SW4E	Space Weather for Engineers
SWAP	Sun Watcher using APS detector and image Processing (PROBA2)
SWE	Space WEather

SWENET	(European) Space WEather NETwork	USET	Uccle Solar Equatorial Table
SWG	Science Working Group	UT(C)	(Coordinated) Universal Time
SWSC	Space Weather and Space Climate journal	UTL	Upper ion Transition Level
SWT	Science Working Team	UV	Ultraviolet
SWWT	(European) Space Weather Working Team	V	Volt
TaD	Topside sounder model profiler – assisted Digisonde	VERSIM	VLF/ELF Remote Sensing of Ionospheres and Magnetospheres
TEC	Total Electron Content	VHDL	VHSIC Hardware Description Language
TECu	Total Electron Content unit (10^{16} electrons per m^2)	VHSIC	Very High Speed Integrated Circuit
tg	Propagation time	VIP	Very Important Person
TID	Travelling Ionospheric Disturbance	VIRGO	Variability of solar IRradiance and Gravity Oscillations
TIM	Total Irradiance Monitor	VIS	VISual
TOA	Top Of Atmosphere	VKI	Von Karman Institute
TOPROF	Towards Operational ground based PROFiling with ceilometers, doppler lidars and microwave radiometers for improving weather forecasts	VLF	Very Low Frequency
TOSCA	Towards a more complete assessment of the impact of solar variability on the Earth's climate	VSWMC	Virtual Space Weather Modelling Centre
TRF	TSI Radiometer Facility	vTEC	vertical TEC
TSI	Total Solar Irradiance	VUB	Vrije Universiteit Brussel
UAV	Unmanned Aerial Vehicle	VUV	Vacuum UV
UK	United Kingdom	VVS	Vereniging Voor Sterrenkunde
ULB	Université Libre de Bruxelles	W	Watt
ULg	Université de Liège	W/m^2	Watt per square meter
US(A)	United States (of America)	WDC	World Data Center
USAF	United States Air Force	WDS	World Data Service
		WG	Working Group
		WLF	White Light Flare
		WMO	World Meteorological Organization
		WP	Work Package
		X-class flare	Extreme x-ray flare
		XUV	Extreme Ultraviolet